THERMO-ECONOMIC EVALUATION OF MAISOTSENKO-DESICCANT COOLING SYSTEMS FOR GAS TURBINE POWER PLANTS

by

Waleed Moustafa El-Damaty

A Thesis presented to the Faculty of the
American University of Sharjah
College of Engineering
In Partial Fulfillment
of the Requirements
for the Degree of

Master of Science in
Mechanical Engineering

Sharjah, United Arab Emirates

October 2018

Approval Signatures

We, the undersigned, approve the master's Thesis of Waleed Moustafa El-Damaty.

Thesis Title: Thermo-Economic Evaluation of Maisotsenko-Desiccant Cooling Systems for Gas Turbine Power Plants

Signature	**Date of Signature** (dd/mm/yyyy)
_____	_____
Dr. Mohamed Gadalla Professor, Department of Mechanical Engineering Thesis Advisor	
_____	_____
Dr. Mehmet Kanoglu Visiting Professor, Department of Mechanical Engineering Thesis Committee Member	
_____	_____
Dr. Zarook Shareefdeen Professor, Department of Chemical Engineering Thesis Committee Member	
_____	_____
Dr. Mamoun Fahed Saleh Abdel-Hafez Head, Department of Mechanical Engineering	
_____	_____
Dr. Ghaleb Husseini Associate Dean for Graduate Affairs and Research College of Engineering	
_____	_____
Dr. Richard Schoephoerster Dean, College of Engineering	
_____	_____
Dr. Mohamed El-Tarhuni Vice Provost for Graduate Studies	

Acknowledgement

First, I would like to thank God for helping me through this important chapter in my life. Then, I would also like thank my parents; without their help, assistance and support, I wouldn't be here today.

I owe special thanks to my advisor and mentor, Dr. Mohamed Gadalla, for providing knowledge, guidance, support, and motivation throughout my research stages. I'm deeply beholden for his great assistance, worthy discussion and suggestions.

I would like also to thank my friend and colleague Mohammad Saghafifar for providing me with his time, help and, most importantly, his experience throughout this journey.

I would like to thank the professors of the Mechanical Engineering department who taught me the master level courses with innovative teaching methods and skills. I really appreciate their dignified advice and motivation.

I would like to thank the Mechanical Engineering department for giving me the opportunity to work as a graduate teaching assistant (GTA) during this period. I have learned many valuable skills from this experience and I am eternally grateful for it.

Abstract

With the everlasting increase in population, a huge surge in the electricity consumption has been recorded. Thus, power plants manufacturers and utility companies need to augment the plants performance to cope with these rising of energy demands. Turbine blade cooling is a vital procedure in gas turbine power plants due to the high turbine inlet temperatures achieved. The main objective of the thesis is to cool down the air bled from the compressor for turbine blade cooling, using Maisotesnko-desiccant cooling systems. This will reduce the amount of bled air and improve the efficiency. In this research, the performance of 50 MWe gas turbine power plants with three different configurations; a simple gas turbine, a gas turbine with an air bottoming cycle (GTABC) and intercooled, reheated and recuperated (IcRhRc) gas turbine integrated with the proposed cooling systems are investigated. Research results indicated that the GTABC yielded an increase in the overall efficiency from 42.57 % without cooling to 43.27%, to 43.54% and to 43.83% for the triple stage Maisotsenko-desiccant (TS-MD), triple stage precooling Maisotsenko-desiccant (TS-PMD) and triple stage extra cooling Maisotsenko-desiccant (TS-EMD), respectively. Furthermore, a maximum reduction in the fuel mass flow rate was observed from 2.713 kg/s to 2.653 kg/s in the TS-EMD system leading to a decrease in the carbon foot print which agrees with recent United Nations sustainability reports. The exergoeconomic results of the IcRhRc gas turbine exhibited a reduction in the exergy destruction rate from 44.86 MW without cooling to 43.34 MW after integrating TS-EMD cooling system. Consequently, the exergy efficiency has increased from 50.92% to 51.43%, to 51.63% and to 51.86% after incorporating TS-MD, TS-PMD and TS-EMD, respectively. Subsequently, the cost rate of exergy destruction has decreased from 924.2$/hr to 879.1$/hr after implementing the TS-EMD cooling system. Moreover, the investment cost flow rate has decreased from 101$/hr to 99.92$/hr after integrating the TS-EMD cooling system. The exergoeconomic factor and relative cost difference were also evaluated to assess each component for further performance improvement.

Keywords: ***Gas turbine power plants; Air bottoming cycles; Intercooled recuperated and reheated gas turbines; Cooling systems; Maisotsenko-desiccant; Thermodynamic optimization; Exergoeconomic analysis***

Table of Contents

Table of Figures

List of Tables

Nomenclature

Symbols

A_Q	Heat transfer area
A_c	Hot gas cross section area
b	Cooling model parameter
c	Cost per unit of exergy
$\dot{C}$	Exergetic cost flow rate
$\dot{C}_D$	Cost rate of exergy destruction
C_p	Specific heat capacity
$\dot{E}$	Exergy flow rate
$\dot{E}_D$	Exergy destruction rate
$\dot{E}_P$	Exergy product rate
$\dot{E}_f$	Exergy fuel rate
f	Exergoeconomic factor
K	Cooling model parameter
$\dot{m}$	Mass flow rate
M	Mach number
St	Stanton number
s	Cooling model parameter
$\dot{Z}$	Investment cost flow rate
Z	Purchase cost associated with the component

Greek letters

$\eta_{iso,air}$	Isothermal efficiency
ζ	Mixing loss factor
α	Ratio between A_Q and A_c
ω	Humidity ratio
ϵ	Exergetic efficiency
r	Relative cost difference

Abbreviation

CC	Combustion chamber
CGAM	Initials of the four investigating researchers
GT	Gas Turbine
HE	Heat exchanger
HPT	High pressure turbine
HPC	High pressure compressor
IcRhRc	Intercooled, Reheated and Recuperated
LPC	Low pressure compressor
LPT	Low pressure turbine
MFFR	Mass flow rate ratio
SS-MD	Single stage Maisotsenko-desiccant
TIT	Turbine inlet temperature
TS-EMD	Triple stage extra cooling Maisotsenko-desiccant
TS-IMD	Two stage Intermediate Maisotsenko-desiccant
TS-MD	Triple stage Maisotsenko-desiccant
TS-PMD	Triple stage precooling Maisotsenko-desiccant
TS-RMD	Two stage recovered Maisotsenko-desiccant

Subscripts

b	Blade
c	Coolant
cs	Cold stream
dp,w	Dew point working air
g	Gas

g,i	Inlet exhaust gases
g,o	Exit exhaust gases
j	Coolant stream
l,e	Lower, Exit
l,i	Lower, Inlet
p	Product air
sa	Supplied air
u,e	Upper, Exit
u,i	Upper, Inlet
Net,top,bot	Net-work in the topping and bottoming cycles

Chapter 1. Introduction

This research work presents a brief outline about gas turbine power plants and the challenges they face in this chapter. Then, it presents the problem investigated in this study as well as the thesis contribution. Lastly, thesis organization is displayed.

1.1. Overview

Electricity has become an essential part of modern life and with the ever-increasing humanity population, the huge surge in electricity consumption is one of the problems that need to be tackled in order to maintain a stable and prosperous life for the upcoming generations. Gas turbine power plants are considered a vital mean in electricity production nowadays due to its flexibility, as they can be converted into combined power plants more easily, low capital cost, simple design and compact size compared to steam turbine power plants [1]. Thus, it is very important to improve the performance of gas turbine power plants to produce more power, using lesser fuel which will in turn reduce the carbon footprints. This comes in agreement with the united nations new guidelines for a more sustainable and green life.

1.2. Thesis Objectives

Pressure, ambient temperature and turbine inlet temperature (TIT) are well known factors that affect the gas turbine performance [2]. Although, the increase of the TIT will improve the performance of the gas turbine, it can cause high thermal stresses and oxidation rates, damaging the turbine blades. Hence, the advancement in material and cooling technologies such as turbine blade cooling is crucial to achieve such high turbine inlet temperatures. The main objective of the thesis is to cool down the air bled from the compressor for turbine blade cooling using Maisotesnko-desiccant cooling systems. This will reduce the amount of bled air, improving the gas turbine efficiency. Moreover, the effect of integrating different configurations of solid desiccant and Maisotsenko cooler cooling systems with three different configurations of gas turbine power plants, including simple gas turbine, gas turbine with air bottoming cycle (GTABC) and intercooled, reheated and recuperated (IcRhRc) gas turbine for inlet air cooling and turbine blade cooling will be investigated.

1.3. Significance of Research

The contributions of this research work can be summarized as follows:

- Propose an unconventional cooling system that can play an important role in the future of gas turbine cooling.
- Propose different configurations of the Maisotsenko-desiccant cooling system and study their effect on the performance of the gas turbine.
- Improve the gas turbine power plant efficiency and reduce the carbon footprints as well for a more sustainable and greener environment.
- Present a detailed exergoeconomic analysis to assess the gas turbine power plant, not from a thermodynamic point of view only, but from an exergoeconomic one as well.

1.4. Thesis Organization

The thesis is structured as follows: Chapter 2 provides background and literature review about gas turbine power plants, recent techniques used for gas turbine cooling, explanation of the used Maisotsenko-desiccant cooling system and the exergoeconomic approach. Problem formulation and research methodology along the different systems configurations are presented in Chapter 3. Chapter 4 discusses the mathematical formulation used for the different systems. Moreover, the thermodynamic model, the exergoeconomic model and the Maisotsenko-desiccant cooling system model are presented and discussed as well. Chapter 5 presents the sensitivity analyses and the optimization procedures performed. Additionally, the obtained thermodynamic and exergoeconomic results are shown, and their effect on the performance of the gas turbine is discussed as well. Finally, Chapter 6 states the conclusion, recommendations and future research work.

Chapter 2. Background and Literature Review

The gas turbine power plant is considered one of the most reliable means in the field of electricity production due to its fast starting and loading, high reliability, compact size, low capital cost and better environmental performance, in comparison to other prime movers, especially the steam turbine plant. [3].

Gas turbines mainly consists of compressor, combustion chamber and gas turbine. The atmospheric air enters the compressor to get compressed to a higher pressure with no heat loss or gain. After leaving the compressor, the air enters the combustion chamber where fuel gets injected, and the combustion process takes place at constant pressure. A hot mixture of combustion gases leaves the combustion chamber at a high temperature where it enters the gas turbine, converting the energy of the hot gases into work [4].

Inlet air conditions and turbine inlet temperature are the main factors affecting the performance of the gas turbine. As the compressor inlet air temperature and humidity decreases, the efficiency and performance of the gas turbine increases. Additionally, the increase in the turbine inlet temperature leads to an augmentation in the gas turbine efficiency. Nevertheless, a reduction of the lifetime of the blades is expected due to the very high temperature of the combustion gases entering the turbine which will lead to undesirable thermal stresses and oxidation rates. Thus, two main cooling approaches can be adopted to improve the performance of gas turbine power plants, First, there is the inlet air cooling where the inlet air entering the compressor is cooled conventionally by utilizing evaporative coolers and mechanical chillers. Second, there is the turbine blade cooling where air is bled from the compressor to cool down the turbine blades. However, the amount of air mass flow rate bled from the compressor presents a penalty on the thermodynamic efficiency of the gas turbine power plant. Thus, it is crucial to try and reduce this air mass flow rate as much as possible without affecting its main task of cooling the turbine blades. Different techniques of cooling will be discussed in the following sections.

2.1. Inlet Air Cooling Methods

Jonsson and Yan [5] discussed the potential of different humidified gas turbines cycles where injecting water/steam leads to an increase in the mass flow rate which

boosts the specific power output. Three main categorizes of the humidified gas turbines were studied: gas turbines with water injection, gas turbine with steam injection and evaporative gas turbines. One of the main factors to affect the performance and the efficiency of the gas turbine is the inlet air cooling where they divided the systems used mainly into evaporative media coolers and mechanical vapor compression.

Kakaras et al. [6] focused on cooling the compressor intake air as a main way to improve the performance of the gas turbine. The air-cooling system proposed consisted mainly of two parts, direct contact air cooler and LiBr absorption chiller which give out water at low temperatures. Computer simulation was conducted for two test cases, simple cycle where the IPSEPRO simulation program was used while ENBIPRO software was used to perform the simulation for the combined cycle. Both cases showed increase in the power output. However, a reduction in the efficiency of the gas turbine in the case of combined cycle was noticed where the absorption chiller was used.

Bassily [7] studied the recuperated gas turbine cycle and the manner of augmenting its efficiency by inlet air cooling and evaporative after-cooling. Relative humidity, ambient air temperature and turbine inlet temperature were the three main factors discussed to test their effect on the performance of the four different layouts of the recuperated gas turbine cycle. The evaporative after-cooling showed an increase in the cycle efficiency by up to 16% while the evaporative cooling of the inlet air increased efficiency by 3.2%. Zadpoor and Golshan [8] discussed the power improvement techniques for gas turbine power plants. They divided the techniques into water/steam injection and inlet air cooling methods. Inlet air cooling was the main focus as it was divided into evaporative cooling methods, the refrigerated inlet cooling systems and the thermal energy storage systems. They proposed a desiccant-based evaporative cooling system to improve the gas turbine cycle performance. The obtained results indicated that the proposed system proved to be more efficient than the other evaporative cooling methods in hot and humid climates.

Oyedepo [9] discussed how to improve the performance of an existing gas turbine power plant in Nigeria by studying the effects of inlet air cooling methods on the gas turbine. The results showed that decreasing the ambient temperature and increasing the turbine inlet temperature will lead to an augmentation in the power output

and efficiency. Another valid method to increase the efficiency is to benefit from any unused or lost energy. Natural gas flow has a valuable pressure exergy which is currently destroyed in throttling valves at exit of the gas fields.

Gord and Magrebi [10] addressed this problem and studied exergy destruction in Iran's natural gas fields. An actual case was discussed where this pressure exergy is calculated. It was found that the maximum available energy is 5600MW, and by considering converting efficiency of 75%, 4200MW, electrical power could be extracted. Gord and Dashtebayaz [11] proposed a new approach to improve performance of a gas turbine. The main idea is to use the cooling capacity of the refinery natural-gas pressure drop station to cool inlet air of the gas turbine. A drop in the gas turbine inlet temperature in the range of 4 to 25°K with an improvement in the performance in range of 1.5-5%.

Boonnasa et al. [12] discussed how to improve the performance of a combined cycle power plant already existing in Bangkok for 8 years. They used a steam absorption chiller with thermal energy storage to cool the intake air to the required levels. Annual increase of 6.24% is noticed in the combined cycle power plant power output. An economic analysis was conducted as well to assure the improvement. The results showed a payback period of 3.81 years with a net present value of 19.44 MU$$ and 40% internal rate of return. An important factor in evaluating the effectiveness of a proposed system is to perform an economic analysis to calculate the economic profits.

Gareta et al. [13] presented a methodology for the economic evaluation of gas turbine air cooling systems in combined cycle applications. The main goal is to focus on the significance of the economic variables due to the selection of air cooling systems for combined cycle power plants which will help in understanding the results better and prove that the most well-known cooling systems might not be the best profitable option after all.

Ameri and Hejazi [14] discussed how to improve the output power of Chabahar by using a steam absorption chiller and an air cooler as well. The results showed an 11.3% increase in the average power output, while the electricity production has increased by 14000 MWh per year. The economic analysis showed that the capital cost of the system is 494 US$ per maximum increased kW while the cost of electricity is

1.45 Cents/kWh compared to the current cost of industrial electricity which is 2.5 Cents/kWh. The internal rate of return is calculated to be 23.4% with a 4.2 years' payback period.

2.2. Turbine Blade Cooling Methods

An alternative way to improve the performance of gas turbine is to increase the turbine inlet temperature (TIT). However, this will lead to reduction in the lifetime of turbine blades which suffers thermal stresses and oxidation rate due to very high temperature. Hence, turbine blade cooling is mandatory to assure long lifetime for the blades, and it can be divided into 3 main categories. First, we have the internal convection cooling technique where the turbine blades are cooled internally by passing the coolant through passages to reduce heat conducted, then there is film cooling technique where a relatively cold air from the internal coolant passages is injected out of the blade surface leading to the formation of a protective layer between the blade and the hot gas. Also, there is the transpiration cooling technique where numerous numbers of holes are made on the blade surface where the coolant flows through, which leads to the creation of coolant film that reduces heat transfer from hot gases to the blade surface. The cooling medium could be water, air or steam. The cooling loop maybe open where the coolant mixes with the hot gases after cooling the blades, or closed where the exiting coolant is mixed with reheated steam [15].

The literature of turbine blade cooling can be divided into two categories. The first category is concerned with determining the amount of coolant mass flow rate, turbine cooling losses and pressure losses. The second category considers heat transfer models, the geometry and shape of the blade holes, different channels design from aerodynamics and fluid point of view. In the first category, Sanjay et al. [15] discussed the different techniques of turbine blade cooling and their effect on the performance of combined cycle from thermodynamic point of view. Seven different configurations including coolant steam and coolant air have been investigated. Internal convection, film and transpiration cooling methods were the main focus under open loop category, while internal convection for closed loop.

Parametric study was conducted by modelling different components of combined cycle and deducting the required governing equations. The results indicated that the closed loop steam cooling presents the highest plant efficiency and specific

work as well as the minimum coolant requirement. Amano [16] discussed the advances in gas turbine blade cooling technology. He presented recent computational methods for internal cooling as well as the current trends in cooling technologies.

Wilcok et al. [17] presented a performance prediction of turbine blade cooling in gas turbines where a thermodynamic cycle analysis computer code was used to calculate the efficiency of plants. Compressor pressure ratio, combustor outlet temperature and turbomachinery polytropic efficiency were the varying variables tested. The results indicated that in order to obtain maximum cycle efficiency, a compromised combination of the varying variables is required due to their significant effect on the performance of the gas turbine.

Louis et al. [18] discussed the different techniques of turbine blade cooling and their influence on the thermodynamic efficiency and specific work of gas turbines where a general model was used to evaluate them. The paper provides a lot of useful information and is cited numerous times, specially in the field of turbine blade cooling since the study was conducted in terms of dimensionless variables to achieve generality and allow access to beneficial guidelines. Sciubba [19] discussed the blade cooling from a different point of view where the blade shape and cooling channel structure were the main focus. He developed a simple analytical thermodynamic model that gives closed form solutions which will help in interpreting the results more accurately. Al-Ali and Janajreh [20] focused on a specific technique of turbine blade cooling which is the jet impingement where an array of high velocity fluid is made to strike a surface leading to formation of a thin boundary layer.

They conducted numerical analysis of different configuration of jet impingement and drew a comparison between them on the basis of effective heat transfer. The results showed that applying turbine blade jet cooling will help in increasing the efficiency and reducing the average blade surface temperature by 20%.

Mohapatra and Sanjay [21] presented a comparison between the effect of two inlet air cooling methods integrated with a combined cycle gas turbine. Parametric study was conducted to test the impact of different varying variables such as compressor pressure ratio, turbine inlet temperature and ambient temperature. The results indicated an improvement of 4.88% in the cycle efficiency and 14.77% in the work output in the

case of vapour compression, while in case of vapor absorption cooling, the cycle work output was enhanced by 17.2% and the cycle efficiency was improved by 9.47%. Sanjay et al [22] studied the effect of different turbine blade cooling methods on a cogeneration cycle and compared between them. The paper provided great insight in the case of different variables optimization for a certain specific work. Sahu and Sanjay [23] investigated the air film blade cooling technique and its effect on thermos-economics of the power plant. Exergy, economics, and exergy costing analysis was conducted. The results showed that the allowable temperature of blade material and turbine inlet temperature have a major impact on blade air coolant requirements.

Jonsson and Bolland [24] developed a simple cooled gas turbine model due to the complexity of most of the available turbine blade cooling models and their appropriateness for cycle analysis that aims for efficiency prediction. Spelling [25] adopted the model, developed by Jonson and Bolland [24], during his doctoral thesis for hybrid solar gas turbine power plants. The objective of model is to determine the fraction of the main compressor mass flow that needs to be extracted for the different cooling purposes.

By considering the turbine as expansion path with continuous work extraction, El-Masri developed a model to calculate the coolant losses occur in various cooling techniques [26]. Horlock et al. [27] reviewed the models used to calculate the coolant mass flow rate for film cooling and the pressure losses occurring during the process.

The combined effect of turbine blade cooling, inlet air cooling and steam injection on a combined cycle power plant were investigated by Singh and Shukla [28]. Vapor absorption cooling were considered for inlet air cooling, and film cooling were considered for turbine blade cooling. The effect of different parameters i.e pressure ratio, TIT and ambient temperature on the combined cycle were considered.

The relation between the gas flow field around the cooled blade was studied by Apostolidis [29] by predicting the cooling requirement and the metal temperature. He recommended a web-based gas turbine simulation code that aims to reduce the drawback of conventional installation. An energetic and exergetic analysis, for an intercooled combustion-turbine based combined cycle power plant, was presented by Sanjay and Prasad [30] where they achieved maximum efficiency by varying the

intercooler pressure ratio. In the second category that is concerned with geometry of holes, channels design and heat transfer models, the pin fin cooling channels design, turbulence models and the pin pressure distribution were studied by Fernandes [31]. Highly advanced geometries were investigated as well to reduce the pressure loss in channels and augment the heat transfer levels. Sunden and Xie [32] overviewed the blade tip leakage flow and heat transfer from 2001 to 2010 and the internal and external cooling technologies as well. The vortex cooling technique was investigated by Du et al. [33] where they conducted numerical simulations to study the thermal effect of vortex cooling with bleed holes. Nagaiah in [34] performed a computational study that aims to control three main factors, the cooling channel heat transfer, cooling channel pressure drop and cooling channel geometry to investigate the film cooling effectiveness and the material used.Zhou in [35] used the PIV and PSP techniques to investigate the effect of density ratios, geometrical parameters and mass flux ratios on the cooling effectiveness. The usage of steam, as a coolant instead of air, was discussed by Siddique in [36]. He also recommended a design cooling configuration for the trailing edge that enhances the heat transfer while reducing the pressure losses.

2.3. Maisotsenko-Desiccant Cooling System

Maisotsenko and Gillan [37] proposed a novel cycle that combines the thermodynamic processes of heat exchange and evaporative cooling with an indirect evaporative cooler. Its main advantage is that it produces temperatures near the dew point temperature of the working gas. Hence, it can be used to cool compressor inlet air below wet bulb temperature. The typical Maisotsenko-desiccant cooling system as shown in Figure 1 comprises of a Maisotsenko cooler, air to air heat exchanger, air to gas heat exchanger and solid desiccant.

Desiccants can be divided into two main sections, solid and liquid desiccants. Zeolite, silica gel, and alumina silicate are the most used materials for solid desiccants. Additionally, the use of composite materials has been investigated as they decrease the regeneration temperature required as well as enhance the moisture adsorption characteristics of the desiccant. Generally, solid desiccants are easier to handle than liquid desiccant. However, the pressure drops of the air passing through solid desiccants is one of its known problems. Solid desiccants come in many forms and shapes such as, cross flow, fixed bed, belt and stationary or rotary wheels. Rotary wheels are one of

the most used shapes as it can operate continuously, and it resists the corrosion. Liquid desiccants utilize lithium chloride or calcium chloride as their adsorbent. Although the capability of liquid desiccants to remove moisture are greater than solid desiccants, they have a major disadvantage that they are carried away by air stream during regeneration and dehumidification [39].

The air stream in Figure 1 can be divided into two streams: lower air stream (regeneration air) and upper air stream (processed air). The lower air stream at state 5 enters the Maisotsenko cooler as atmospheric air to get cooled reaching state 6. The upper air stream is then used to heat it as it passes through the heat exchanger to reach state 7. Next, the exhaust gases from the turbine outlet heat the air to state 8. Following that, the vapour pressure on the desiccant surface is increased, surpassing the surrounding air pressure, as the heated air passes through it in a process named regeneration to restore the moisture removal capabilities of the desiccant. Air is driven to the environment at state 9.

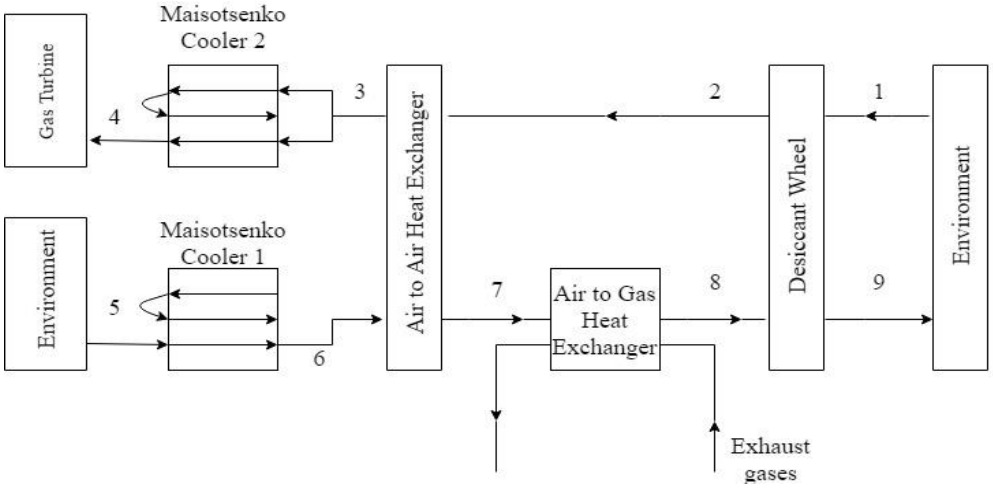

Figure 1: Single stage Maisotsenko-desiccant cooling system

The upper air stream at state 1 enters the desiccant, reaching state 2 after being dehumidified. Afterwards, the air exchanges heat with the lower air stream as it passes through an air to air heat exchanger reaching state 3. At state 3, the processed air stream is divided into two equal air streams. One of the streams enters the working dry channel of the Maisotsenko cooler while the other stream enters the product channel of the Maisotsenko cooler, and it is cooled to the dew point temperature of the air in the working channel at state 4. Air at state 4 can be used as inlet air to the compressor as well as cooling the coolant line which will help in reducing the amount of coolant that

is depleted from the compressor exit. Caliskan et al. [38] conducted energy and exergy analyses as well as sustainability assessment for an air-cooling system based on Maisotsenko cycle.

The results indicated a maximum exergy efficiency of 19.14% while 8.45% for the minimum exergy efficiency with an energetic COP of the cycle to be 2.30, while 0.19 and 0 were the observed maximum and minimum exergetic COPs of the cycle, respectively.

Saghafifar and Gadalla [39] proposed an innovative inlet air cooling technology for gas turbine power plants by integrating solid desiccant and Maisotsenko cooler. Two different climates were investigated to evaluate the performance of the inlet air cooling systems. The results showed that Maisotsenko evaporative desiccant inlet air cooling is a very economic choice as an inlet cooling method with a life span of 25 years. Saghafifar and Gadalla [40] presented a new system by integrating PV/T solid desiccant air-conditioning systems and Maisotsenko cooler in order to cool buildings. A detailed thermodynamic analysis is conducted as well as a comparative analysis in order to clarify the pros and cons of integrating the Maisotsenko cooler with conventional desiccant air conditioning units. The results showed an average COP of 0.2495 and 0.2713 for the two proposed configurations.

Gadalla and Saghafifar [41] presented a double-stage solid desiccant air conditioning system where they analysed its performance and conducted transient optimization of air precooling in it. Three different configurations of two-stage desiccant air conditioning systems integrated with Maisotsenko cooling cycle are proposed. The results indicated that air precooling is considered to improve two stage desiccant air conditioning systems' COP.

The assessment of gas turbine systems can be divided into two categories. The first category focuses mainly on the thermodynamic analysis considering the thermal efficiency and the performance of the system from the first law of thermodynamics point of view. The second category studies the exergoeconomic analysis considering the exergetic efficiency and performance of the system from the second law of thermodynamics point of view.

2.4. Thermodynamic Approach

In this area, a significant body of research has been conducted regarding the analysis of gas turbine power plants as done by Bhargava et al. [42], Sanjay et al. [43], Goktun et al. [44] and Mcdonald et al. [45]. Bhargava [46] and Sanjay et al. [47].

They studied the cooled gas turbines by using the coolant that prevents overheating, that damages the turbine blades, and allows for higher TIT leading to a better performance by the system. The effect of blade cooling on the performance of the system was investigated by Horlock [48], Young [49], Sanjay et al [50] and Hwan Kwon [51]. Moreover, the effect of air film cooled gas turbines and the longer lives of the turbine blades achieved by maintaining the blade temperature below a certain value were studied by Sanjay et al. [52] and Young et al. [53].

2.5. Exergoeconomic Approach

Researchers started to adopt a relevant new approach called the exergoeconomic analysis because the environmental effect and the cost of the power plant have been as important as its thermal efficiency recently.

The main idea behind exergoeconomic analysis is that it combines economic concepts with thermodynamic principles from the second law of thermodynamics point of view to analyze gas turbine power plants. This aids in determining the total cost of the power plant and to the manner of improving the performance of the system by knowing critical information about the system performance and its economic variables.

A great improvement in this research area has started during the late eighties and nineties where the CGAM problem [54] was introduced. It was a simple gas turbine with a cogeneration energy system named after the initials of the researchers investigated the topic namely C. Frangopoulos [55], G. Tsatsaronis [56], A. Valero [57] and M. von Spakovsky [58].

Several exergoeconomic analyses were conducted by a lot of researchers during recent years. Sahoo [59] performed an exergoeconomic analysis for a cogeneration power plant. He optimized it by using a programming methodology. The results indicated that the cost of electricity and product cost is 9.9% lower in comparison to the base case. A 10% increase in capital investment were also noticed along 3.23 years of payback period. This shows a promising potential in the author’s work of

optimization a cogeneration power plant. An innovative thermoeconomic concept called the “wonergy” was introduced by Kim [60]. For validation, he applied it to the CGAM problem. He categorized the exergoeconomics into three fields: cost analysis, cost allocation and cost optimization where he developed one equation in each field to be used as an evaluation for any energy. He defined the wonergy as an energy that can equally evaluate the worth of each product.

Vandani et al. [61] investigated the environmental impact along the energy and exergy of natural gases. Bakhshmand et al. [62] used an evolutionary algorithm to assess and optimize a triple pressure combined cycle power plant where they conducted an exergoeconomic analysis.

The results showed that optimization process improved the energetic and exergetic efficiencies by 3 % and decreased the costs by 9%. Additionally, the specific cost of product of the plant is reduced from 21.48 (€/h) for the base case to 20.90 (€/h) for the optimum case leading to a 3% reduction in the specific cost of product.

Cooling the inlet air is usually accompanied by improvement in the gas turbine efficiency and performance**.** The reduction in the compressor inlet temperature will increase the density of air leading to an increase in the mass flow rate. Marzouk and Hanafi [63] assessed a gas turbine with inlet air cooling by conducting an exergoeconomic analysis. They studied the chiller cooling and evaporative cooling economically and thermally for a 264 MW gas turbine plant located at Korymat, southern Egypt. The results showed that the annual power gained by evaporative cooling is 86,118 MW with a net cash flow of $4,503,548. As for the chiller cooling, the annual power gained was 117,027 MWh with a net cash flow of $3,787,537.

In case of coal fired power plants, Xiong et al. [64] optimized it thermoeconomically. They adopted two optimization strategies, local optimization and global optimization, to reduce the total annual cost of the plant. The results indicated a 2.5% reduction in the total annual cost and a 3.5% decrement in the total investment cost. Seyyedi et al. [65] developed a new approach for thermal power plants optimization thermoeconomically by applying it to the CGAM problem. The proposed methodology involved the determination of the sum of the investment and exergy destruction cost flow rates for each component, and sensitivity analysis to study the

importance of each decision variable and structural optimization method which is applied to minimize the total cost flow rate, respectively. Karaali and Oztürk [66] developed a new thermoeconomic optimization method by improving a thermoeconomic analysis method that is called non-linear simplex direct search method. The method was applied to four cogeneration cycles that are air-fuel preheated simple cycle, inlet air cooling cycle and air preheated.

The optimum electricity costs were 0,0432 $/kWh for simple cycle, 0,0514 $/kWh for inlet air cooling cycle, 0,0577 $/kWh for air preheated cycle and 0,058 $/kWh for air-fuel preheated cycle. Ahmadi et al. [67] focused on the optimization of combined cycle power plants from the exergoeconomic and environmental point of view.

The three main objectives of the optimization were the CO2 emissions of the overall plant, the combined cycle power plant exergetic efficiency and the total cost rate of the system products. By integrating the environmental impact in terms of CO2 emissions with the exergoeconomic, a new objective function was added.

The exergy and exergoeconomic analyses results showed that the largest exergy destructions occur in the combined cycle power plant combustion chamber. A reduction in the combined cycle power plant cost of exergy destruction could be obtained by increasing the gas turbine inlet temperature. Moreover, using a low fuel injection rate into the combustion chamber and choosing the appropriate components will reduce the CO2 emissions.

In the area of exergoeconomic analysis for air film blade cooling, Sahu and Sanjay [68,69,70,71,72] conducted an exergoeconomic analysis for a basic and reheated gas turbine cycle, basic and combined gas turbine cycle, basic and intercooled gas turbine cycle, basic and intercooled recuperated gas turbine cycle, and the power utilities of a basic gas turbine cycle, where all of them were integrated with air film blade cooling.

In [68], where a comparative exergoeconomic analysis of basic and reheat gas turbine with air film blade cooling was conducted, the comparative results showed a total cost rate of 20.172 $/h and 29.156 $/h, plant specific work equal to 422.49 kJ/kg

and 576.40 kJ/kg for basic and reheat gas turbine cycle-based power utility and cost of electricity equal to 3.31 cents/kWh and 3.45 cents/kWh, and respectively.

In [69], where a comparative exergoeconomics of power utilities of an air-cooled gas turbine cycle and combined cycle configurations was conducted, the results showed that the combined cycle-based utility showed higher exergy efficiency of 21.16% in comparison to basic gas turbine-based utility with a higher cost of electricity 13.3% which is nearly equal to 3.32 cents/kWh.

Moreover, the combined cycle will develop 21% higher power output equivalent to 48.71 MW in case of a 4.47 % higher total cost rate. The results obtained in the thermoeconomic investigation of basic and intercooled gas turbine incorporating air-film blade cooling [70] showed that the total cost rate of Intercooled gas turbine cycle is a little higher in the base case parameters, compared to the basic gas turbine while delivering lower electricity cost 2.872 cents/ kWh. Additionally, the Intercooled gas turbine-based power utility produces about 40% higher plant specific work where it requires 47.34% higher fuel during operation.

In [71], a thermoeconomic investigation of power utilities of an intercooled recuperated gas turbine cycle featuring cooled turbine blades was conducted. The results showed that the related cost of electricity is 20% lower, and the total cost rate is 16.33% higher for Intercooled Recuperated gas turbine in comparison to basic gas turbine for same operating parameters. Results also showed a 50% higher plant specific work as well as a 27.8% higher fuel flow rate in case of Intercooled Recuperated gas turbine as compared to basic gas turbine.

The results for the base case in the exergoeconomic investigation of power utility based on air film blade cooled gas turbine cycle [72] showed energy efficiency equal to 40.26%, total cost rate of 19.64 $/h, electricity cost of 2.97 cents/kwh and a plant specific work of 433.89 kJ/kg.

As it can be seen from the literature survey, the factors that affect the designe and performance of gas turbine power plants have changed along the past years. Nowadays, the cost of gas turbine power plants and their environmental effects have been considered as important as the thermodynamic performance during their design and operation. Exergoeconomic analysis combines energy analysis and economic

evaluation of energy system which are crucial to design and cost-effective operation of the energy system. Exergoeconomic analysis usually includes cost analysis, thermodynamic performance improvement and optimization of energy systems. Crucial information that helps in foreseeing the thermodynamic performance along many economic variables related to power plants are acquired from the exergoeconomic analysis.

Chapter 3. Research Methodology and System Configurations

This chapter is devoted to the formulation of the problem of deficiencies in cooling system techniques for gas turbine power plants and the manner through which they can be addressed appropriately.

3.1. Problem Formulation

Hot and humid climates of Gulf countries have always been a challenge for researchers and scientists during their continuous work for a better gas turbine performance. Cooling systems were developed to overcome the drawbacks of hot and humid climates which negatively affect the performance of the gas turbine. Either inefficient cooling systems or costly ones are the available options in Gulf countries.

Evaporative cooling is most suited for hot dry areas as it uses the latent heat of vaporization to cool ambient temperature from the dry-bulb to the wet-bulb temperature. However, it has limited potential in regions of high summer humidity [73]. As for the high-pressure fogging, in spite of the fact that it has a substantially higher cooling potential than evaporative cooling, the requirement for demineralized water expands the complexity and capital cost of the system [74]. Furthermore, the high water requirements, being up to five times that of evaporating cooling [75], makes it a poor choice. Absorption chillers can perform very well in countries with ambient air temperature above 40°C since aqua-ammonia absorption chillers can reduce inlet air temperatures to around 10°C [76] with an online power increase of almost 20% for simple-cycle CT, and a lesser value for combined-cycle CT. However, the systems have high capital costs, and are complex to install and maintain. As for the turbine blade cooling techniques, the amount of air bled from the compressor to cool down the turbine blades presents a penalty on the efficiency of the system, reducing the performance of the gas turbine power plants.

3.2. Research Methodology

The research strategy depends on two main factors that affect the performance of the gas turbine: inlet air cooling and turbine blade cooling. A novel cooling system was developed to overcome the drawbacks of inlet air cooling and turbine blade cooling. Three different configurations of gas turbine were adopted to investigate the effect of the Maisotsenko-desiccant cooling systems on their performance.

3.3. System Configurations

The performance of three different configurations of gas turbine will be studied after being integrated with the Maisotsenko-desiccant cooling systems. The first configuration is the simple gas turbine shown in Figure 2. The main idea behind this principle is that a cooling fluid line is taken from the compressor exit at state 2 which will get mixed with the hot combustion gas at the combustion chamber exit at state 3 in order to maintain the temperature at acceptable levels, before entering the turbine at state 4. The coolant line will act as the turbine blade cooling where a specific temperature will be maintained in order to avoid thermal stresses and oxidation rates that might occur due to very high temperatures. In other words, in order to prevent the temperature of the blades from bypassing a specified limit when exposed to a mass flow of hot combustion gases at combustor exit temperature, it will require a certain mass flow of coolant at temperature of compressor exit.

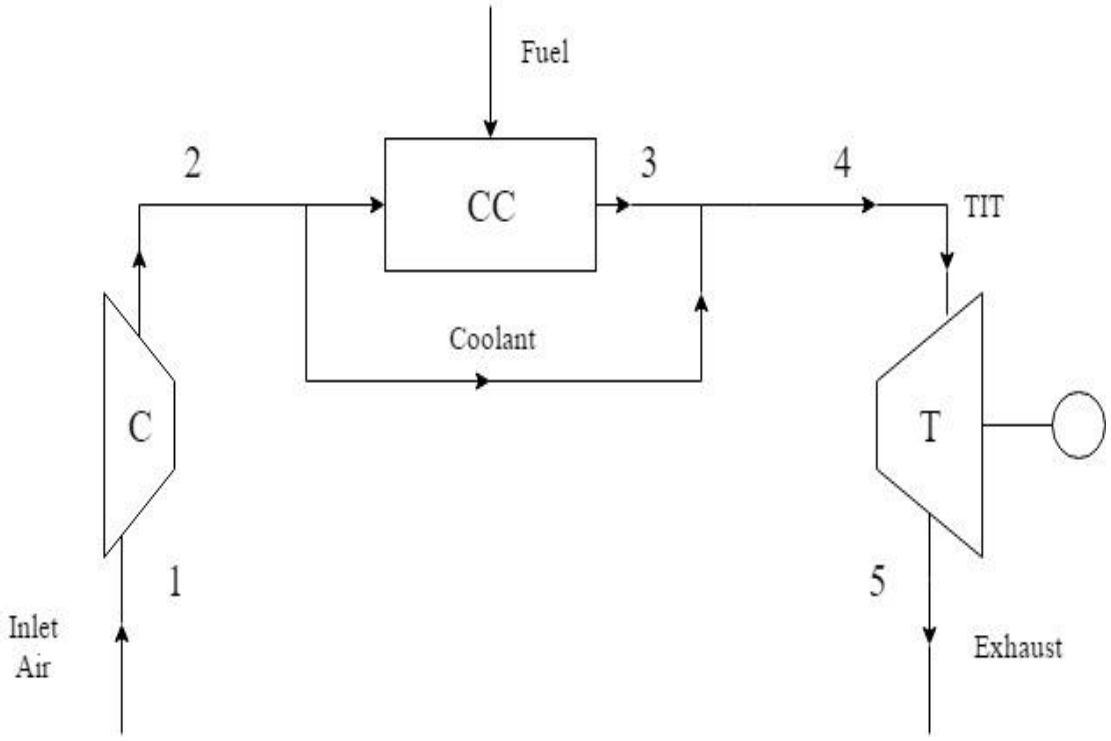

Figure 2: Simple gas turbine

The second configuration is gas turbine with air bottoming cycle (GTABC) shown in Figure 3. During the GTABC cycle, the air passes into the compressor of the top cycle at state 1 to get compressed to a higher temperature and pressure reaching state 2.

Next, it flows into the combustion chamber where fuel is added for a complete combustion process. This will result in fluent gases at very high temperatures which head towards the turbine at TIT. Thermal stress to the turbine blades and shortage in its lifetime are the main outcomes of these high temperature gases (1500 K).

Hence, air is bled from the compressor at state 5, 6 and 7 to cool down the turbine blades in order to prevent them from being damaged. The coolant air cools the turbine blades internally as it enters the turbine from the blade root by passing through the internal passage inside the hollow blade. An air film is formed over the blade surface which reduces heat transferred to the blade, as the coolant air exits from the leading edge of the blade. Subsequently, the exhaust air at state 4 flows to the bottoming cycle, heating the compressed air from state 10 to reach state 11. Next, air enters the bottoming cycle turbine, expanding in it as the exhaust gases leave the system at state 12.

Additionally, the coolant lines bled from the compressor and the input air to the compressors will be cooled down by the outlet cold air from the cooling systems. Thus, the amount of coolant mass flow rate required to be bled to cool down the turbine blades will be reduced, decreasing the penalty on thermal efficiency, which will improve the performance of the gas turbine and the overall efficiency of the system.

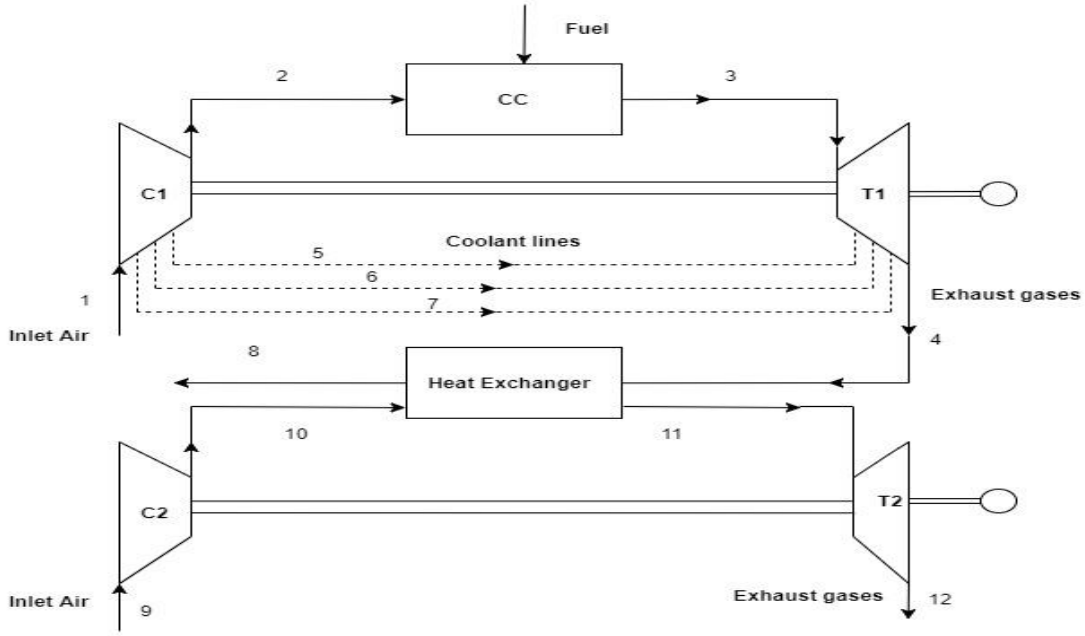

Figure 3: GTABC incorporating turbine blade cooling

The third and last configuration is the intercooled, reheated and recuperated gas turbine (IcRhRc) shown in Figure 4. The specific net-work of the gas turbine is defined as the difference between the turbine specific work output and the compressor specific work input. Thus, it can be enhanced by increasing the turbine work output or/and decreasing the compressor work input

By utilizing an intercooler for a multi stage compressor and a reheater for a multi stage turbine, the two goals can be achieved. This is based on a simple principle which states that the steady flow compression or expansion work is proportional to the specific volume of the fluid. From this principle came the idea of reheater to make the specific volume as high as possible during the expansion process and the idea of intercooling to make the specific volume of air as low as possible during the compression process. Since the reheater increases the temperature at which heat is rejected and the intercooler decreases the temperature at which head is added, intercooling and reheating will always reduce the thermal efficiency unless they are integrated with a recuperator.

In the intercooled, reheated and recuperated gas turbine cycle, the air at state 1 flows into the low-pressure compressor to get compressed to state 2 where it gets cooled to a lower temperature before being led to the high-pressure compressor to be compressed to state 4.

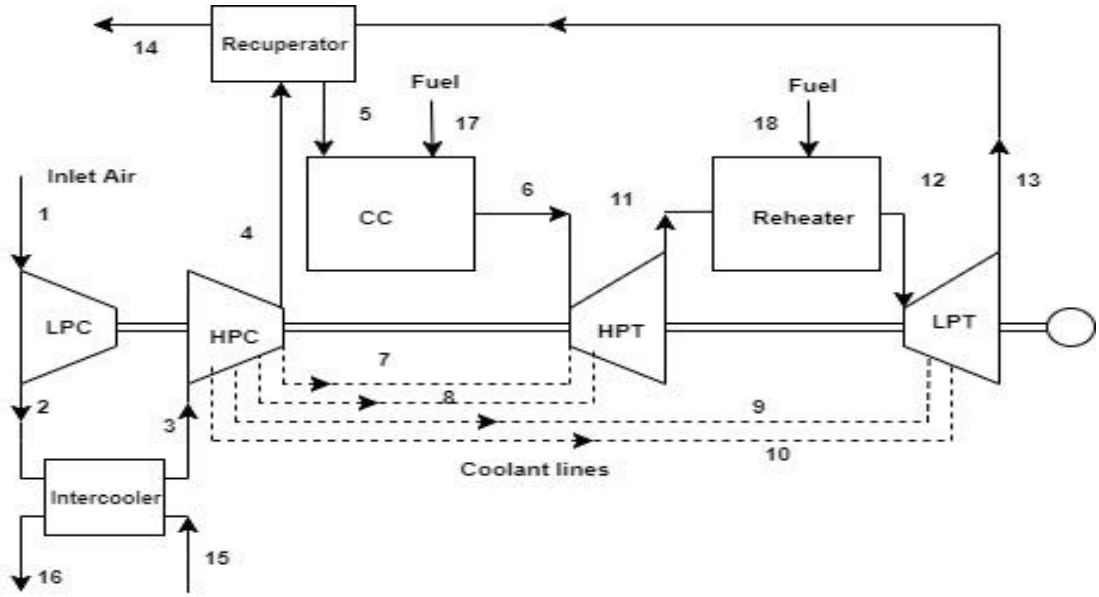

Figure 4: IcRhRc gas turbine cycle

After that, the outlet stream of the low- pressure turbine heats the air after it enters the recuperator reaching state 5. Next, air enters the combustion chamber where a complete combustion takes place. At state 6, the gas enters the high-pressure turbine to expand before being led to the reheater to be reheated reaching state 12. After that, it reaches state 13 after being expanded in the low-pressure turbine. Next, it is led to the recuperator to heat the air coming from the high-pressure compressor. Coolant lines are being bled from the high-pressure compressor to cool down the turbine blades in the high-pressure turbine and the low-pressure turbine.

Different configurations of the Maisotsenko-desiccant cooling system were used to investigate their effect on the performance of the different configurations of the gas turbine. Although there are many configurations for the Maisotsenko-desiccant cooling system, the main working principle is still the same as explained before in Figure 1. For the first configuration of a simple gas turbine, single stage Maisotsenko-desiccant, two-stage intermediate Maisotsenko desiccant, two-stage precooled Maisotsenko desiccant and two-stage recovered Maisotsenko desiccant cooling systems were implemented as they are shown in Figures 1, 5, 6 and 7, respectively.

The gas turbine with air bottoming cycle and the intercooled, reheated and recuperated gas turbine second and third configurations utilized the triple-stage Maisotsenko desiccant, triple-stage precooling Maisotsenko desiccant and triple-stage extra cooling Maisotsenko desiccant cooling systems as they are shown in Figures 8, 9 and 10, respectively.

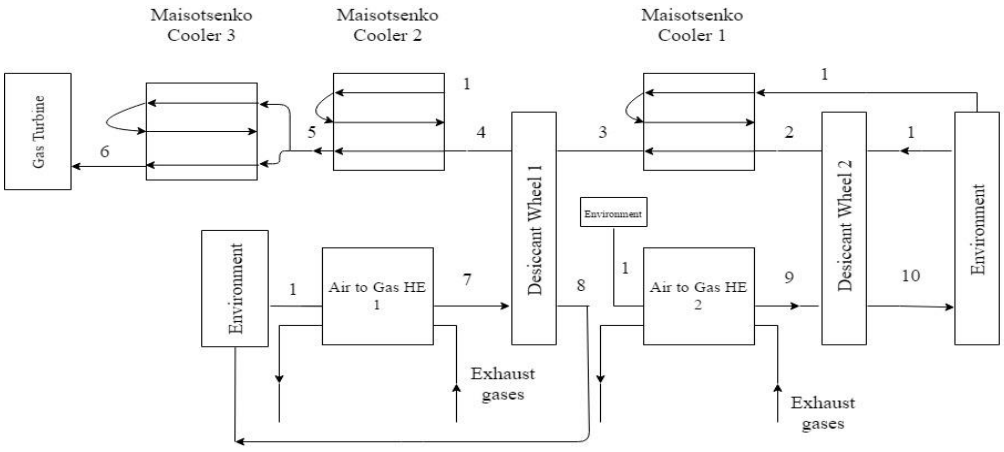

Figure 5: Two-stage intermediate Maisotsenko-desiccant (TS-IMD)

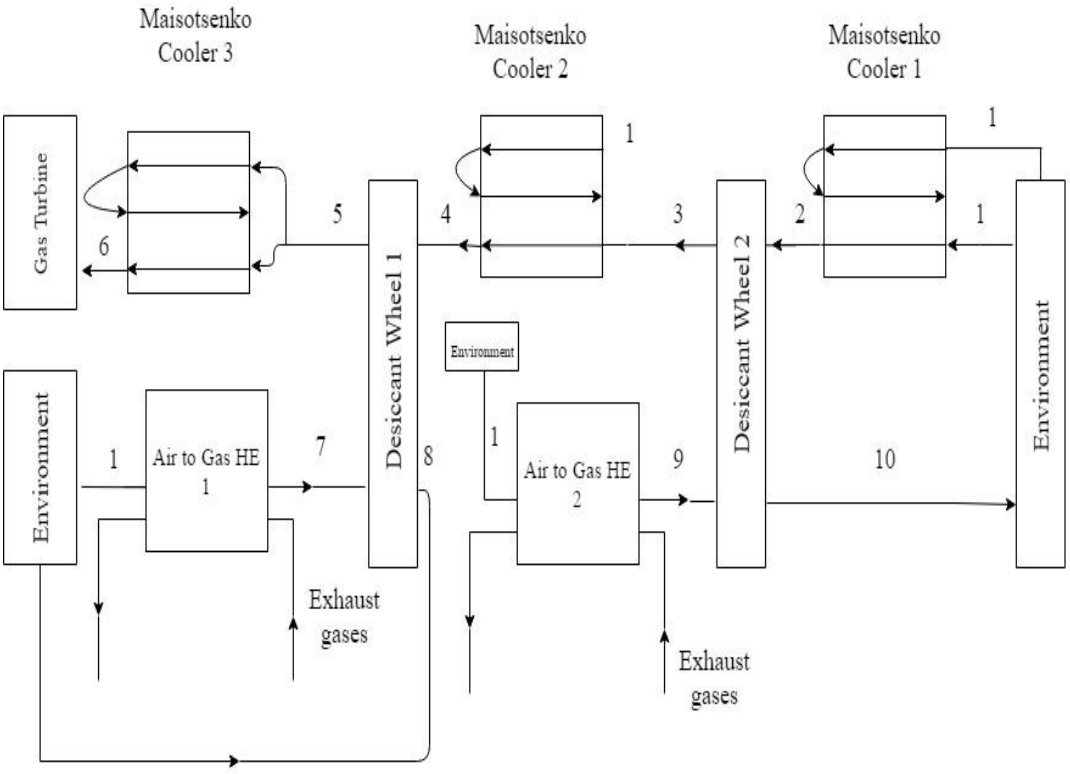

Figure 6: Two-stage precooled Maisotsenko-desiccant (TS-PMD)

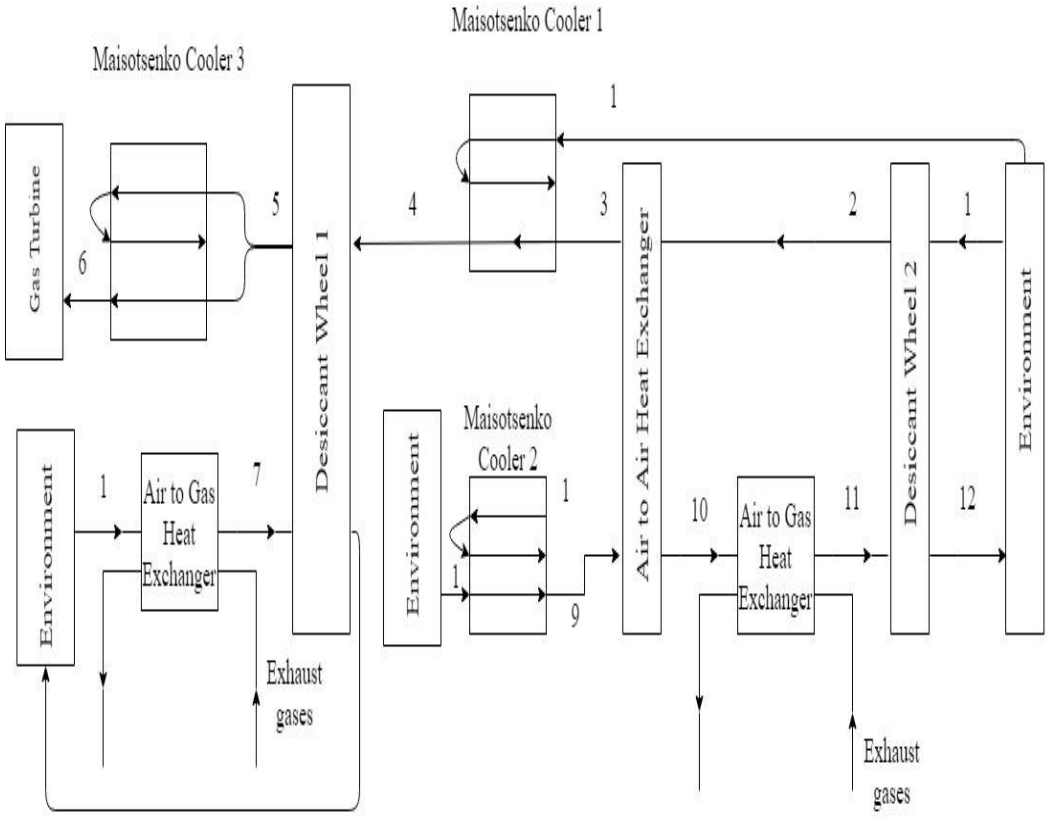

Figure 7: Two-stage recovered Maisotsenko-desiccant (TS-RMD)

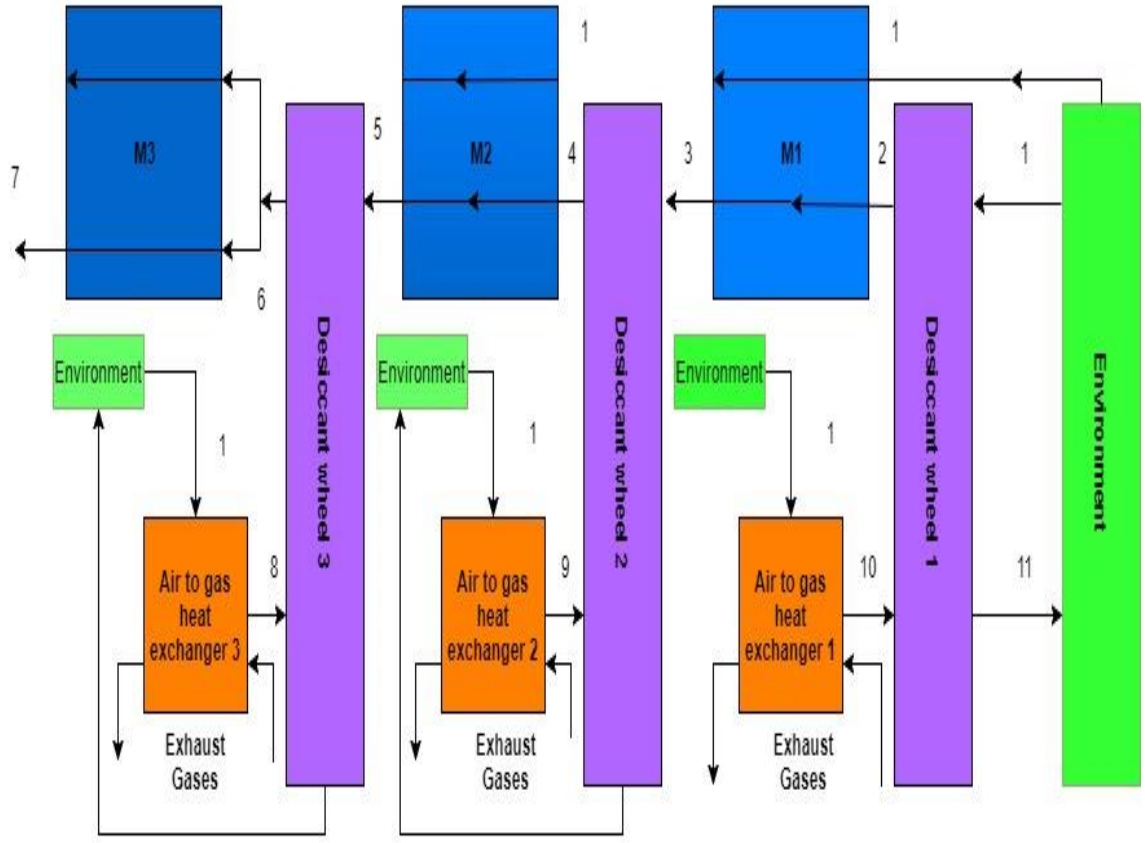

Figure 8: Triple-stage Maisotsenko-desiccant (TS-MD)

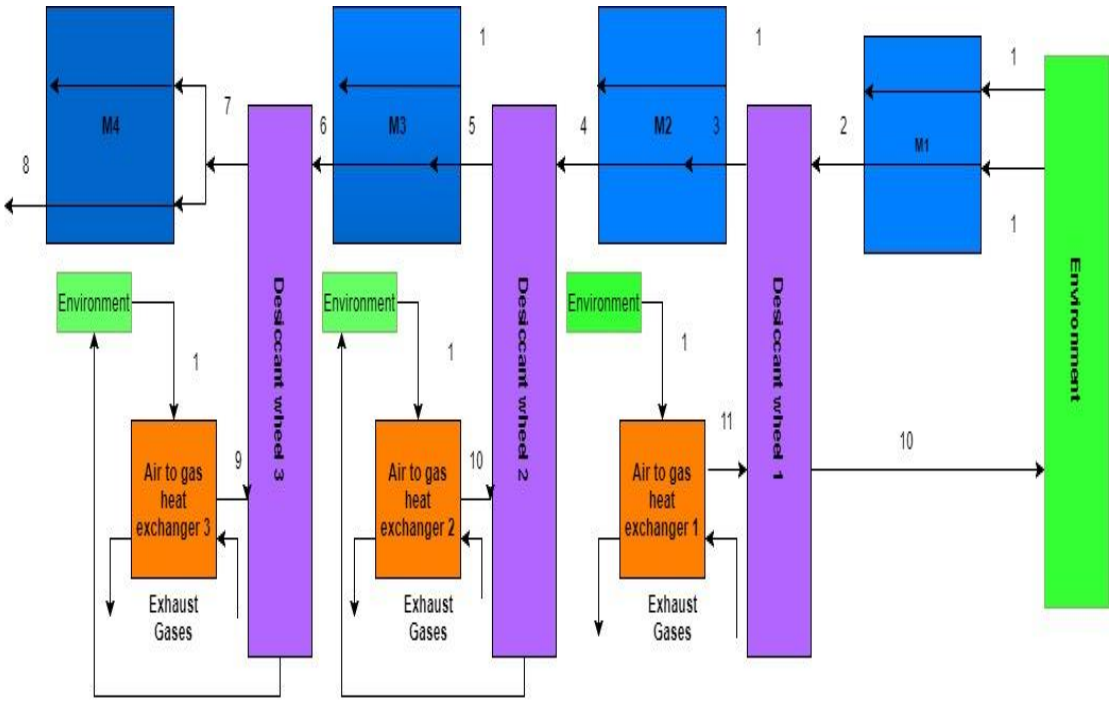

Figure 9: Triple-stage precooling Maisotsenko-desiccant (TS-PMD)

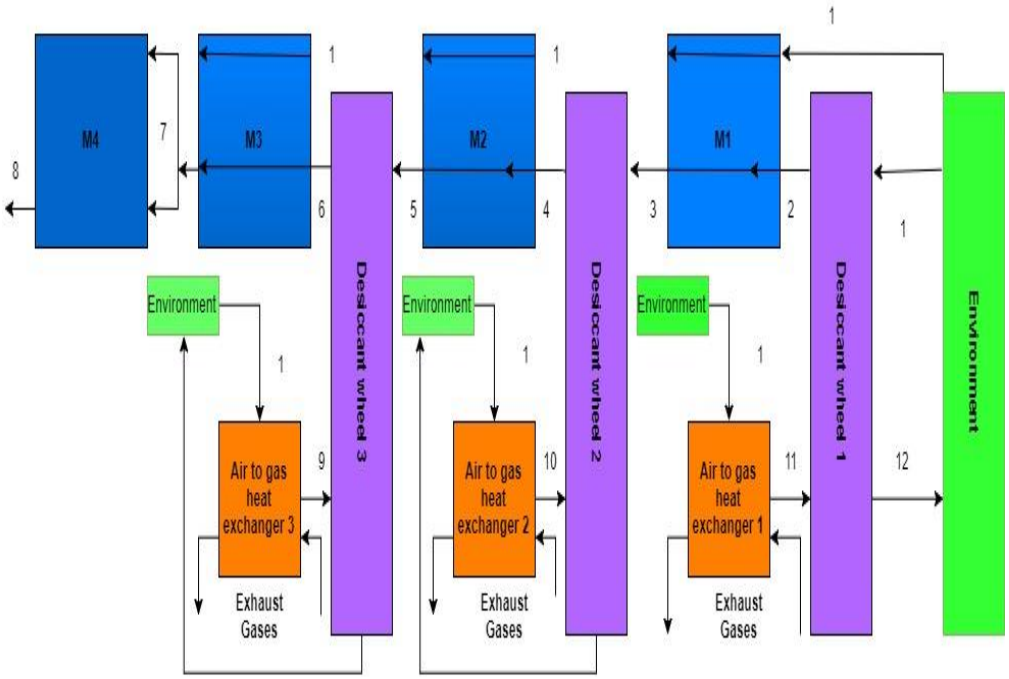

Figure 10: Triple-stage extra cooling Maisotsenko-desiccant (TS-EMD)

Two examples of the two-stage and triple-stage configurations will be described to give insight of how the system works. From the two-stage configurations, the (TS-IMD) shown in Figure 5 will be clarified. In the upper air stream, ambient air is heated and dehumidified from state 1 to state 2 in desiccant wheel 2.

Afterwards, the desiccated air is cooled down to the ambient air dew point temperature reaching state 3 as it enters the product channel of Maisotsenko cooler 1. Next, the cooled air at state 3 flows into desiccant wheel 1, getting dehumidified and heated to state 4. The air at state 4 gets cooled to the ambient air dew point temperature reaching state 5 as it enters the product channel of Maisotsenko cooler 2. Finally, the air is divided into two equal streams and enters Maisotsenko cooler 3 where it gets cooled to its dew point temperature before going to the gas turbine.

In the lower air stream, ambient air is heated from state 1 to 7 and from 1 to 9 in the air to gas heat exchanger. Next, the heated air streams flow through the desiccant wheels 1 and 2 for regeneration purposes from state 7 to 8 and from 9 to 10 and are then released to the environment. From the triple-stage configurations, the (TS-MD) displayed in Figure 8 will be explained. The air streams in the cycle cab be divided into two types; first, there is the (upper stream) processed air that gets heated and dehumidified from state 1 to 2 in desiccant wheel 1. Next, the desiccated air goes into

the product channel of Maisotsenko cooler 1 where it is cooled to the ambient air dew point temperature reaching state 3. Following that, air enters desiccant wheel 2 to get dehumidified even further to state 4.

Afterwards, the air gets cooled down as it enters Maisotsenko cooler 2 before in going into desiccant wheel 3 for dehumidification reaching state 6. Following that, air stream is split into two equal streams. One of the streams will enter the product channel of Maisotsenko cooler 3 where it gets cooled down to the dew point temperature of the air in the working channel reaching state 7, which will be used for cooling purposes for the gas turbine, while the other stream will go into the working dry channel of Maisotsenko cooler 3. The second type of air stream in the system is the (lower stream) regeneration air. This type of air is used to increase the vapor pressure on their surface so that it surpasses the surrounding air pressure, helping the desiccants regain their moisture removal potential in a process known as regeneration. This is achieved as it flows into the desiccants, after being heated in air to gas heat exchangers by the exhaust gases from the gas turbine.

Chapter 4. Mathematical Formulation

This chapter will address the main mathematical equations and the exergoeconomic model developed for the analysis of the gas turbine and the integrated Maisotsenko-desiccant cooling system.

4.1. Simple Gas Turbine (First Configuration)

The gas turbine model specification is shown in Table 1. The turbine inlet temperature (TIT) is fixed at 1500°K, the blade temperature at 1133°K, the temperature at combustion exit at 1698°K and the power output is designed to be of 50 MWe. Pressure ratio of 17 was chosen with pressure loss of 10mbar at the compressor inlet and the turbine exit as well. The mechanical efficiency is 99.6% while the combustion chamber efficiency is 98%.

Table 1: First gas turbine model specification

Parameter	Assigned value
Net power output (MWe)	50
Combustion chamber efficiency (%)	98
Combustion chamber pressure drop (%)	3
Pressure loss at turbine exit (mbar)	10
Turbine polytropic efficiency (%)	85
Turbine inlet temperature (K)	1500
Blade temperature (K)	1133
Reference temperature (K)	298
Mechanical efficiency (%)	99.6
Compressor polytropic efficiency (%)	91.5
Compressor pressure ratio	17
Pressure loss at compressor inlet (mbar)	10
Temperature combustion chamber exit (K)	1698

In all three models, it is assumed that specific heat of gas varies with temperature only in the form of polynomials given as:

$$c_p = a + bT + cT^2 + dT^3 \tag{4.1}$$

where, *a*, *b*, *c* and *d* are coefficient of polynomials, values of which are taken from the work of Touloukian and Tadash [78]

The relation between the mass flow rate of coolant and the mass flow rate of gas can be deducted from [24,79]

$$\frac{\dot{m}_c c_{p,c}}{\dot{m}_g c_{p,g}} = b\left(\frac{T_3 - T_b}{T_b - T_2}\right)^s \tag{4.2}$$

where (*b*) is the cooling model parameter that replaces the constant ($\alpha = \frac{A_Q}{A_c}$), (*St*) which is the Stanton number and the cooling efficiency. The (*s*) value ranges from 1 to 2 where 1 denotes the convective cooling. (*s*) represents the impact of the hot gas inlet temperature. ($c_{p,c}$) and ($c_{p,g}$) are the specific heat capacities of the coolant and the hot gas respectively. ($\dot{m}_c$) is the coolant mass flow rate and the ($\dot{m}_g$) is the gas mass flow rate. ($c_{p,c}$) and ($c_{p,g}$) are calculated at the average values between the blade temperature (T_b) and the compressor exit (T_2) and combustor exit temperatures (T_3), respectively.

A reduction in the momentum of the hot gas takes place due to the mixing of the cooling fluid with the hot gas path, as the cooling fluid has to be accelerated to the speed and direction of the hot gas. Equation (4.3), which is a momentum balance for the mixing, is used to expressas the pressure loss for the hot gas. The pressure loss can be converted to a reduction of the turbine polytropic efficiency or added to the combustor pressure loss. Equation (4.4) relates the pressure drop to the loss of polytropic efficiency. Equation (4.5) defines the efficiency loss ($\Delta\eta$).

$$\frac{\Delta P}{P_4} = -\frac{\dot{m}_c}{\dot{m}_g} K_g {M_g}^2 \zeta \qquad (\Delta P < 0) \tag{4.3}$$

$$\frac{\eta_{p,uc,t} + \Delta\eta}{\eta_{p,uc,t}} = \frac{\ln(\frac{P5}{P4})}{\ln(\frac{P5}{P4 + \Delta P})} \tag{4.4}$$

$$\eta_{p,c,t} = \eta_{p,uc,t} - \Delta\eta \qquad \Delta\eta > 0 \tag{4.5}$$

The mixing loss factor (ζ) accounts for the direction in which the cooling fluid is injected into the hot gas flow. It is equal to unity If the injection is perpendicular to the hot gas flow. Parameter (K) summarizes the Mach number (Mg), the heat capacity ratio (K_g) and (ζ). For most air gas turbines, (K_g)is about 1.3 and (Mg) is 0.6-0.8. A rough estimate gives (ζ) as 0.3-0.6. Hence, (K) should be in the range 0.15-0.5 approximately [24].

In the proposed cooling model, no dissociation and complete combustion were assumed. Furthermore, the cooling fluid is mixed with the combustor exit gas at state (3) before the turbine inlet at state (4). Hence, the whole thermodynamic mixing loss is taken at the turbine inlet. Thus, in comparison to a real turbine, the mixing losses are overestimated, where in real turbines, the mixing occurs at a much smaller temperature difference. Assuming that the temperature at the combustor exit (T_3) is 1698°K helps in calculating the required temperature (T_{req}) of the coolant line needed in order to maintain the temperature at the turbine inlet (TIT=T_4) equal to 1500°K as follows

$$\dot{m}_g h_3 + \dot{m}_c h_{req} = (\dot{m}_g + \dot{m}_c) h_4 \tag{4.6}$$

4.2. Gas Turbine with Air Bottoming Cycle (Second Configuration)

The gas turbine specifications are presented in Table 2. The turbine inlet temperature (TIT) is 1500°K, the blade temperature at 1150°K and the power output is designed to be 50 MWe. Pressure ratio of a range between 4-8 for the bottom cycle and range of 14-24 for the top cycle were chosen to represent the gas turbine performance, with heat exchanger pressure drop and combustion chamber pressure drop of 2%.

In this model, the compressor work is calculated as follows:

$$\dot{W}_c = \dot{m}_e . h_e + \sum \dot{m}_{coolanT,j} . h_{coolant,j} - \dot{m}_\iota . h_i \tag{4.7}$$

where ($h_{coolant,j}$) is the corresponding enthalpy and ($\dot{m}_{coolanT,j}$) is the coolant mass flow rate extracted from the compressor.

The relation between the mass flow rate of coolant and the mass flow rate of gas can be deducted from [23] as:

$$\frac{\dot{m}_c}{\dot{m}_g} = \frac{c_{pg}(T_{g,i} - T_b)}{c_{p,coolant}(T_b - T_{coolant,i})} * \frac{S_{t,i} . S_g . F_{sa}}{\in_{cool} . t . cos\alpha} * (1 - \eta_{iso,air}) \tag{4.8}$$

where, $(S_g.F_{sa}/t.cos\alpha)$ indicates the turbine blade geometry, $(\eta_{iso,air})$ is the isothermal effectiveness and (S_t) is the Stanton number.

The turbine work is calculated by:

$$\dot{W}_T = \sum \dot{m}_{coolanT,j}\,.\,h_{coolant,j} + \dot{m}_i.h_i - \dot{m}_e.h_e \tag{4.9}$$

Pinch analysis was used to formulate the air to air heat exchanger in the gas turbine cycle. The pinch point is located at the hot stream entry and the cold stream exit, where the minimum temperature difference between the hot and cold streams occurs [21], If the heat capacitance of the hot stream is greater than the heat capacitance of the cold stream. In that case the following equations can be used:

$$T_{o,cs} = T_{i,hs} - \Delta T_{pinch} \tag{4.10}$$

$$T_{o,hs} = T_{i,hs} - \frac{\dot{m}_{a,bot}.c_{pa}.(T_{o,cs} - T_{i,cs})}{\dot{m}_g.c_{pg}} \tag{4.11}$$

While in the other case, where the heat capacitance of the cold stream is greater, the following equations are implemented:

$$T_{o,hs} = T_{i,cs} - \Delta T_{pinch} \tag{4.12}$$

$$T_{o,cs} = T_{i,cs} - \frac{\dot{m}_g.c_{pg}.(T_{o,hs} - T_{i,hs})}{\dot{m}_{a,bot}.c_{pa}} \tag{4.13}$$

where $(T_{i,hs})$, $(T_{i,cs})$, $(T_{o,cs})$ and $(T_{o,hs})$ are the hot and the cold fluid streams inlet and exit temperatures in K. $(\dot{m}_{a,bot})$ is the bottoming cycle air mass flowrate in kg/s and (ΔT_{pinch}) is the designed pinch temperature difference in K.

The net power of the gas turbine cycle can be calculated using:

$$\dot{W}_{Net} = \dot{W}_{Net,top} + \dot{W}_{Net,bot} \tag{4.14}$$

$$\dot{W}_{Net,top} = \dot{m}_3 h_3 - \dot{m}_4 h_4 - \dot{m}_2 h_2 + \dot{m}_1 h_1 \tag{4.15}$$

$$\dot{W}_{Net,bot} = \dot{m}_{a,bot}(w_{t,bot} - w_{c,bot}) \tag{4.16}$$

The mass flow rate ratio can be calculated by:

$$MFFR = \frac{\dot{m}_{a,bot}}{\dot{m}_{a,top}} \tag{4.17}$$

To calculate the topping cycle mass flow rate, the following equation was developed:

$$\dot{m}_{a,top} = \frac{\dot{W}_{Net}}{\frac{\dot{W}_{Net,top}}{\dot{m}_{a,top}} + MFFR.(w_{t,bot} - w_{c,bot})} \quad (4.18)$$

where $(w_{t,bot})$ and $(w_{c,bot})$ are the bottom cycle turbine and compressor specific work in kJ/kg, respectively.

Table 2: Second gas turbine model specifications

Parameter	Assigned value
Net power output (MWe)	50
Combustion chamber efficiency (%)	98
Compressor isentropic efficiency (%)	85
Generator efficiency (%)	98.5
Fuel low heating value (kJ/kg)	42000
Turbine inlet temperature (K)	1500
Blade temperature (K)	1150
Turbine isentropic efficiency (%)	87
Reference temperature (K)	288
Mechanical efficiency (%)	98.5
Topping cycle pressure ratio	14-24
Bottoming cycle pressure ratio	4-8
Heat exchanger pinch temperature (K)	10
Mass flow rate ratio (MFFR)	0-1.2

4.3. Intercooled, Reheated and Recuperated Gas Turbine (Third Configuration)

The gas turbine specifications are presented in Table 3. The turbine inlet temperature (TIT) is 1500°K, the blade temperature is 1150°K and the power output is designed to be at 50 MWe.

Pressure ratio of 20 was chosen after optimization. Pressure loss of 2% was chosen for the intercooler, recuperator and combustion chamber. The mechanical efficiency is 98.5% and the combustion chamber efficiency is 98%.

4.3.1. Thermodynamic analysis. Assumptions for the model can be summarized as follows:

1- Ideal gas mixtures principles apply for the air and the combustion products.

2- Pressure drop in the combustion chamber is 2% of the entry pressure.

3- The system operates at steady state and the pressure loses due to friction in pipelines are neglected.

5- The dead state or the reference environment chosen for this study is 288 K and 1 bar.

6- At the reference environment, the air is assigned zero entropy, enthalpy and exergy.

7- The inlet air streams have the same chemical composition as the ambient.

8- The fuel is natural gas and complete combustion is assumed in the CC.

In this model, the equations used for the compressor work, turbine work and the relation between the mass flow rate of coolant and the mass flow rate of gas are similar to the previous configuration.

The enthalpy, entropy and exergy can be calculated by:

$$h = \int_{T_0}^{T} C_p(T)dT \tag{4.19}$$

$$s = \int_{T_0}^{T} C_p(T)\frac{dT}{T} - Rln(\frac{p}{p_0}) \tag{4.20}$$

$$E = h - T_0 * s \tag{4.21}$$

where (s) is the specific entropy kJ/kgK, (h) is the specific enthalpy in kJ/kg, and (E) is the specific exergy kJ/kg.

The net power of the gas turbine cycle can be calculated using:

$$\dot{W}_{Net} = \dot{W}_{Net,Turbine} - \dot{W}_{Net,Compressor} \tag{4.22}$$

$$\dot{W}_{Net,Turbine} = \dot{W}_{HPT} + \dot{W}_{LPT} \quad (4.23)$$

$$\dot{W}_{Net,Compressor} = \dot{W}_{HPC} + \dot{W}_{LPC} \quad (4.24)$$

Table 3: Third gas turbine model specification

Parameter	Assigned value
Pressure ratio	20
Combustion chamber efficiency (%)	98
Combustion chambers pressure drop (%)	2
Compressor isentropic efficiency (%)	85
Fuel low heating value (kJ/kg)	42000
Turbine isentropic efficiency (%)	87
Net power output (MWe)	50
Intercooler pressure drop (%)	2
Recuperator pressure drop (%)	2
Blade Temperature (K)	1150
Turbine inlet temperatures (K)	1500
Inlet pressure (bar)	1
Inlet temperature (K)	288
Mechanical efficiency (%)	98.5
Generator efficiency (%)	98.5
Reference temperature (K)	288

4.3.2. Exergoeconomic analysis. With the constant increase in the quality of life, the demand for electricity has risen. This has put pressure on the health of the environment and on our finite resources. Thus, it is only rational to look for efficient conversion systems. In the field of electricity generation, gas turbine power plants can be considered as the prime candidate with more feasibility, lower capital cost, simpler design, compact size and higher efficiency compared to steam turbine power plants.

The factors that affect the designing and performance of gas turbine power plants have changed along the past years. Nowadays, the cost of gas turbine power plants and their environmental effects have been considered as important as the thermodynamic performance during their design and operation. Moreover, the increased competition in the energy market has drawn the attention in recent years to the exergoeconomic analysis. Therefore, researchers started to adopted exergoeconomic analysis to assess gas turbine power plants, using thermodynamic principles from the second law of thermodynamics point of view and the economic concepts as well. In other words, exergoeconomic analysis combines energy analysis and economic evaluation of energy systems which are crucial to design and cost-effective operation of the energy system. Exergoeconomic analysis usually includes cost analysis, thermodynamic performance improvement and optimization of energy systems. Crucial information that helps in foreseeing the thermodynamic performance along many economic variables related to power plants are acquired from the exergoeconomic analysis.

Performing the exergy analysis of the cycle is considered as the first step to execute an exergoeconomic analysis. Exergy analysis detects thermodynamic irreversibilities present within a system by determining their location, magnitude and source. The information obtained from exergy analysis can help improve the cost effectiveness of a system and the general productivity as well. The exergy of each stream of a cycle can be obtained by an exergy analysis. Moreover, it provides information about the exergy destruction and the exergetic efficiencies for each component in the cycle. The product and fuel exergy of each component are determined based on exergy of each stream.

Fuel exergy is defined by the resources used to produce the desired result while the product exergy is the desired outcome of the component. The product and fuel exergy of components are used to determine the exergy destruction and exergetic efficiencies using the upcoming equations:

$$\text{Exergy destruction ratio} = \frac{\dot{E}_D}{\dot{E}_{D\,Total}} x100 \qquad (4.25)$$

$$\in = \frac{\dot{E}_P}{\dot{E}_F} x100 \tag{4.26}$$

4.3.2.1. Economic model. The cost of the final product is considered to be one of the most important factors affecting the selection of a design option for a thermal system. The effective assessment of a gas turbine power plant requires the estimation of the major costs expended. In order to calculate the total cost of the cycle, the sources of cost should be identified first. Typically, the total cost consists of the capital investment in purchasing the equipment, operating & maintenance cost and the fuel used. Cost functions for equipment purchase cost (Z) are shown in Table 4 and Table 5 [84].

In contrast to fuel costs, operation costs and maintenance costs which are continuous by nature, investment cost is a one-time cost. However, we are going to include operation and maintenance costs with the total capital investment for simplicity. Usually, the total capital investment consists of fixed capital investment and other outlays. The fixed capital investment includes direct costs such as purchased equipment costs, purchased equipment installation, piping, electrical equipment, materials and service facility. Additionally, it includes some indirect costs depicted by construction costs and supervision. The other outlays may include start-up costs, working capital, costs of licensing, research and development and allowance for funds used during construction. Operation and maintenance costs can be divided into fixed and variable costs. Fixed operation and maintenance costs include costs for operating labor, maintenance labor, maintenance materials, administration and support, distribution, marketing and research and development. The variable operating costs depend on the average annual system capacity factor.

The equation that defines the total capital investment by considering the maintenance and operating cost parameters for the Kth component is described as:

$$\dot{Z_k} = \frac{Z_k * CRF * \varphi}{N} \tag{4.27}$$

Where (N) shows the number of plant operation in hour annually (N= 8000 h), (φ) indicates maintenance factor (φ = 1.06), *CRF* is the annual capital recovery factor (*CRF* =18.2%) and (Z_k) is the purchase cost of the kth component ($) [84]. Fuel costs are usually part of the operating and maintenance costs. Nevertheless, fuel costs are going

to be considered separately in this work due to the importance of fuel costs in thermal systems. The fuel cost rate can be calculated by:

$$\dot{C}_f = c_f * \dot{m}_f * LHV \tag{4.28}$$

where (c_f=0.004 \$/MJ) is the fuel cost per energy unit. The total cost rate of operation is the summation of the fuel cost rate and the total capital investment costs as it can be determined by:

$$\dot{C_T} = c_f * \dot{m}_f * LHV + \sum_{k=1}^{n} \dot{Z}_k \tag{4.29}$$

where ($\dot{C_T}$) is the total cost rate of operation and (n) is the number of components.

Table 4: Equations to calculate the purchase cost (Z) for the components

Component	Purchase cost equation
Compressor	$Z_C=(\frac{G_{11}*\dot{m_{a,i}}}{G_{12}-\eta_{AC}})(\frac{P_e}{P_i})ln(\frac{P_e}{P_i})$
Intercooler	$Z_{IC}=G_{51}(\frac{\dot{m_{a,i}}(h_{IC,a,i}-h_{IC,a,e})}{U(\nabla TLM)})^{0.6}$
Recuperator	$Z_{RC}=G_{51}(\frac{\dot{m_{g,i}}(h_{RC,g,i}-h_{RC,g,e})}{U(\nabla TLM)})^{0.6}$
Combustion chamber	$Z_{CC}=(\frac{G_{21}*\dot{m_{a,i}}}{G_{22}-\frac{P_e}{P_i}})(1+\exp(G_{23}*T_e-G_{24})$
Gas Turbine	$Z_{CC}=(\frac{G_{31}*\dot{m_{g,e}}}{G_{32}-\eta_{GT}})ln(\frac{P_i}{P_e})(1+\exp(G_{23}*T_i-G_{24})$

Table 5: Components constants to determine the purchase cost

Component	Constant of the purchase cost equation
Compressor	G_{11}=39.50 \$/kg/s G_{12}=0.9
Intercooler	G_{51}=2290 \$/m^2 U=0.018 kW/(m^2K)
Recuperator	G_{51}=2290 \$/m^2 U=0.018 kW/(m^2K)
Combustion chamber	G_{21}=25.65 \$/kg/s G_{22}=0.995 G_{23}=0.018 K^{-1} G_{24}=26.4
Gas Turbine	G_{31}=266.3 \$/kg/s G_{32}=0.920 G_{33}=0.036 K^{-1} G_{24}=54.4

4.3.2.2. Cost model. The exergy costing approach is used to determine the cost flow rate of streams. The F-P-L (fuel-product-loss) principle has been utilized for the streams cost assigning according to [56]. Once the cost assigning equations are solved, the cost of each stream can be calculated. In some cases, auxiliary equations are needed as the number of variables are usually higher than the available equations developed as mentioned in [85].

The equations governing the cost for different streams are given by [85]:

$$\dot{C}_\iota = c_i * \dot{E}_\iota = c_i(\dot{m}_\iota * \dot{e_\iota}) \tag{4.30}$$

$$\dot{C_e} = c_e * \dot{E}_e = c_e(\dot{m}_e * \dot{e_e}) \tag{4.31}$$

$$\dot{C_w} = c_w * \dot{W} \tag{4.32}$$

$$\dot{C_q} = c_q * \dot{E_q} \tag{4.33}$$

where (c_i), (c_e), (c_w), and (c_q) define the average costs per unit of exergy in dollars per Mega Joule ($/MJ). The aforementioned formulas are too specific. Thus, they can be summarized into one general equation for cost assignment of a component as follows:

$$\sum_e \dot{C_{e,k}} + \dot{C_{w,k}} = \dot{C_{q,k}} + \sum_i \dot{C_{\iota,k}} + \dot{Z_k} \tag{4.34}$$

The auxiliary equations required are given accordingly [86]:

$$\text{Intercooler:} \quad \frac{\dot{C_2}}{\dot{E_2}} = \frac{\dot{C_3}}{\dot{E_3}} \tag{4.35}$$

$$\text{HPC:} \quad \frac{\dot{C_4} - \dot{C_3}}{\dot{E_4} - \dot{E_3}} = \frac{\dot{C_7} - \dot{C_3}}{\dot{E_7} - \dot{E_3}} = \frac{\dot{C_8} - \dot{C_3}}{\dot{E_8} - \dot{E_3}} = \frac{\dot{C_9} - \dot{C_3}}{\dot{E_9} - \dot{E_3}} = \frac{\dot{C_{10}} - \dot{C_3}}{\dot{E_{10}} - \dot{E_3}} \tag{4.36}$$

$$\text{Recuperator:} \quad \frac{\dot{C_{13}}}{\dot{E_{13}}} = \frac{\dot{C_{14}}}{\dot{E_{14}}} \tag{4.37}$$

$$\text{HPT:} \quad \frac{\dot{C_{11}}}{\dot{E_{11}}} = \frac{\dot{C_6} + \dot{C_7} + \dot{C_8}}{\dot{E_6} + \dot{E_7} + \dot{E_8}} \tag{4.38}$$

$$\text{LPT:} \quad \frac{\dot{C_{13}}}{\dot{E_{13}}} = \frac{\dot{C_{12}} + \dot{C_9} + \dot{C_{10}}}{\dot{E_{12}} + \dot{E_9} + \dot{E_{10}}} \tag{4.39}$$

The main equations that govern the thermo-economics of the gas turbine cycle are given by [85]:

Average fuel cost per exergy unit of component:

$$c_{F,k} = \frac{\dot{C_{F,k}}}{\dot{E_{F,k}}} \tag{4.40}$$

Average product cost per exergy unit of component:

$$c_{P,k} = \frac{\dot{C_{P,k}}}{\dot{E_{P,k}}} \tag{4.41}$$

Cost rate of exergy destruction:

$$\dot{C_D} = \dot{E_D total} * c_{F,k} \tag{4.42}$$

Exergoeconomic factor:

$$f_k = \frac{\dot{Z_k}}{\dot{Z_k} + \dot{C_{D,k}}} \tag{4.43}$$

Relative cost difference:

$$r_k = \frac{c_{P,k} - c_{F,k}}{c_{F,k}} \tag{4.44}$$

4.4. Maisotsenko-Desiccant Cooling Systems

The typical Maisotsenko-desiccant cooling system consists of a Maisotsenko cooler, air to air heat exchanger, air to gas heat exchanger and solid desiccant. Maisotsenko cooler combines the thermodynamic processes of heat exchange and evaporative cooling with an indirect evaporative cooler. Its main advantage is that it produces temperatures near the dew point temperature of the working gas. Desiccants can be divided into two main sections: solid and liquid desiccants. Zeolite, silica gel, and alumina silicate are the most used materials for solid desiccants. Additionally, the use of composite materials has been investigated as it decreases the regeneration temperature required as well as enhances the moisture adsorption characteristics of the desiccant. Generally, solid desiccants are easier to handle than liquid desiccant. However, the pressure drops of the air passing through solid desiccants is one of its known problems. Solid desiccants come in many forms and shapes such as, cross flow, fixed bed, belt and stationary or rotary wheels. Rotary wheels are one of the most used shapes as it can operate continuously and it resists the corrosion. Liquid desiccants utilize lithium chloride or calcium chloride as their adsorbent. Although the capability of liquid desiccants to remove moisture are greater than solid desiccants, they have a major disadvantage that they are carried away by air stream during regeneration and dehumidification.

4.4.1. Desiccant wheel. Regarding the mathematical formulation of the desiccant wheel, the presented model by [80] is chosen. Nobrega and Brum [81] were able to develop the model by converting the mass and energy equations of the desiccant

wheel into a system of linear hyperbolic partial differential equations and solving them by wave shock method. Panaras et al. [82] presented an experimental validation of the chosen desiccant wheel model.

The formulation can be summarized as follows [80]:

$$f_{1,i} = \frac{-2865}{(t_i + 273)^{1.49}} + 4.344(\frac{\omega_i}{1000})^{0.8624} \tag{4.45}$$

$$f_{2,i} = \frac{(t_i + 273)^{1.49}}{6360} - 1.127(\frac{\omega_i}{1000})^{0.07969} \tag{4.46}$$

$$\eta_{F1} = \frac{f_{1,(u,e)} - f_{1,(u,i)}}{f_{1,(l,i)} - f_{1,(u,i)}} \tag{4.47}$$

$$\eta_{F2} = \frac{f_{2,(u,e)} - f_{2,(u,i)}}{f_{2,(l,i)} - f_{2,(u,i)}} \tag{4.48}$$

$$\dot{m}_u(\, t_e - t_i) = \dot{m}_l(\, t_i - t_e) \tag{4.49}$$

$$\dot{m}_u(\, \omega_e - \omega_i) = \dot{m}_l(\, \omega_i - \omega_e) \tag{4.50}$$

where (t_i) and (ω_i) are the temperature and humidity ratio of each state. $(f_{1,i})$ and $(f_{2,i})$ are the combined potential for the desiccant. (η_{F1}) and (η_{F2}) are the efficiencies of the desiccant wheel.

Their values might range from 0.09 and 0.76 in case of moderate level of operation and between 0.05 and 0.95 in case of high performance, respectively [77].$(\dot{m}_l)$ and $(\dot{m}_u)$ are the lower and upper air streams mass flow rates in kg/s.

4.4.2. Air to gas heat exchanger. The exhaust gas from the gas turbine will act as the source of heat required in order to achieve the regeneration temperature required for the desiccant to increase its vapor pressure on its surface so that it surpasses the surrounding air pressure in a process known as regeneration that helps the desiccant regain its moisture removal potential. The exhaust gas outlet temperature can be calculated by the following formula [39]:

$$t_{g,o} = t_{g,i} - \frac{\dot{m}_l(h_e - h_i)}{\dot{m}_g c_{pg}} \tag{4.51}$$

$$h = (1.005 + 1.8723\ \omega)t \tag{4.52}$$

where ($t_{g,o}$) and ($t_{g,i}$) are the outlet and inlet exhaust gas temperatures in K, and (h) is the specific enthalpy of the moist air in kJ/kg. (c_{pg}) is the exhaust gas specific heat capacity in kJ/Kg and ($\dot{m}_g$) is the exhaust gas mass flow rate in kg/s.

4.4.3. Maisotsenko coolers. The integration of double stage and triple stage Maisotsenko-desiccant cooling systems with gas turbines power plants were investigated by El-Damaty and Gadalla [87,88]. The outlet air temperature of the product air be calculated by [37]:

$$E_{dp} = \frac{T_{PI} - T_{PO}}{T_{PI} - T_{dp,w}} \tag{4.53}$$

where (E_{dp}) is the dew point effectiveness of the Maisotsenko cooler. Its value is taken to be 0.8 based on the results presented in [83] (T_{PI}) and (T_{PO}) are the product air streams inlet and outlet temperature, while ($T_{dp,w}$) is the dew point temperature of the working air.

Chapter 5. Results and Discussion

In this chapter, all the obtained results from the analysis and optimization of the proposed configurations will be presented and discussed. All three configurations of the gas turbine are integrated with Maisotsenko-Desiccant cooling systems. Initially, the first configuration of a simple gas turbine will be discussed. Next, the results of the analysis and optimization of the second configuration of a gas turbine with air bottoming cycle will be evaluated. Following that, the thermodynamic and exergoeconomic results obtained for the third configuration of intercooled, reheated and recuperated gas turbine cycle will be presented.

5.1. Simple Gas Turbine Cycle

The gas turbine performance at ISO conditions of ambient temperature of 15°C and relative humidity of 60% is shown in Table 6. Moreover, the table presents the results of gas turbine performance for ambient temperature at 40°C which the researcher called the "Base Case". It displays also the exhaust gas temperature (T_5), the temperature at the compressor exit(T_2) in °C, the air mass flow rate ($\dot{m}_{air}$) and the fuel mass flow rate($\dot{m}_{fuel}$) in kg/s, the coolant fraction which is the ratio between the coolant mass flow rate to the air mass flow rate in % and the coolant mass flow rate($\dot{m}_{coolant}$) in kg/s. The performance of the cooling system different configurations SS-MD, TS-IMD is shown in Table 7 while the performance for TS-PMD and TS-RMD are presented in Table 8. The gas turbine performance after implementing the different configuration of the cooling system is shown in Table 9 and 10. ($\dot{m}_u$) is the upper stream mass flow rate, ($\dot{m}_l$) is the lower stream air mass flow rate and ($\dot{m}_{outlet}$) is the mass flow rate of air which is going to be driven to the cooling line in the gas turbine, all in kg/s; ($T_{g,out}$) is the temperature of the exhaust gases at the outlet of the air to gas heat exchanger and (T_{outlet}) is the temperature of air that is going to be led into the gas turbine, both are in °C. ($\dot{Q}_{Regeneration}$) is the amount of heat rate needed to operate the regeneration process for the desiccant wheel which is the amount of heat rate recovered from the gas turbine exhaust gas in kW while ($\dot{Q}_{Cooling}$) is the cooling capacity of the inlet cooling system in kW, and COP is the coefficient of performance.

The simulations performed in all three configurations of the gas turbine, that include simple gas turbine, gas turbine with air bottoming cycle and intercooled recuperated and reheated gas turbine, were done using EES and MATLAB software.

The numbers in Table 7 and 8 showed that the air mass flow rate ($\dot{m}_{outlet}$) that is going to be bled to the coolant line in the gas turbine is the lowest in the TS-IMD configuration with 5.421 where it is 5.459 for TS-PMD, 5.517 for SS-MD and 5.478 for TS-RMD. The lower and upper stream air mass flow rate ($\dot{m}_l \; and \; \dot{m}_u$) is nearly the same for all the configurations with 282.8 kg/s. The TS-IMD configuration has the lowest (T_{outlet}) of 18.6℃ ,which is the temperature of air coming out of the cooling system, followed by the TS-PMD with 22℃ , then 23.5℃ for the TS-RMD and lastly the SS-MD with 27℃. Making TS-IMD the best choice out of the 4 configurations. Moreover, ($T_{g,out}$), which is the temperature of exhaust gases at the outlet of the air to gas heat exchanger, is the lowest in the case of TS-IMD and TS-PMD with 507℃ followed by the TS-RMD and SS-MD configurations.

Table 6: Simple gas turbine performance

Parameter	ISO	Base Case
Compressor inlet temp (°C)	15	40
Relative humidity (%)	60	55
Temperature at comp. exit (°C)	411	467
Temperature required (°C)	309	416
Efficiency (%)	34.32	33.33
Fuel mass flow rate (kg/s)	2.85	2.935
Air mass flow rate (kg/s)	122.7	136
Coolant mass flow rate (kg/s)	28.98	35.32
Cooling Fraction (%)	23.62	25.96
Exhaust gas temperature (°C)	636	640

Table 7: SS-MD and TS-IMD cooling systems performance

Configurations	SS-MD	TS-IMD
Humidity ratio (kg/kg)	0.02611	0.02611
Relative humidity (%)	55	55
$T_{ambient}$(°C)	40	40
$\dot{m}_{outlet}$(kg/s)	5.517	5.421
$\dot{m}_l = \dot{m}_u$(kg/s)	282.9	282.7
T_{outlet}(°C)	27	18.6
$T_{g,out}$(°C)	598	507
$\dot{Q}_{Cooling}$(KW)	1862	3041
$\dot{Q}_{Regeneration}$(KW)	7546	23838
COP	0.2468	0.1276

Table 8: TS-PMD and TS-RMD cooling systems performance

Configurations	TS-PMD	TS-RMD
Humidity ratio (kg/kg)	0.02611	0.02611
Relative humidity (%)	55	55
$T_{ambient}$(°C)	40	40
$\dot{m}_{outlet}$(kg/s)	5.459	5.478
$\dot{m}_l = \dot{m}_u$(kg/s)	282.8	282.9
T_{outlet}(°C)	22	23.5
$T_{g,out}$(°C)	507	539.5
$\dot{Q}_{Cooling}$(KW)	2579	2338
$\dot{Q}_{Regeneration}$(KW)	23844	17976
COP	0.1081	0.1301

Table 9: Gas turbine performance with SS-MD and TS-IMD cooling systems

Parameter	SS-MD	TS-IMD
Compressor inlet temperature (°C)	27	18.6
Relative humidity (%)	55	55
Pressure (bar)	1	1
Temperature at compressor exit (°C)	438.5	420
Temperature required (°C)	357	321
Efficiency (%)	33.84	34.17
Air mass flow rate (kg/s)	128.6	124.4
Coolant mass flow rate (kg/s)	31.64	29.65
Cooling Fraction (%)	24.6	23.84
Exhaust gas temperature (°C)	638	637

Table 10: Gas turbine performance with TS-PMD and TS-RMD cooling systems

Parameter	TS-PMD	TS-RMD
Compressor inlet temperature (°C)	22	23.5
Relative humidity (%)	55	55
Pressure (bar)	1	1
Temperature at compressor exit (°C)	427	430.6
Temperature required (°C)	335.5	342
Efficiency (%)	34.04	33.98
Air mass flow rate (kg/s)	126.1	126.8
Coolant mass flow rate (kg/s)	30.34	30.79
Cooling Fraction (%)	24.14	24.28
Exhaust gas temperature (°C)	637	637.4

The performance of the gas turbine after integrating the different configuration of the cooling systems is displayed in Table 9 and 10. TS-IMD scored the highest increase in the gas turbine efficiency in comparison to the other configurations as it increased from the base case at 33.33% to 34.17%. This was anticipated since the TS-IMD has the lowest air temperature out of all the configurations with (T_{outlet}) of 18.6°C. Additionally, TS-IMD has the highest reduction in the amount of coolant that needs to be taken from the compressor exit as it decreased from 35.32 kg/s to 29.65 kg/s, leading to a reduction in the cooling fraction from 25.96 % to 23.84%.

5.1.1. Sensitivity analysis. A sensitivity analysis was conducted to study the influence of various variables on the coolant mass flow rate and the gas turbine efficiency. The effect of pressure ratio on the gas turbine efficiency and the coolant mass flow rate is shown in Figure 11. At constant ambient temperature and turbine inlet temperature, the increase in pressure ratio will lead to an increase in the coolant mass flow rate along an increase in the gas turbine efficiency as well.

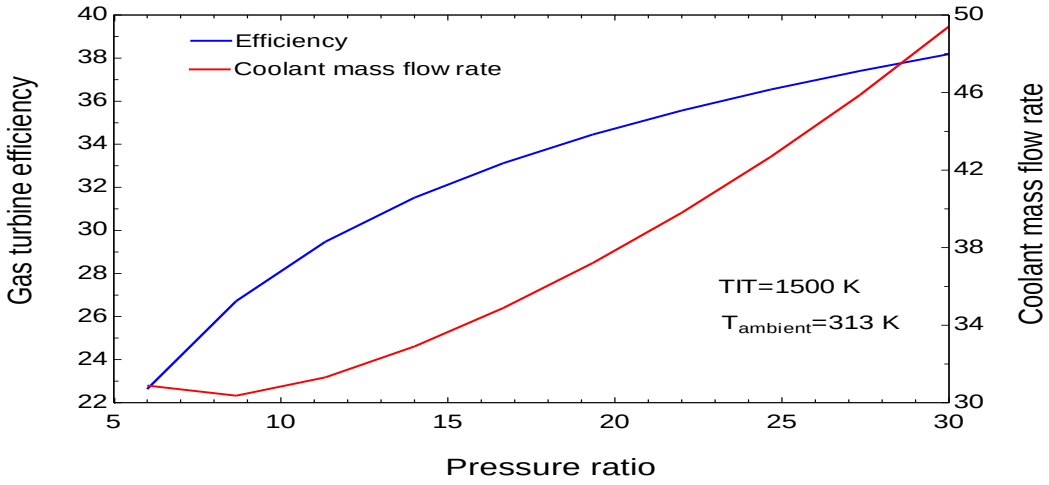

Figure 11: Effect of pressure ratio on gas turbine efficiency (%) and coolant mass flow rate (kg/s)

The effect of turbine inlet temperature (TIT) on the coolant mass flow rate and the gas turbine efficiency is shown in Figure 12. The increase in the turbine inlet temperature will cause an increase in the gas turbine efficiency, at constant pressure ratio of 17, ambient air temperature of 313°K and combustor exit temperature (T3) of 1698°K. However, a reduction in the amount of coolant mass flow rate required is noticed with the augmentation in the turbine inlet temperature. This was expected since increasing the value of (TIT) will bring it closer to the value of combustor exit

temperature (T3) 1698°K. Thus, a less amount of coolant mass flow rate will be needed to lower the temperature from (T3) at combustor exit to the turbine inlet temperature (TIT).

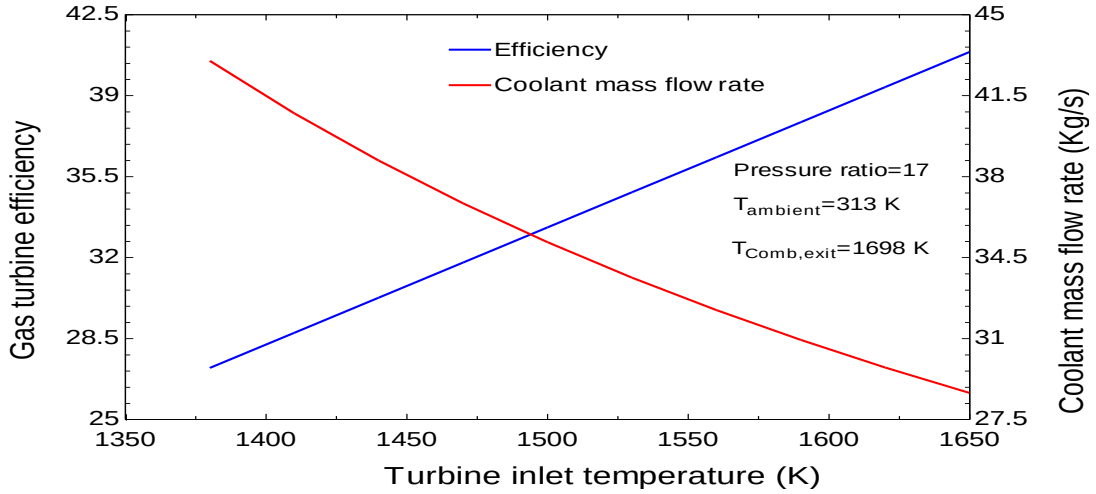

Figure 12: Effect of turbine inlet temperature (°K) on gas turbine efficiency (%) and coolant mass flow rate (kg/s)

The performance of each configuration of the cooling systems is displayed in Figure 13 by studying the effect of ambient air temperature on the outlet temperature. As shown, the SS-MD gives out the highest temperature while TS-IMD configuration yielded the lowest outlet temperatures followed by the TS-PMD and TS-RMD. Thus, the TS-IMD configuration had the best performance out of the four configurations.

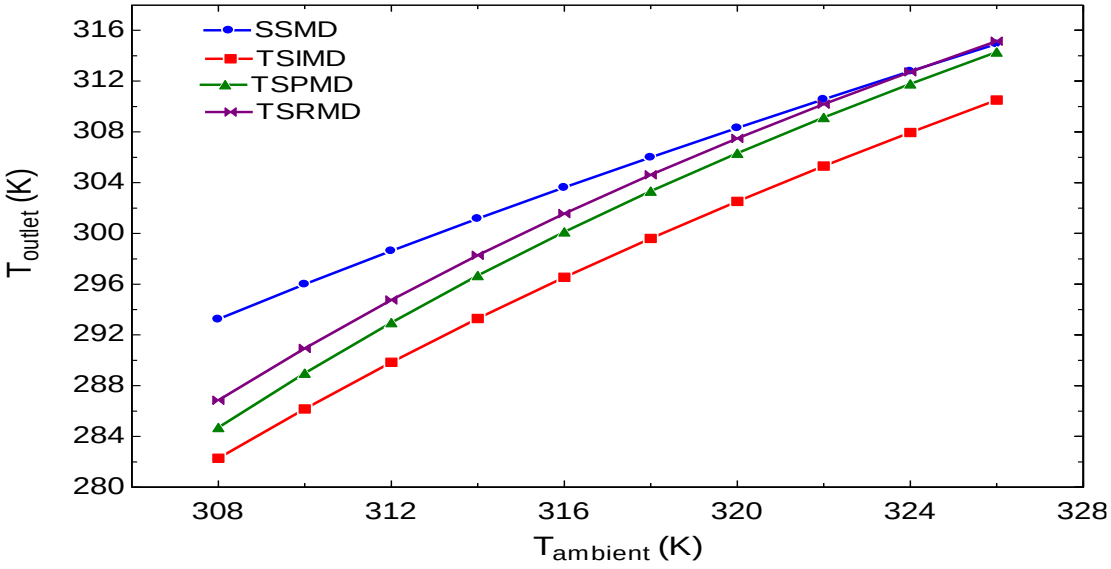

Figure 13: Effect of ambient air temperature (°K) on the outlet temperature (°K) for each configuration of the cooling systems

The influence of air temperature on the gas turbine efficiency in each configuration of the cooling systems is displayed in Figure 14 and 15. It can be seen that as the ambient air temperature decreases, the gas turbine efficiency increases. This takes place because lowering the compressor inlet temperature will lead to a higher air density and a higher mass flow rate improving the overall performance. Hence, it can be deducted that the TS-IMD configuration will provide the highest gas turbine efficiency since it yielded the lowest temperatures.

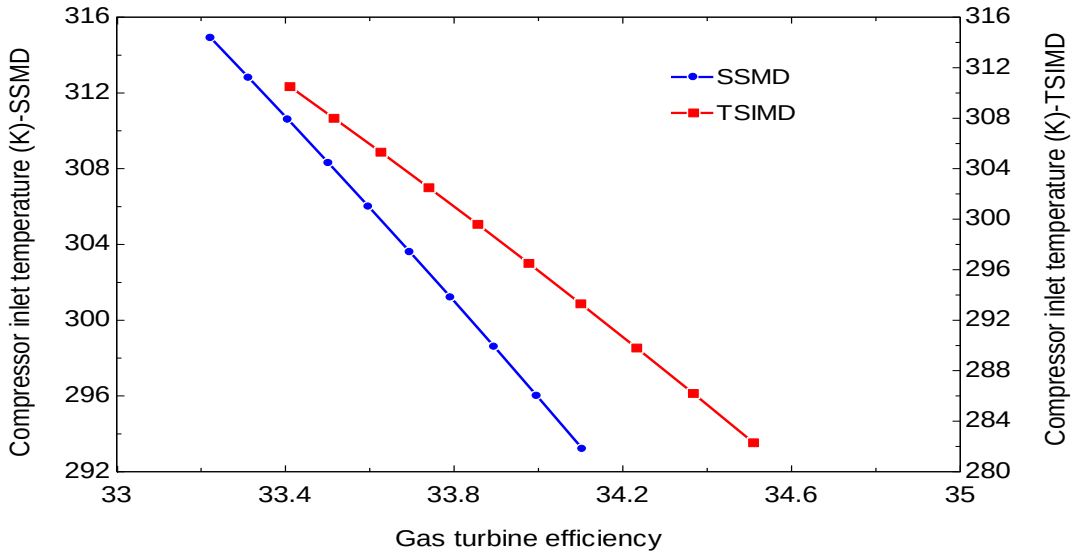

Figure 14: Effect of ambient air temperature (°K) in the case of SSMD and TSIMD on the gas turbine efficiency (%)

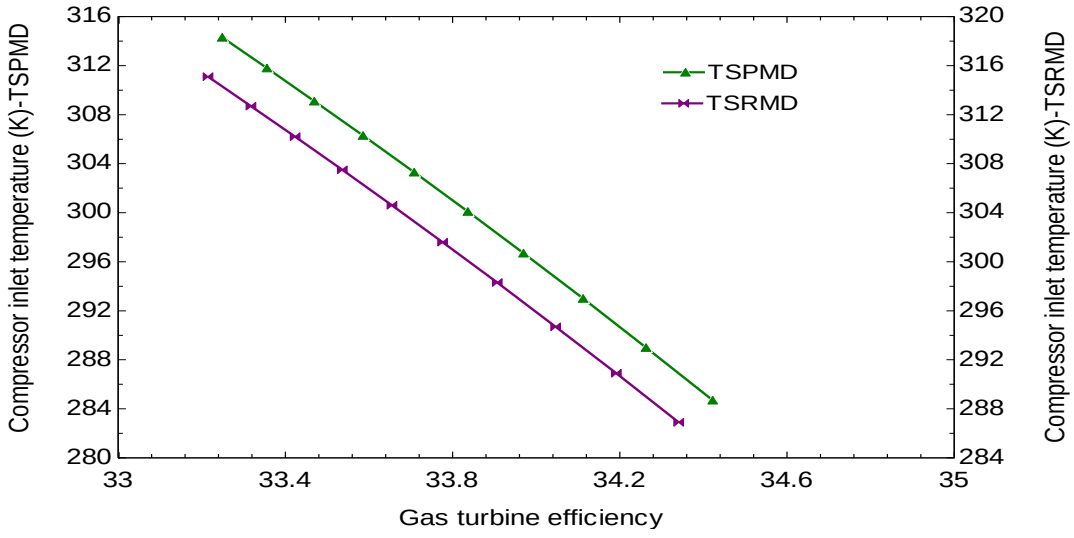

Figure 15: Effect of ambient air temperature (°K) in case of TSPMD and TSRMD on the gas turbine efficiency (%)

Figures 16 and 17 displayed the effect of cooling on the coolant mass flow rate. As the air temperature decreases, the amount of coolant mass flowrate will decrease as well. Thus, the use of cold air, coming from the cooling systems to cool down the coolant line even further, will reduce the amount of required coolant mass flow rate even more. Additionally, the TSIMD configuration is expected to be the configuration with the lowest required coolant mass flow rate since it yielded the lowest temperatures.

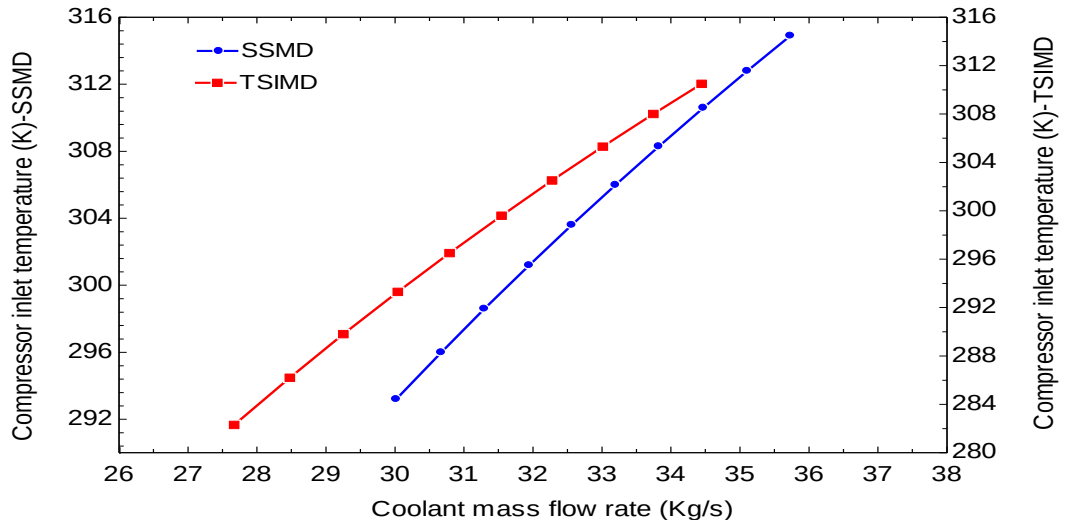

Figure 16: Effect of ambient air temperature (°K) in case of SSMD and TSIMD on the coolant mass flow rate (kg/s)

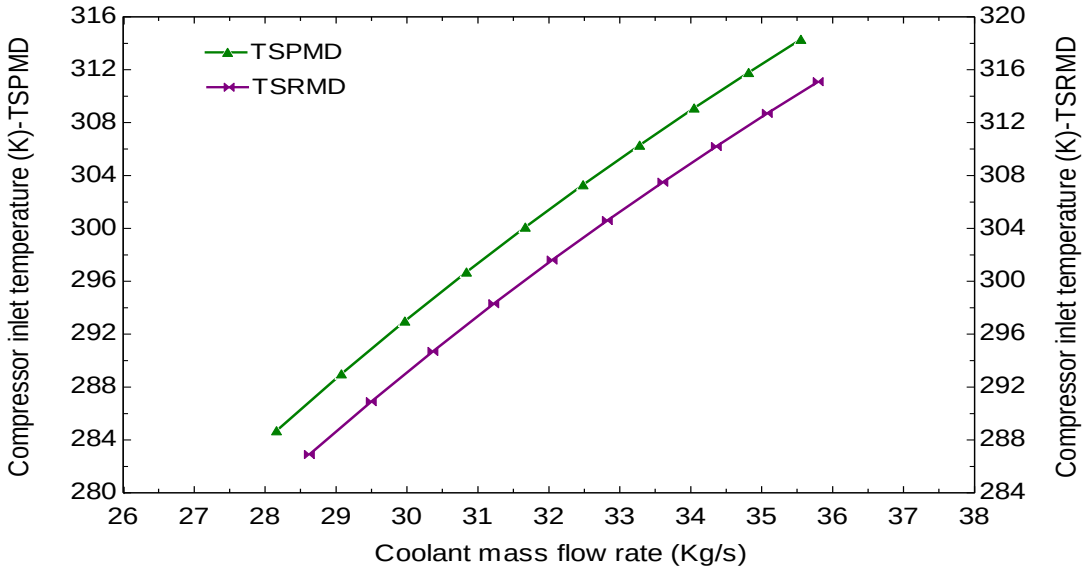

Figure 17: Effect of ambient air temperature(°K) in case of TSPMD and TSRMD on the coolant mass flow rate (kg/s)

Figure 18 showed the effect of ambient air on the COP. The SS-MD configuration has the highest COP compared to others configurations. However, since additional amounts of heat are available at our disposal from the gas turbine exhaust gases, the coefficient of performance is not considered to be the best indicator for the performance of this system.

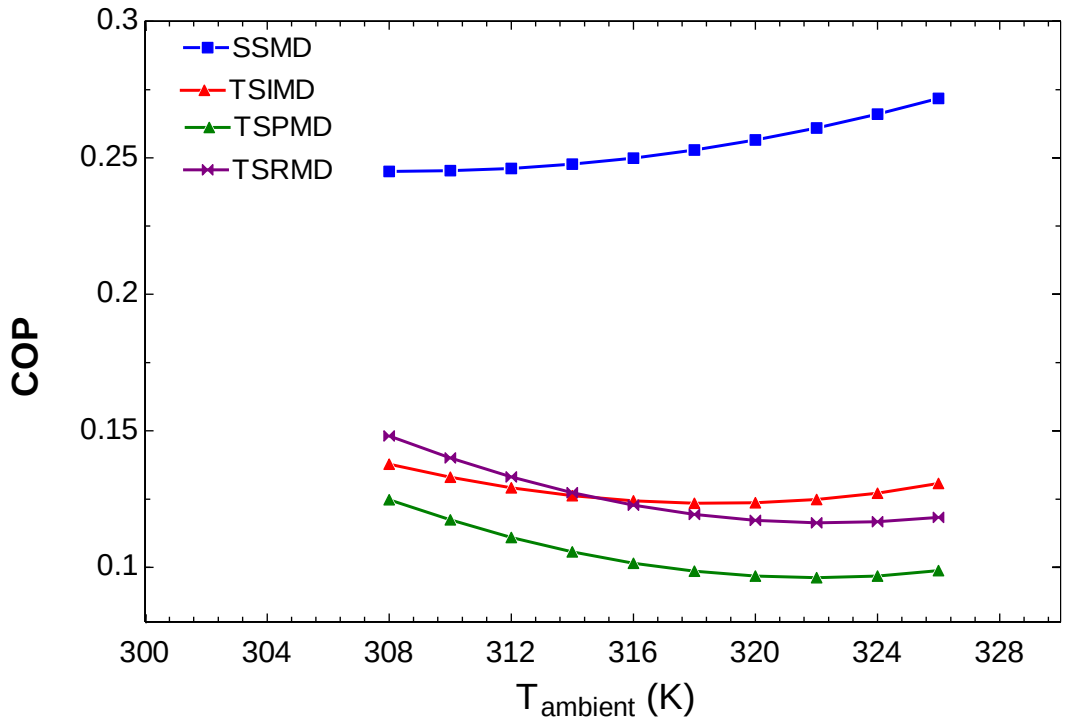

Figure 18: Effect of ambient air temperature(°K) for each configuration of the cooling systems on the COP

5.2. Gas Turbine with Air Bottoming Cycle (GTABC)

Sensitivity analysis was conducted to study the influence of different variables on the coolant mass flow rate and the gas turbine efficiency. Additionally, optimization analysis was conducted to determine the best operating parameters of the gas turbine as well as the cooling systems.

5.2.1. Optimization and sensitivity analysis. One of the most important parameters in the analysis of the gas turbine with air bottoming cycle performance is the mass flow rate ratio (MFFR). Thus, Figures 19,20 and 21 displayed the effect of MFFR on the overall efficiency of the gas turbine at different bottoming and topping cycle pressure ratios. As displayed by the results, the optimum value for MFFR was 1.2 at all conditions. Hence, this value was chosen for the rest of the analysis.

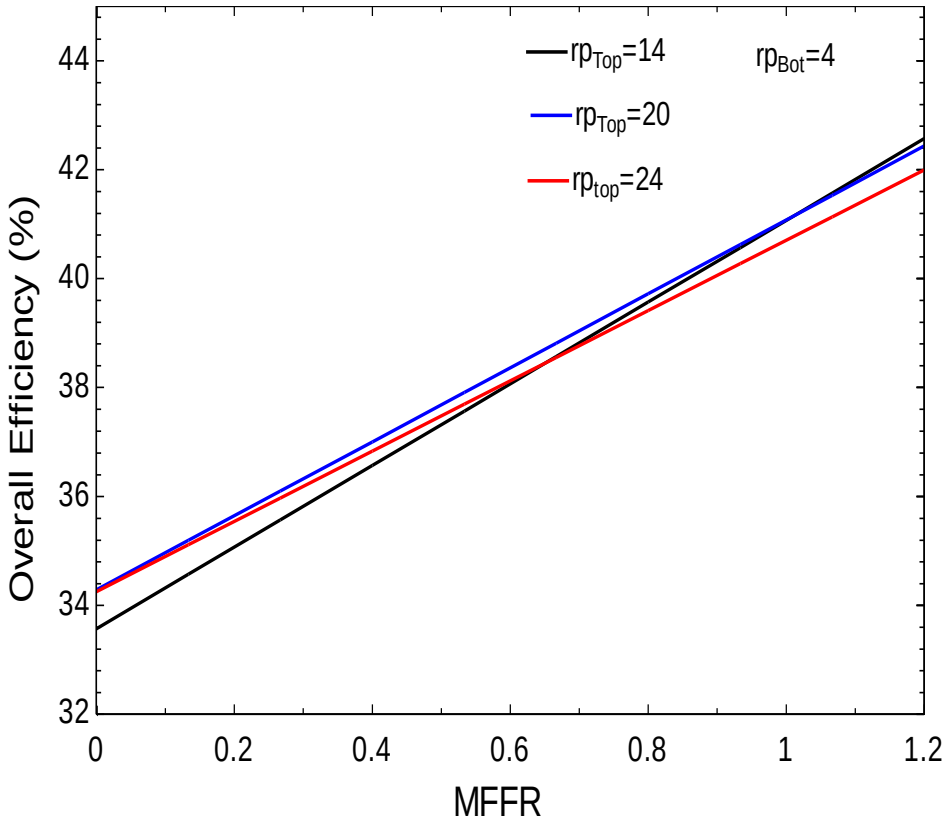

Figure 19: Effect of MFFR on the overall efficiency at bot cycle pressure ratio=4

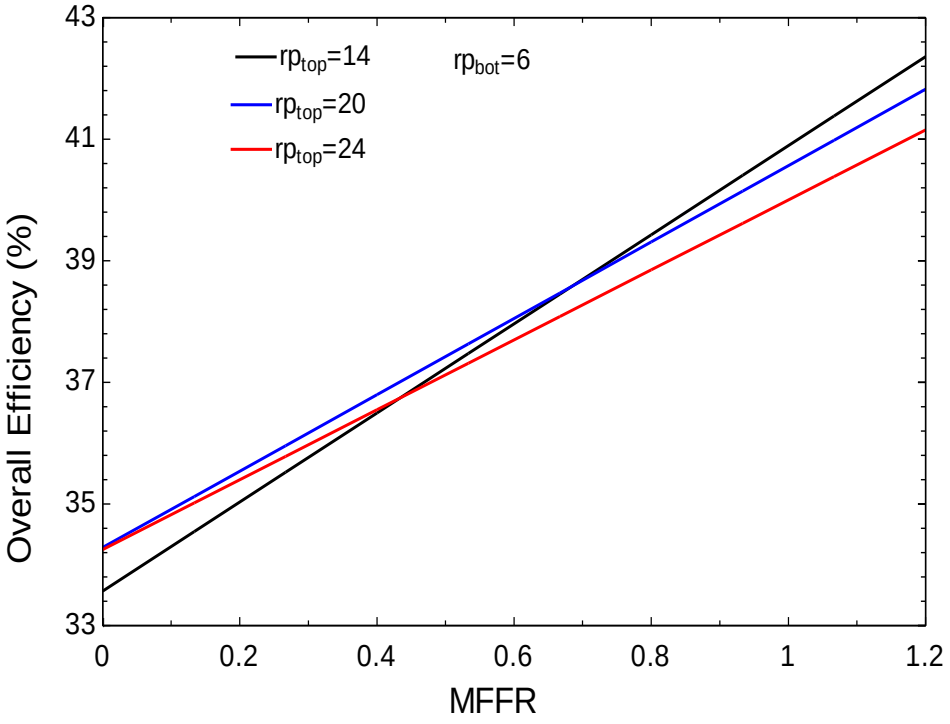

Figure 20: Effect of MFFR on the overall efficiency at bot cycle pressure ratio=6

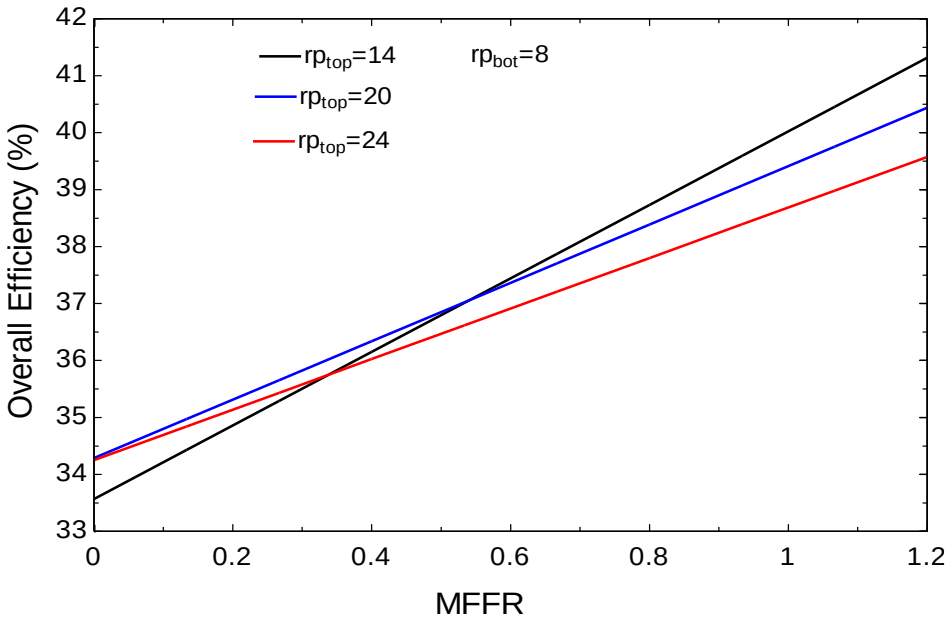

Figure 21: Effect of MFFR on the overall efficiency at bot cycle pressure ratio=8

The optimization of the bottoming and topping cycle pressure ratios to obtain the highest overall efficiency and the smallest coolant mass flow rate is presented in Figure 22 and 23, respectively. The effect of topping cycle pressure ratio on the overall efficiency at different bottoming cycle pressure ratio is presented in Figure 22. As shown in the figure, the bottoming cycle pressure ratio of 4 has yielded the highest overall efficiency out of the three values. Moreover, the overall efficiency tends to increase with the increase, followed by a decrease, of the topping cycle pressure ratio. This can be explained as a lower exhaust gases temperature, which is being driven to the bottoming cycle, and is achieved by increasing the topping cycle pressure ratio. This leads to an increase in the efficiency of the topping cycle along a reduction in the bottoming cycle efficiency.

This tradeoff is the main reason behind this behavior of increasing and decreasing afterwards. The effect of topping cycle pressure ratio on the coolant mass flow rate at different bottoming cycle pressure ratio is displayed in Figure 23**.** Again, bottoming cycle of pressure ratio 4 produced the lowest coolant mass flow rate. Thus, this value was assigned for the bottoming cycle pressure ratio for the rest of the analysis. Figure 23 showed that amount of coolant mass flow rate increases with the increase of the topping cycle pressure ratio, which is logical since as the pressure ratios increase, the coolant lines temperature will increase. Hence, higher amounts of coolant will be needed to cool down the turbine blades.

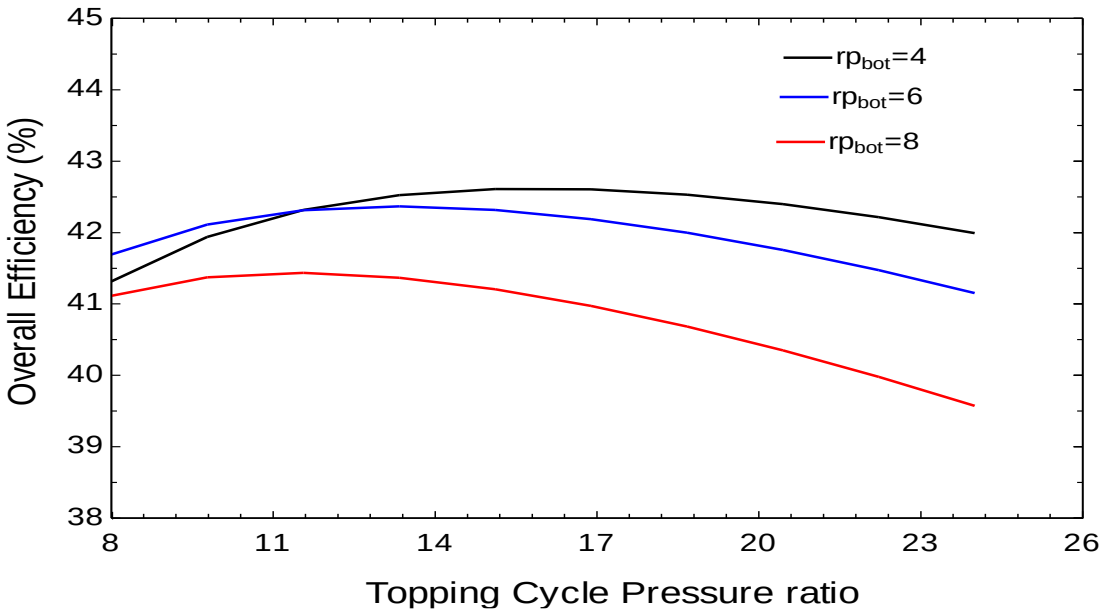

Figure 22: Effect of top cycle pressure ratio on the overall efficiency at different bot cycle pressure ratios

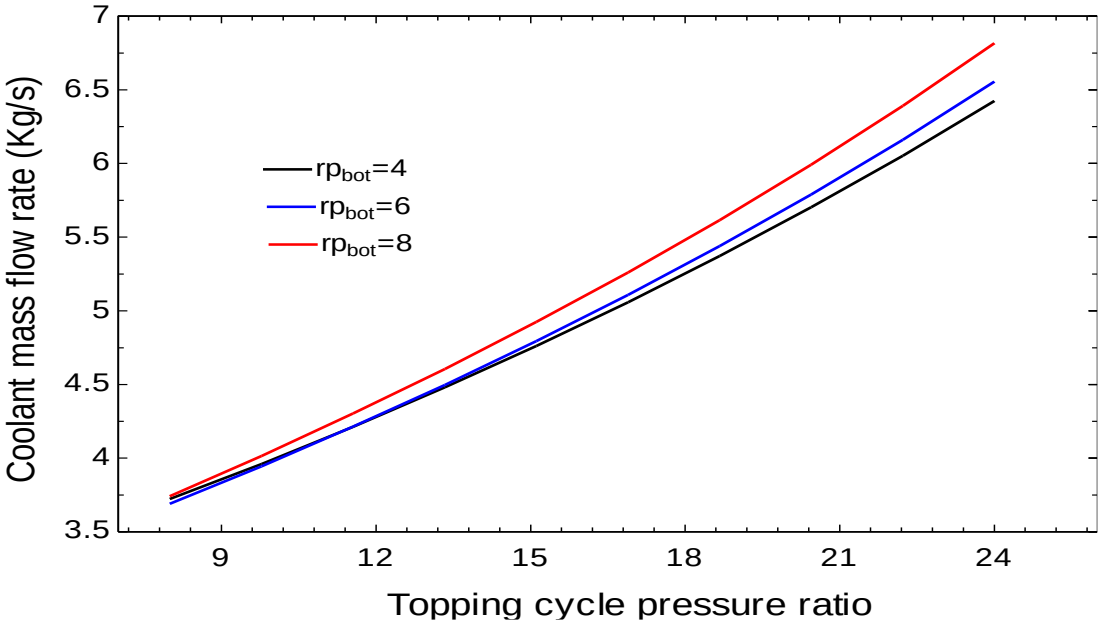

Figure 23: Effect of top cycle pressure ratio on the coolant mass flow rate at different bot cycle pressure ratios

The effect of inlet air temperature on the overall efficiency at different topping cycle pressure ratios is shown in Figure 24. It comes in agreement with the world known fact that the reduction of the inlet air temperature will lead to an increase in the overall efficiency of the gas turbine. Out of the three values for the topping cycle pressure ratio, 14 yielded the highest overall efficiency.

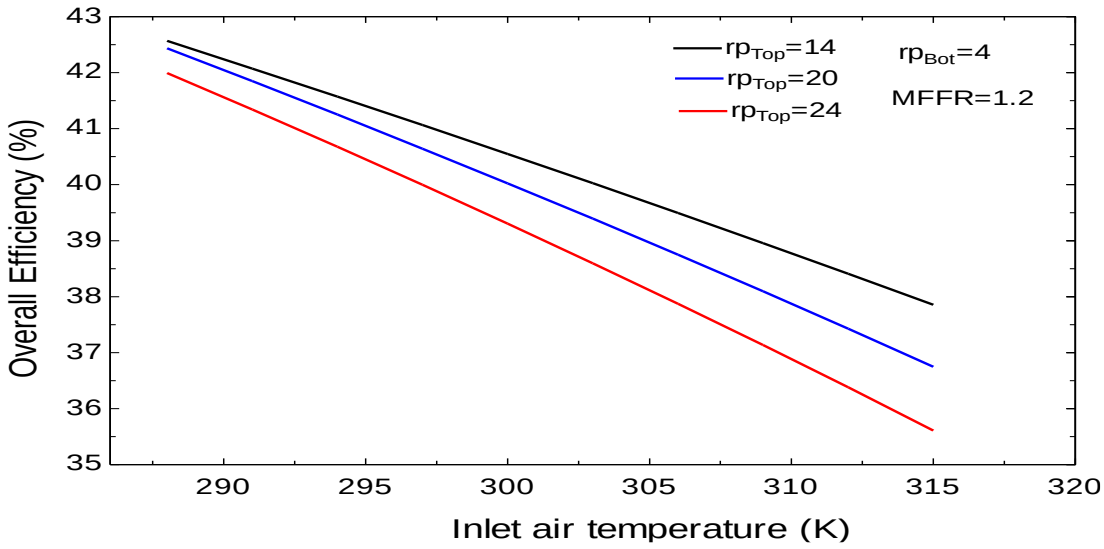

Figure 24: Effect of inlet air temperature on the overall efficiency at different top cycle pressure ratios

The effect of turbine inlet temperature (TIT) on the overall efficiency at different topping cycle pressure ratios is displayed in Figure 25. Again, Figure 25 agrees with the fact stating that increasing the TIT will lead to an increase in the gas turbine efficiency. For our picked value of TIT (1500°K), topping cycle pressure ratio of 14 achieved the highest overall efficiency.

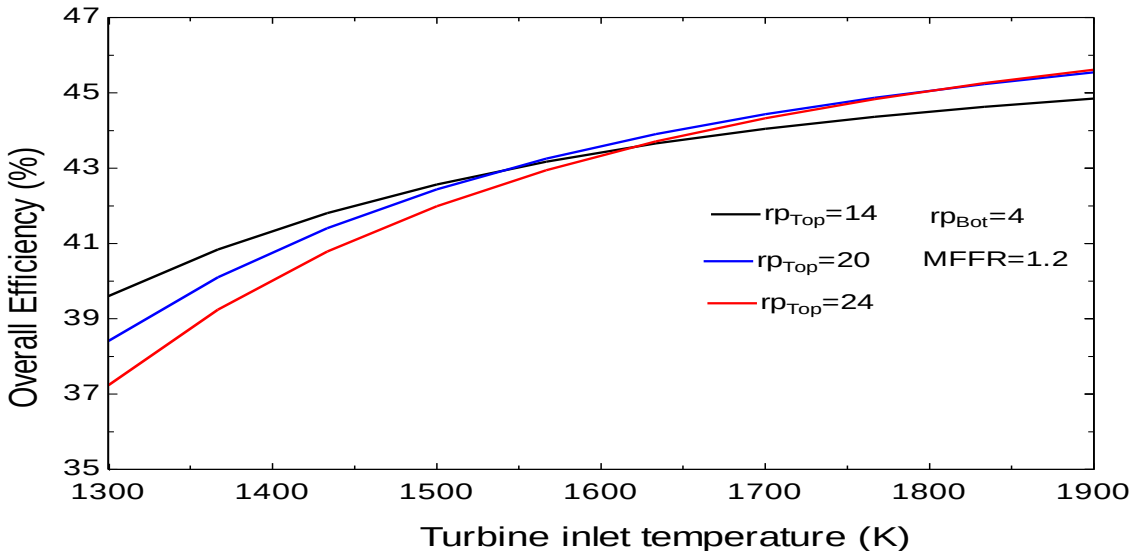

Figure 25: Effect of turbine inlet temperature on the overall efficiency at different top cycle pressure ratios

The effect of turbine inlet temperature on the coolant mass flow rate at different topping cycle pressure ratios is shown in Figure 26. The amount of coolant mass flow rate increases with the increase of the turbine inlet temperature.

This occurs due to the fact that increasing the turbine inlet temperature will raise the turbine blades temperature, which means that larger amounts of coolant mass flow rate will be required to cool it. A topping cycle pressure ratio of 14 yielded the lowest amount of coolant mass flow rate. Thus, due to the aforementioned conclusions, topping cycle of pressure ratio 14 was chosen for the rest of the analysis.

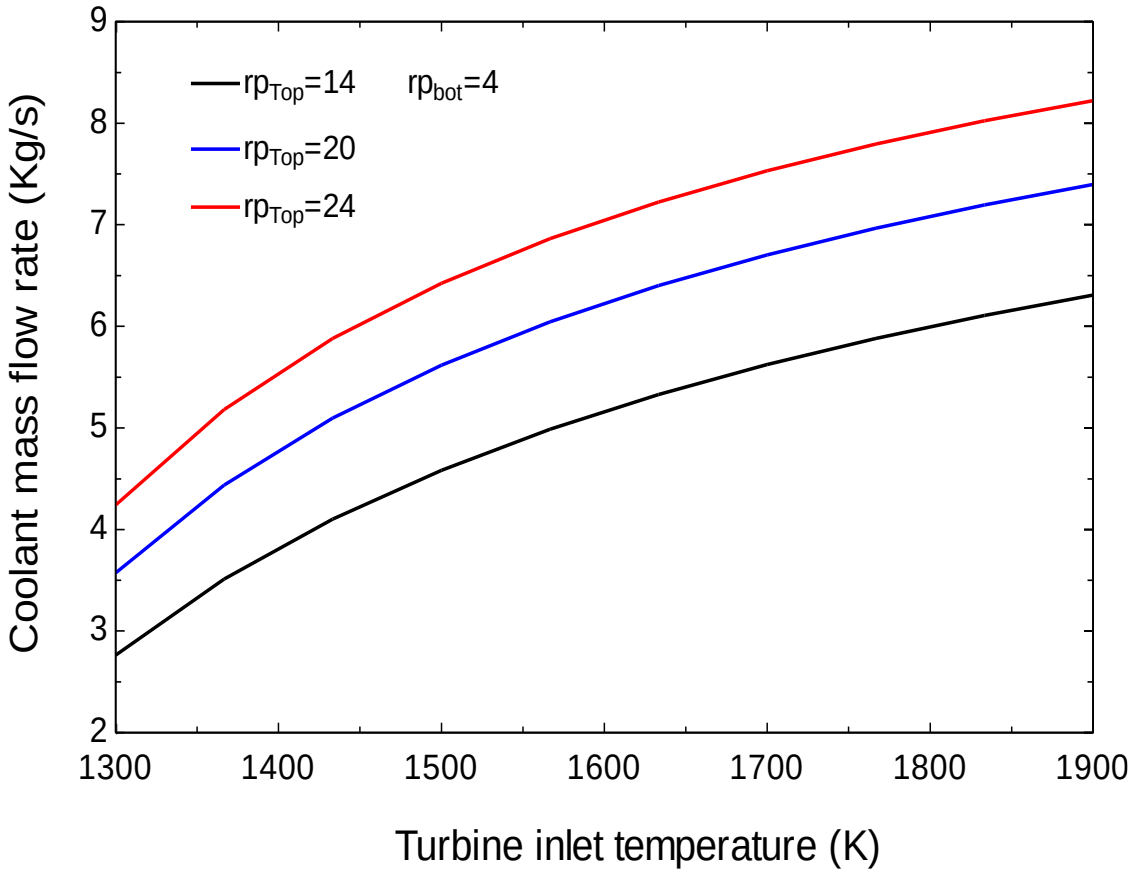

Figure 26: Effect of turbine inlet temperature on the coolant mass flow rate at different top cycle pressure ratios

The effect of inlet air temperature on the outlet air temperature for each configuration of the cooling system at different relative humidity is presented in Figure 27. As shown in the figure, out of the three values of relative humidity, 50% produced the coolest outlet air temperature. At relative humidity of 50%, TS-MD produced the highest outlet air temperature while TS-EMD yielded the coolest outlet air temperature. The effect of inlet air temperature on the outlet air humidity ratio for each configuration of the cooling system at different relative humidity is shown in Figure 28. When the inlet air temperature increases, the outlet air humidity ratio increases with relative humidity of 50% yielding the lowest humidity ratio out of the three cases.

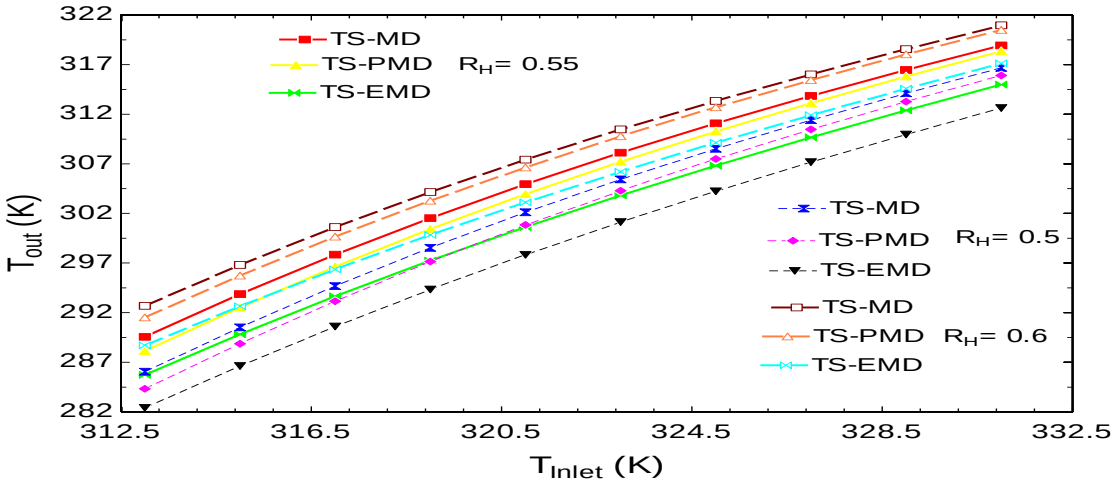

Figure 27: Effect of inlet air temperature on the outlet air temperature for each configuration of the cooling system at different relative humidity

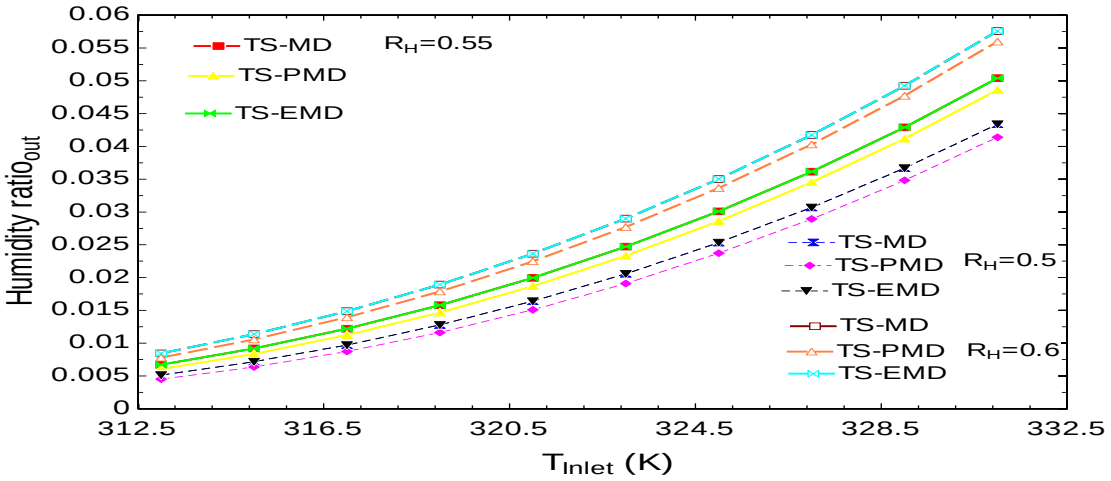

Figure 28: Effect of inlet air temperature on the outlet air humidity ratio for each configuration of the cooling system at different relative humidity

Figure 29 discussed the effect of relative humidity on the outlet air temperature for each configuration of the cooling system at different inlet air temperatures. It was noticed that the outlet air temperature increases when the relative humidity increases. Inlet air temperature of 40 (°C) produced the coolest outlet air temperature which was in the case of TS-EMD while TS-MD produced the highest outlet air temperature. The effect of relative humidity on the outlet air humidity ratio for each configuration of the cooling system at different inlet air temperatures is discussed in Figure 30. The augmentation of relative humidity has led to a slight increase in the outlet air humidity ratio with 40 (°C) of the inlet air temperature produced the lowest values for humidity ratio.

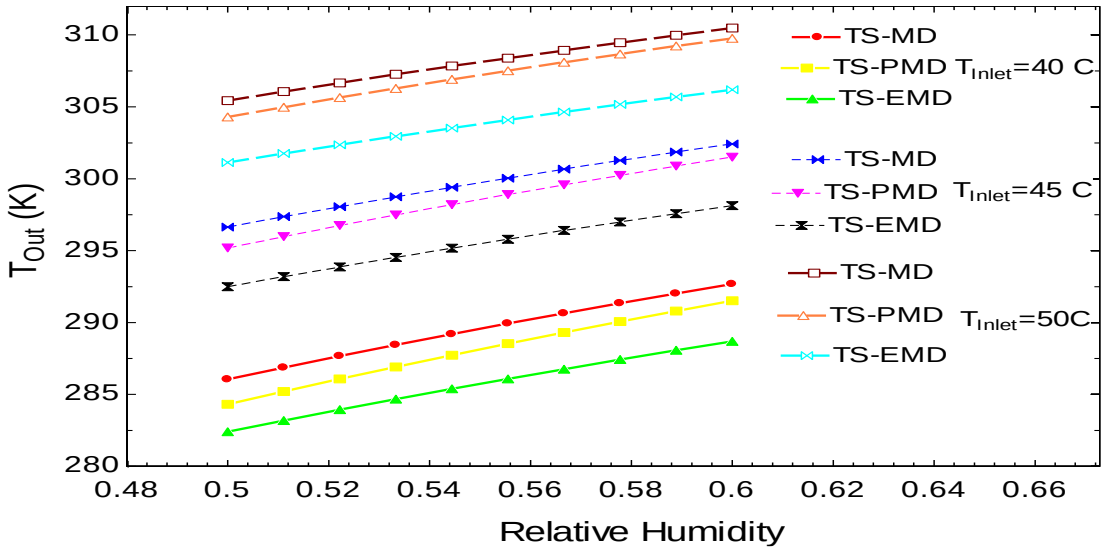

Figure 29: Effect of relative humidity on the outlet air temperature for each configuration of the cooling system at different inlet air temperatures

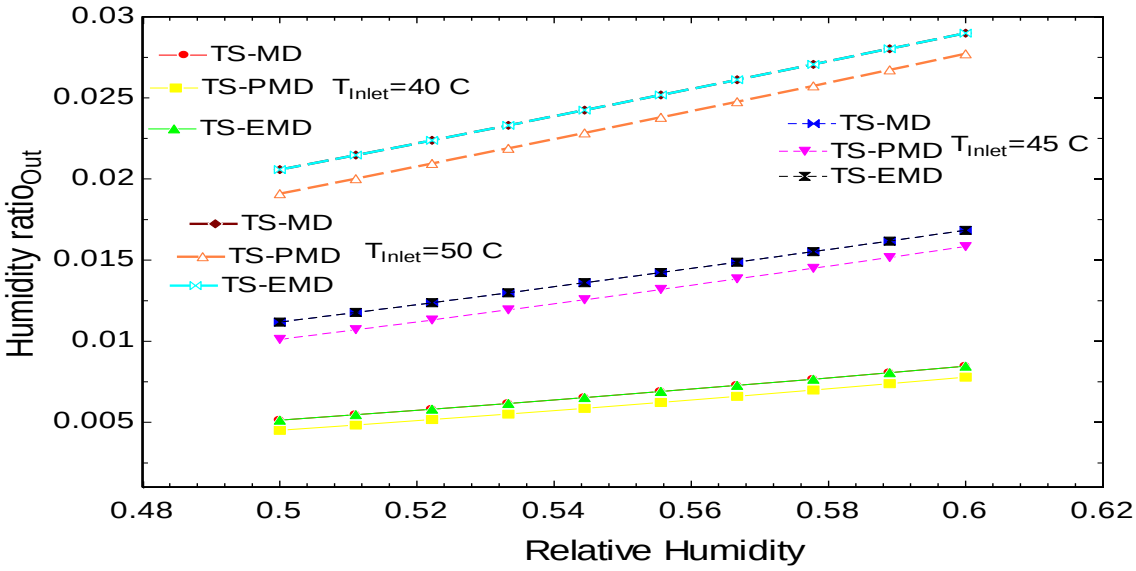

Figure 30: Effect of relative humidity on the outlet air humidity ratio for each configuration of the cooling system at different inlet air temperatures

The effect of regeneration temperature on the outlet air temperature and humidity ratio for each configuration of the cooling system at different inlet air temperatures is displayed in Figure 31 and 32. A reduction in the outlet air temperature as well as the humidity ratio was noticed as the regeneration temperature increased. The lowest value for the outlet air temperature and humidity ratio was achieved at 40 (°C) of inlet air temperature. TS-MD yielded the highest outlet air temperature while TS-EMD produced the lowest outlet air temperature.

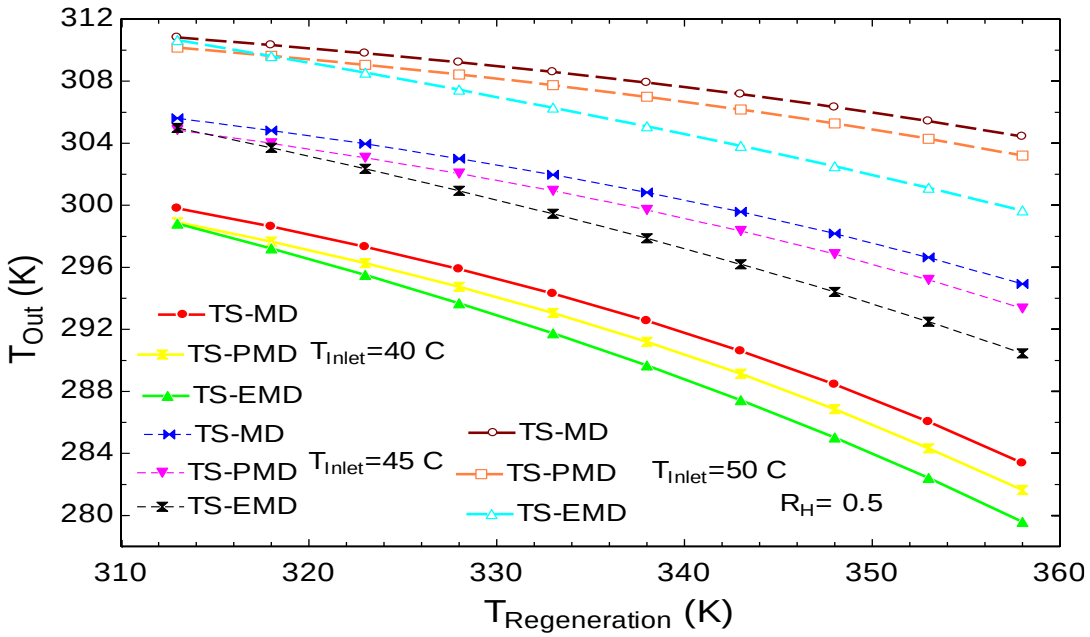

Figure 31: Effect of regeneration temperature on the outlet air temperature for each configuration of the cooling system at different inlet air temperatures

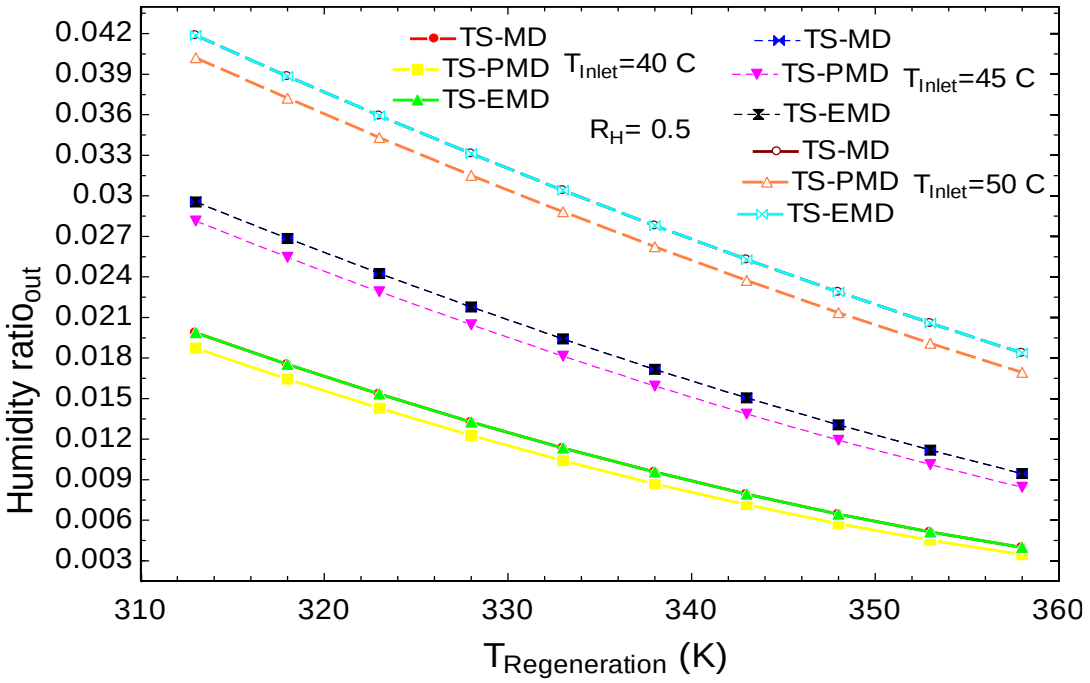

Figure 32: Effect of regeneration temperature on the outlet air humidity ratio for each configuration of the cooling system at different inlet air temperatures

As a result of the previous conclusions obtained, relative humidity of 50%, inlet air temperature of 313(°K) and regeneration temperature of 353(°K) were chosen as the operating parameters for the cooling systems.

The gas turbine performance after being optimized is shown in Table 11, where the bottoming cycle pressure ratio is 4, the topping cycle pressure ratio is 14 and the MFFR is 1.2. ISO conditions of ambient temperature of 15°C, relative humidity of 60% and pressure of 1 bar are applied. It showed also the overall efficiency: top cycle and bottom cycle specific work in kJ/kg, the fuel mass flow rate($\dot{m_{fuel}}$), the gas mass flow rate ($\dot{m}_g$), bottoming cycle air mass flow rate ($\dot{m}_{a,bot}$), topping cycle air mass flow rate($\dot{m_{a,Top}}$) and the coolant mass flow rate($\dot{m_{coolant}}$) , all in kg/s. The coolant fraction which is the ratio between the coolant mass flow rate to the air mass flow rate in % is displayed as well.

Table 11: Gas turbine performance after optimization

Parameter	Value
Compressor inlet temperature (°C)	15
Relative humidity (%)	60
Pressure (bar)	1
Topping cycle pressure ratio	14
Bottoming cycle pressure ratio	4
Mass flow rate ratio (MFFR)	1.2
Top cycle air mass flow rate (kg/s)	97.11
Bottom cycle air mass flow rate (kg/s)	116.5
Overall Efficiency (%)	42.57
Fuel mass flow rate (kg/s)	2.713
Gas mass flow rate (kg/s)	95.24
Coolant mass flow rate (kg/s)	4.584
Cooling Fraction (%)	4.72
Top cycle specific work (kJ/kg)	441.4
Bottom cycle specific work (kJ/kg)	96.79

Table 12 displayed the performance of TS-MD, TS-PMD and TS-EMD after being optimized. Furthermore, Table 13 showed the gas turbine performance after implementing the different configuration of the cooling systems, where ($\dot{m}_u$) is the upper stream mass flow rate in kg/s, ($\dot{m}_l$) is the lower stream air mass flow rate in kg/s, (T_{outlet}) is the temperature of air that is going to be driven to the gas turbine input as well as the coolant line in°K. Relative humidity of 50%, ambient air temperature of 313(°K) and regeneration temperature of 353 (°K) were chosen as a result of optimization of the operating parameters of the cooling systems.

The optimization studied the effect of different inlet air temperature on the outlet air temperature and humidity ratio at different relative humidity levels. Moreover, the influence of relative humidity on the exit air temperature and humidity ratio at altered inlet air temperatures were investigated. Additionally, the effect of regeneration temperature on the outlet temperature as well as the humidity ratio was discussed as well. The performance of the three different configurations of the cooling systems, after being optimized, is presented in Table 12. As shown, TS-MD yielded the highest outlet air temperature and largest air mass flow rate, while TS-EMD produced the coolest outlet air temperature and the lower air mass flow rate. The performance of the gas turbine, after being integrated with the three cooling systems, is displayed in Table 13. The gas turbine performance without cooling system produced an overall efficiency of 42.57 %, topping cycle air mass flow rate of 97.11 kg/s, coolant mass flow rate of 4.584 kg/s, bottoming cycle air mass flow rate of 116.5 kg/s, cooling fraction of 4.72% and fuel mass flow rate of 2.713%. After integrating the cooling systems, the gas turbine performance showed an augmentation in the overall efficiency at 43.27%, 43.54% and 43.83% for TS-MD, TS-PMD and TS-EMD, respectively. It also showed a reduction in the amount of coolant mass flow rate at 3.708 kg/s, 3.66 kg/s and 3.607 kg/s for TS-MD, TS-PMD and TS-EMD, respectively. The cooling systems assisted in the reduction of the amount of air mass flow rate in the topping and bottoming cycle to 94.36 kg/s, 93.44kg/s and 92.43 kg/s for topping cycle air mass flow rate and to 113.2 kg/s, 112.1 kg/s and 110.9 kg/s for bottoming cycle air mass flow rate for TS-MD, TS-PMD and TS-EMD, respectively. A reduction in the cooling fraction was observed as well, reaching values of 3.93%, 3.917% and 3.902% for TS-MD, TS-PMD and TS-EMD, respectively.

The fuel mass flow rate was reduced to 2.669 kg/s, 2.653kg/s and 2.635 kg/s for TS-MD, TS-PMD and TS-EMD, respectively. From the obtained outcomes, one can say that the best results for the gas turbine performance were obtained in the case of TS-EMD implementation followed by TS-PMD then TS-MD.

Table 12: TS-MD, TS-PMD and TS-EMD cooling systems performance after optimization

Configurations	TS-MD	TS-PMD	TS-EMD
Inlet pressure (bar)	1	1	1
Relative humidity (%)	50	50	50
$T_{ambient}$(°K)	313	313	313
$T_{Regeneration}$(°K)	353	353	353
Humidity ratio (kg/kg)	0.005137	0.004513	0.005137
$\dot{m}_l = \dot{m}_u$ (kg/s)	418.82	414.74	410.26
T_{outlet}(°K)	286	284.3	282.4

Table 13: Gas turbine performance with TS-MD, TS-PMD and TS-EMD cooling systems

Parameter	SS-MD	TS-PMD	TS-EMD
Compressor inlet temperature (°K)	286	284.3	282.4
Relative humidity (%)	50	50	50
Pressure (bar)	1	1	1
Top cycle air mass flow rate (kg/s)	94.36	93.44	92.43
Bot cycle air mass flow rate (kg/s)	113.2	112.1	110.9
Overall efficiency (%)	43.27	43.54	43.83
Gas mass flow rate (kg/s)	93.32	92.43	91.46
Fuel mass flow rate (kg/s)	2.669	2.653	2.635
Coolant mass flow rate (kg/s)	3.708	3.66	3.607
Cooling Fraction (%)	3.93	3.917	3.902
Top cycle specific work (kJ/kg)	432.6	436.7	441.4
Bot cycle specific work (kJ/kg)	94.68	95.68	96.79

The effect of inlet air temperature in the three cases TS-MD, TS-PMD and TS-EMD on the overall efficiency is presented in Figure 33. As seen, the ambient air temperature decreases, the gas turbine overall efficiency increases. This is because as the compressor inlet temperature decreases, the air density and mass flow rate increase, yielding a better overall performance.

Hence, since the TS-EMD configuration produced the lowest temperatures, it will provide the highest gas turbine overall efficiency. The influence of inlet air temperature in case of TS-MD, TS-PMD and TS-EMD on the coolant mass flow rate is displayed in Figure 34. As shown, the reduction of the ambient air temperature will lead to a decrease in the amount of coolant mass flowrate. Hence, by cooling down the coolant lines, used for turbine blade cooling, to even lower temperatures by cold air coming from the cooling systems, lower amount of coolant mass flow rate will be required to cool down the turbine blades.

Additionally, since that the TS-EMD configuration yielded the lowest temperatures, it is only reasonable to be the configuration with smaller amounts of coolant mass flow rate.

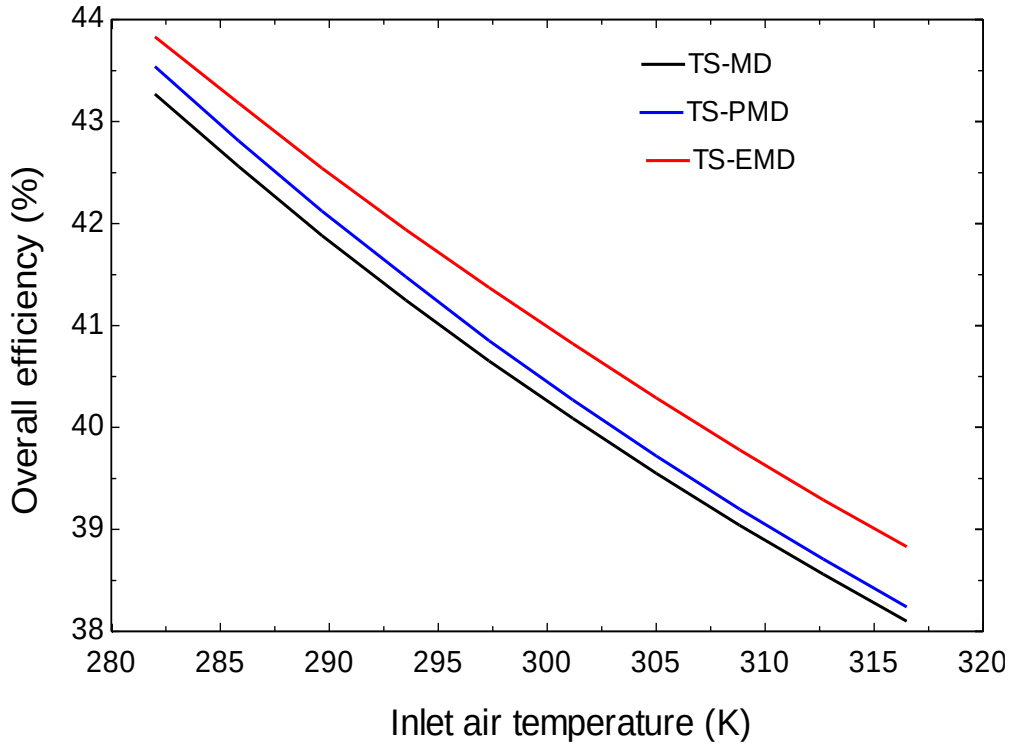

Figure 33: Effect of inlet air temperature in the case of TS-MD, TS-PMD and TS-EMD on the gas turbine overall efficiency

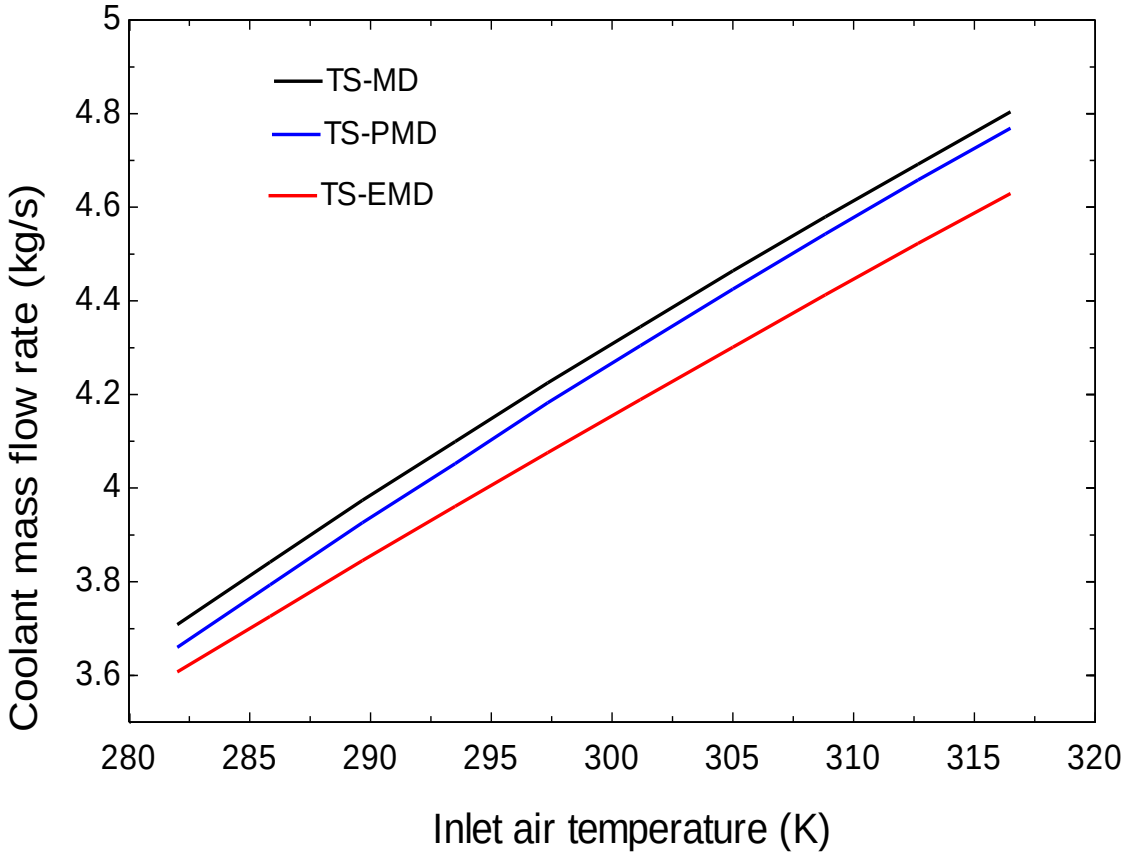

Figure 34: Effect of inlet air temperature in the case of TS-MD, TS-PMD and TS-EMD on the coolant mass flow rate

5.3. Intercooled, Reheated and Recuperated Gas Turbine (IcRhRc)

Optimization and sensitivity analysis were performed in order to determine the most appropriate pressure ratio to use, investigate the effect of turbine inlet temperature (TIT) and pressure ratio on the turbine thermal efficiency, exergetic efficiency, net specific work and the total cost rate.

5.3.1. Optimization and sensitivity analysis. The pressure ratio plays a major rule in any gas turbine cycle. Hence, it is vital to choose a suitable value for it to obtain the best performance of the system. Figure 35 investigated the effect of turbine inlet temperature (TIT) on the thermal efficiency as well as the exergetic efficiency at different pressure ratios. The figure displayed that the pressure ratio of 20 yielded the highest value for thermal and exergetic efficiency, followed by 26 then 30. Thus, a pressure ratio of 20 was chosen for the rest of the analysis.

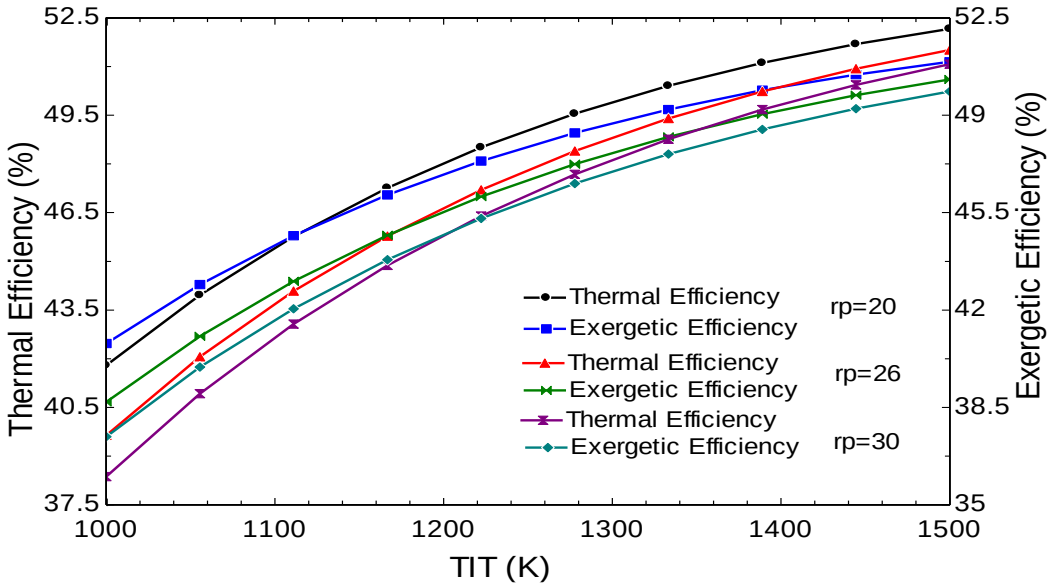

Figure 35: Effect of turbine inlet temperature(K) on the gas turbine thermal and exergetic efficiency (%) at different pressure ratios

The effect of turbine inlet temperature (TIT) on the gas turbine thermal efficiency and the net specific work is displayed in Figure 36. An augmentation in the thermal efficiency was noticed when the (TIT) increased. This comes in agreement with the various published work previously. Additionally, the augmentation in the (TIT) will lead to an increase of the net specific work of the cycle since the gases will be at higher temperatures before being expanded in the turbines. This comes in agreement with the results obtained from [89,90]

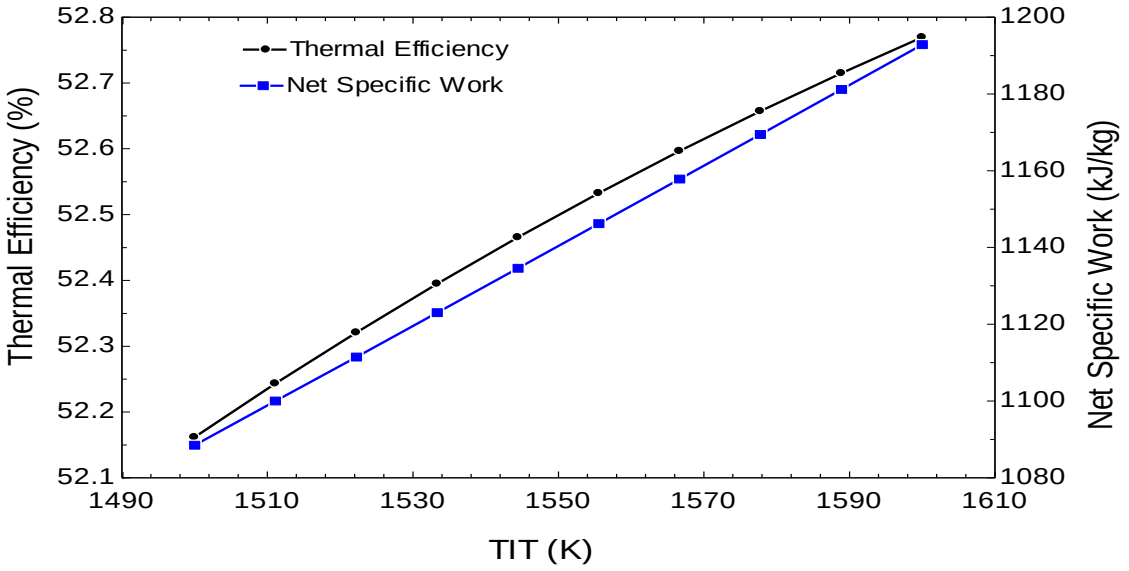

Figure 36: Effect of turbine inlet temperature (K) on the gas turbine thermal efficiency (%) and the net specific work (kJ/kg)

The effect of turbine inlet temperature on the gas turbine exergetic efficiency and the total cost rate is presented in Figure 37. As the turbine inlet temperature rises, more advanced materials and unconventional cooling technologies will be required in order to protect the turbine blades from any damages. Thus, these advanced materials are going to be more expensive than the ordinary ones. Making the total cost rate increase with the surge in the inlet temperature of the turbine.

Moreover, the figure showed that the increase in the (TIT) has led to an increase in the exergy efficiency. This is because the augmentation in (TIT) will increase the net specific work, which will increase the exergetic efficiency of the cycle. However, it is expected that at higher (TIT), more fuel will be needed to reach these higher (TIT) values which will reduce the exergetic efficiency.

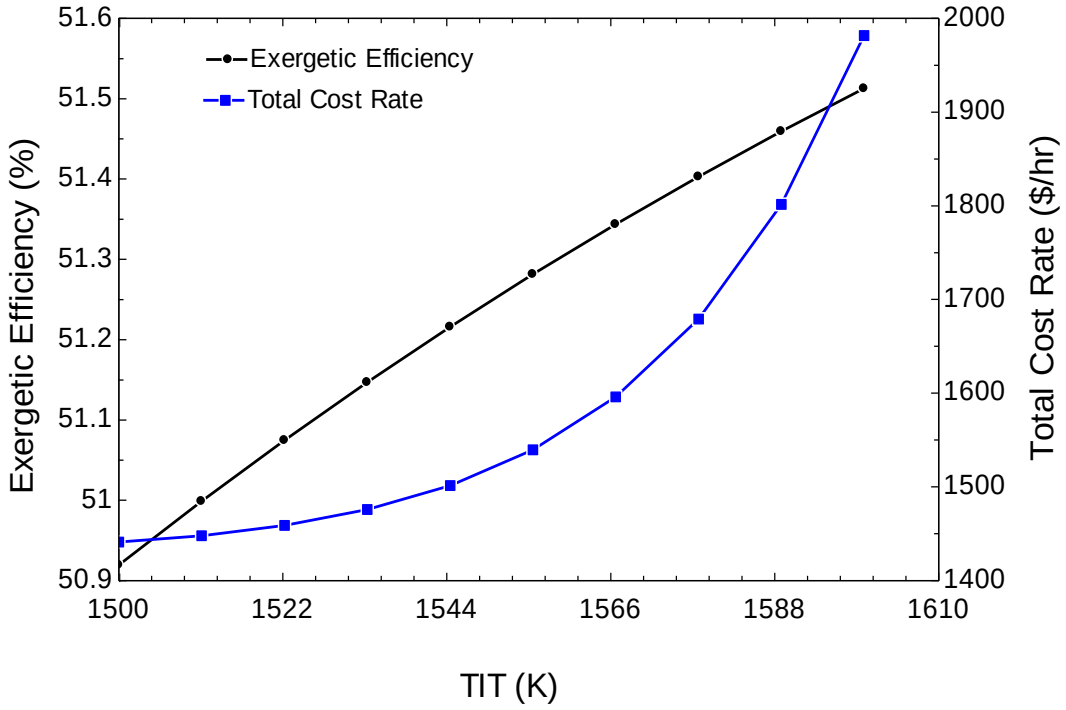

Figure 37: Effect of turbine inlet temperature (K) on the gas turbine exergetic efficiency (%) and the total cost rate ($/hr)

Figure 38 displayed the effect of pressure ratio on the gas turbine thermal efficiency and the net specific work. As it can be seen, the augmentation of pressure ratio will lead to an increase in the net specific work, where the save in the compression work is overcoming the increase in compression work. However, the increase in the pressure ratio is met with a reduction in the thermal efficiency due to the increase in the compression work.

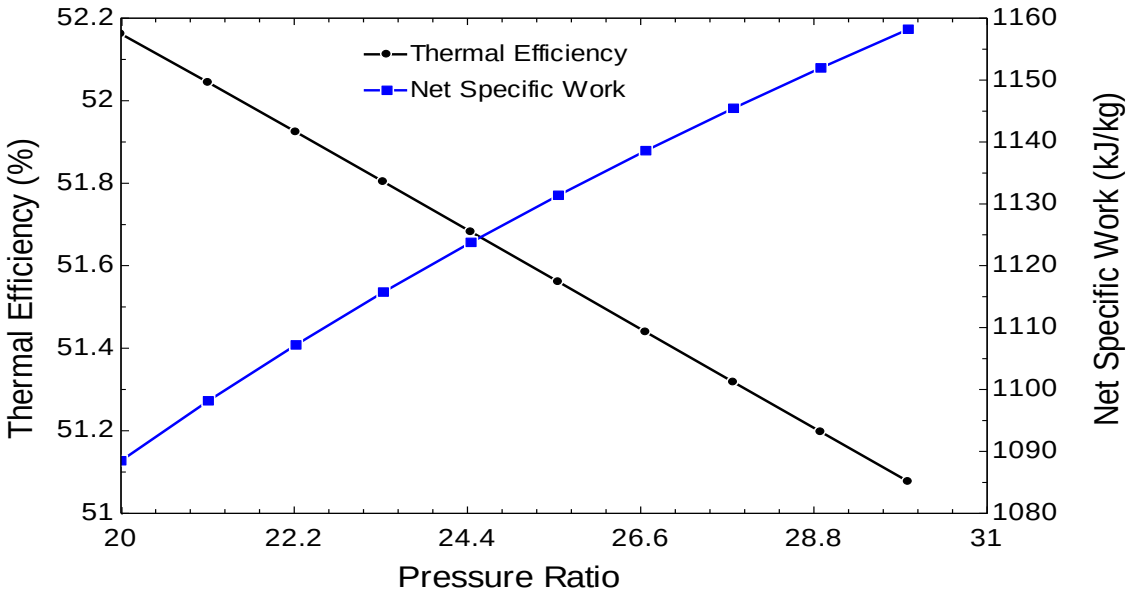

Figure 38: Effect of pressure ratio on the gas turbine thermal efficiency (%) and the net specific work (kJ/kg)

The effect of pressure ratio on the gas turbine exergetic efficiency and the total cost rate is shown in Figure 39. The increase in pressure ratio usually leads to an increase in the exergetic efficiency. This occurs because the increase in the pressure ratio means lower fuel requirements and higher compression work. However, If the high compression work overcomes the lower fuel requirements, the exergetic efficiency will start decreasing as displayed. Moreover, the increase in pressure ratio will increase the total cost rate due to the higher investment costs.

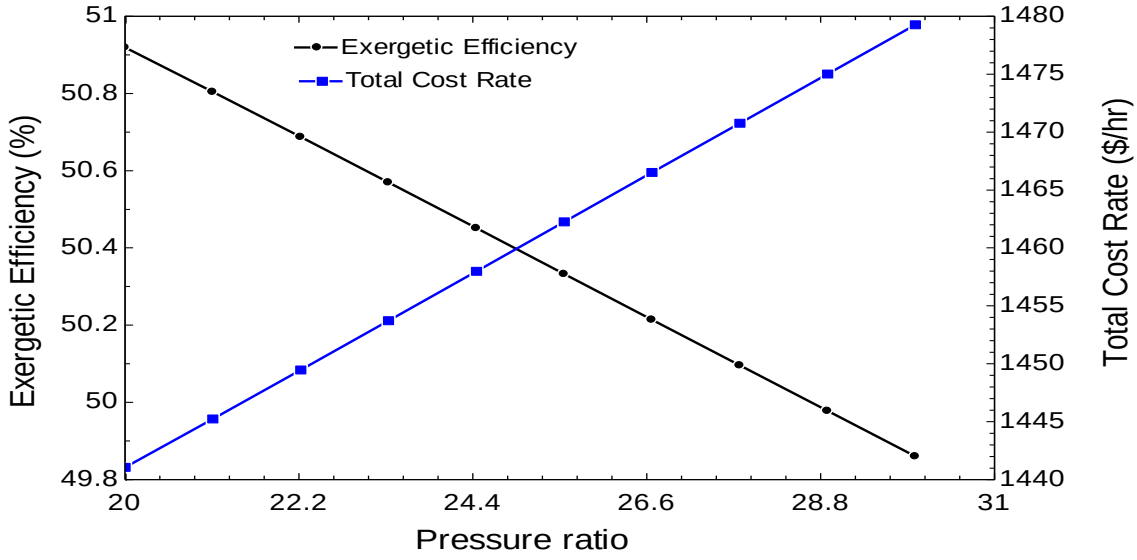

Figure 39: Effect of pressure ratio on the gas turbine exergetic efficiency (%) and the total cost rate ($/hr)

5.3.2. Thermodynamic results. The performance of the three Maisotsenko-desiccant cooling systems TS-MD, TS-PMD and TS-EMD is showed in Table 14. Tables 15, 16, 17 and 18 showed the performance of the gas turbine cycle from the thermodynamics point of view with and without integrating the cooling systems.

As it can be seen, in the base case, where no cooling systems are integrated, the total coolant mass flow rate required to cool down the turbine blades was 3.349 kg/s, while the total coolant mass flow rate was found to be 3.01 kg/s, 2.995 kg/s and 2.977 kg/s after integrating the cooling systems TS-MD, TS-PMD and TS-EMD, respectively. Thus, in comparison to the base case, a lower cooling fraction is going to be needed in the case of integrating the cooling systems. This reduction in the amount of coolant mass flow rate bled from the compressor to cool down the turbine blades will reduce the penalty on the thermal efficiency of the system as expected.

In comparison to the base case, where the thermal efficiency was 52.16%, the thermal efficiency has increased to 52.69%, 52.89% and 53.12% after integrating the cooling systems TS-MD, TS-PMD and TS-EMD, respectively. Moreover, a reduction in the amount of total fuel mass flow rate required was noticed after integrating the cooling systems in comparison to the base case. This reduction will help in decreasing the carbon foot print which is a major concern nowadays to the United Nations according to their latest strategies and guidelines where they are working towards a more sustainable and greener environment [91]. Furthermore, the net specific work of the cycle has increased from 1089 kJ/kg in the base case to 1091 kJ/kg, 1093 kJ/kg and 1095 kJ/kg in the case of TS-MD, TS-PMD and TS-EMD implementation, respectively.

The obtained results show a very promising potential, especially in the industry sector where the increase in the efficiency can save millions of dollars. Moreover, the reduction in carbon foot print, which is defined as the amount of carbon dioxide released into the atmosphere as a result of the activities of a particular individual, organization, or community, is of major importance from environmental point of view as the world is trying to unite together to face the upcoming climate change challenges.

Table 14: TS-MD, TS-PMD and TS-EMD cooling systems performance

Configurations	TS-MD	TS-PMD	TS-EMD
Inlet pressure (bar)	1	1	1
Relative humidity (%)	50	50	50
$T_{ambient}$(°K)	313	313	313
$T_{Regeneration}$ (°K)	353	353	353
Humidity ratio (kg/kg)	0.005137	0.004513	0.005137
(kg/s)$\dot{m}_l = \dot{m}_u$	418.82	414.74	410.26
T_{outlet}(°K)	286	284.3	282.4

Table 15: Thermodynamic results of the gas turbine without integrating the cooling systems

Parameter	Value
Thermal efficiency (%)	52.16
Air mass flow rate (kg/s)	64.43
Total Coolant mass flow rate (kg/s)	3.349
Cooling fractions (%)	5.198
Total Fuel mass flow rate (kg/s)	2.214
Total Compressors specific work (kJ/Kg)	759.9
Total Turbines specific work (kJ/kg)	1848
Net specific work (kJ/kg)	1089
Total Compressor power (MW)	25.552
Total Turbine power (MW)	75.552

Table 16: Thermodynamic results of the gas turbine integrated with TS-MD

Parameter	Value
Thermal efficiency (%)	52.69
Air mass flow rate (kg/s)	63.57
Total Coolant mass flow rate (kg/s)	3.01
Cooling fractions (%)	4.739
Total Fuel mass flow rate (kg/s)	2.192
Total Compressors specific work (kJ/kg)	490
Total Turbines specific work (kJ/kg)	1581
Net specific work (kJ/kg)	1091
Total Compressor power (MW)	24.785
Total Turbine power (MW)	74.785

Table 17: Thermodynamic results of the gas turbine integrated with TS-PMD

Parameter	Value
Thermal efficiency (%)	52.89
Air mass flow rate (kg/s)	63.3
Total Coolant mass flow rate (kg/s)	2.995
Cooling fractions (%)	4.732
Total Fuel mass flow rate (kg/s)	2.184
Total Compressors specific work (kJ/kg)	482.5
Total Turbines specific work (kJ/kg)	1576
Net specific work (kJ/kg)	1093
Total Compressor power (MW)	24.475
Total Turbine power (MW)	74.475

Table 18: Thermodynamic results of the gas turbine integrated with TS-EMD

Parameter	Value
Thermal efficiency (%)	53.12
Air mass flow rate (kg/s)	63
Total Coolant mass flow rate (kg/s)	2.977
Cooling fractions (%)	4.724
Total Fuel mass flow rate (kg/s)	2.174
Total Compressors specific work (kJ/kg)	474.6
Total Turbines specific work (kJ/kg)	1570
Net specific work (kJ/kg)	1095
Total Compressor power (MW)	24.133
Total Turbine power (MW)	74.133

Nowadays, the cost of power plants and the environmental effects have been considered as important as the thermodynamic performance during the design of power plants. Thus, exergoeconomic analysis was adopted by researchers to assess gas turbine power plants, using the thermodynamic principles from the second law of thermodynamics point of view and the economic concepts as well. Crucial information that helps in foreseeing the thermodynamic performance and many economic variables related to power plants are acquired from the exergoeconomic analysis.

5.3.3. Exergoeconomic results. The performance of the gas turbine cycle from the exergoeconomic point of view, with and without integrating the cooling systems, is presented in Tables 19, 20, 21 and 22. As observed, when integrating TS-MD, TS-PMD and TS-EMD, the exergy destruction rate of the overall system has decreased in the base case from 44.86 MW to 44 MW, 43.7 MW and 43.34 MW, respectively. Hence, an increase in the exergetic efficiency of the overall system from 50.92% in the base case to 51.43%, 51.63% and 51.86% was noticed by integrating TS-MD, TS-PMD and TS-EMD cooling systems, respectively. This was expected due to the reduction in the exergy rate of destruction of the overall system.

Furthermore, a reduction in the investment cost flow rate of the overall system has been detected from 101.8 $/hr in the base case to 100.7 $/hr, 100.3 $/hr and 99.92 $/hr in the case of TS-MD, TS-PMD and TS-EMD integration, respectively. Consequently, the cost rate of exergy destruction of the overall system has decreased from 924.2 $/hr in the base case to reach 899.4 $/hr, 890 $/hr and 879.1 $/hr by integrating the TS-MD, TS-PMD and TS-EMD, respectively.

Another significant factor is the exergoeconomic factor, which describes how well each component and the overall system are performing. For instance, the exergoeconomic factor of the first and the second combustion chambers are recorded to be 2.03 and 2.65, respectively. This means that the cost rate of exergy destruction in both cases is the most dominant factor. Thus, an increase in the capital investment is recommended to improve the component efficiency. One more valuable factor that was investigated as well is the relative cost difference which dictates the relative increase in the average cost per exergy unit between fuel and product of the component. This means that in a cost optimization iteration, if the cost of fuel for a component changed from one iteration to the other, the main objective is to reduce the relative cost difference not the fuel average cost per exergy unit. The integration of the cooling systems has led to a reduction in the relative cost difference of the overall system from 97.06 % in the base case to 95.12%, 94.35% and 93.51% in the case of TS-MD, TS-PMD and TS-EMD, respectively.

Table 19: Exergoeconomic results of the gas turbine without integrating the cooling systems

Component	$\dot{E}_D$ (MW)	$\dot{E}_D$ (%)	$\in$ (%)	$\dot{Z}$ ($/hr)	$\dot{C}_D$ ($/hr)	f (%)	r (%)
LPC	1.239	2.76	89.58	8.222	28.73	22.25	14.97
Intercooler	1.384	3.084	46.09	14.65	36.89	28.42	163.4
HPC	1.266	2.82	90.74	8.503	29.35	22.46	13.16
Recuperator	4.693	10.46	79.95	15.82	107.8	12.8	28.76
CC1	17.26	38.47	81.16	7.108	342.6	2.03	23.7
HPT	2.255	5.02	93.83	19.79	53.1	27.15	4.126
CC2	14.39	32.07	82.9	7.459	273.2	2.65	21.19
LPT	2.383	5.31	93.71	20.29	52.57	27.85	4.123
Overall System	44.86	100	50.92	101.8	924.2	9.925	97.06

Table 20: Exergoeconomic results of the gas turbine integrated with TS-MD

Component	$\dot{E}_D$ (MW)	$\dot{E}_D$ (%)	$\in$ (%)	$\dot{Z}$ ($/hr)	$\dot{C}_D$ ($/hr)	f (%)	r (%)
LPC	1.093	2.484	90.51	8.112	25.16	24.38	13.87
Intercooler	1.33	3.022	45.93	14.53	34.86	29.42	166.8
HPC	1.115	2.534	91.6	8.39	25.67	24.64	12.17
Recuperator	4.561	10.37	80.29	15.69	104.3	13.08	28.25
CC1	17.12	38.9	81.15	7.047	337.2	2.047	23.71
HPT	2.228	5.063	93.85	19.55	52.07	27.29	4.091
CC2	14.21	32.07	82.9	7.368	268.6	2.67	21.2
LPT	2.346	5.331	93.73	20.02	51.52	27.98	4.09
Overall System	44	100	51.43	100.7	899.4	10.18	95.12

Table 21: Exergoeconomic results of the gas turbine integrated with TS-PMD

Component	$\dot{E}_D$ (MW)	$\dot{E}_D$ (%)	$\in$ (%)	$\dot{Z}$ ($/hr)	$\dot{C}_D$ ($/hr)	f (%)	r (%)
LPC	0.9783	2.239	91.34	8.078	22.45	26.46	12.9
Intercooler	1.292	3.022	45.87	14.49	33.49	30.02	169.1
HPC	1.109	2.958	91.59	8.355	25.45	24.72	12.2
Recuperator	4.555	10.42	80.26	15.65	104.1	13.07	28.3
CC1	17.05	39.03	81.14	7.018	334.5	2.055	23.72
HPT	2.218	5.077	93.85	19.47	51.7	27.35	4.082
CC2	14.15	32.39	82.9	7.337	267	2.675	21.2
LPT	2.346	5.345	93.73	19.94	51.28	27.99	4.087
Overall System	43.7	100	51.63	100.3	890	10.13	94.35

Table 22: Exergoeconomic results of the gas turbine integrated with TS-EMD

Component	$\dot{E}_D$ (MW)	$\dot{E}_D$ (%)	$\in$ (%)	$\dot{Z}$ ($/hr)	$\dot{C}_D$ ($/hr)	f (%)	r (%)
LPC	0.8504	1.962	92.3	8.041	19.45	29.24	11.79
Intercooler	1.234	2.848	46.55	14.45	31.56	31.4	167.4
HPC	1.102	2.543	91.58	8.316	25.21	24.81	12.22
Recuperator	4.549	10.5	80.22	15.61	103.9	13.06	23.74
CC1	16.98	39.19	81.14	6.986	331.5	2.064	23.72
HPT	2.208	5.095	93.86	19.38	51.28	27.42	4.073
CC2	14.09	32.5	82.9	7.304	265.2	2.68	21.2
LPT	2.324	5.363	93.73	19.84	51	28.01	4.085
Overall System	43.34	100	51.86	99.92	879.1	10.21	93.51

Chapter 6. Conclusion and Recommendation

In this research, three different configurations of a 50 MWe gas turbine power plants integrated with different configurations of Maisotsenko-Desiccant cooling systems were analysed. The three gas turbine configurations included simple gas turbine, gas turbine with air bottoming cycle and intercooled, recuperated and reheated gas turbine. Optimization and sensitivity analysis were performed to assess the gas turbine power plant and optimize its performance. An exergoeconomic analysis was conducted on the third configuration of an intercooled, recuperated and reheated gas turbine to assess gas turbine power plants, using the thermodynamic principles from the second law of thermodynamics point of view and the economic concepts as well.

6.1. Conclusion

In the first proposed configuration of a simple gas turbine, four different configurations of Maisotsenko-Desiccant cooling systems were analysed. Detailed analysis showed that the highest increase in the efficiency was from 33.33% to 34.17% of the gas turbine in the case of integrating the TS-IMD configuration.

Although the COP was the highest in the case of SS-MD configuration, it might not be the best choice as coefficient of performance is not the best indicator for the performance of this system. This is due to the excess amounts of heat available at our disposal from the gas turbine exhaust gases. Additionally, the gas turbine efficiency and the required coolant mass flow rate, the factors which are considered the main focus of the research, were the best in the case of integrating the two-stage intermediate Maisotsenko desiccant (TS-IMD). Thus, one can say that the (TS-IMD) system in the first gas turbine configuration would be the best choice.

In the second configuration of gas turbine with air bottoming cycle (GTABC), three different configuration of cooling systems were proposed to study the effect of implementing them with a cooled gas turbine incorporated with air bottoming cycle for turbine blade cooling and inlet air cooling as well. The results indicated an increase in the coolant mass flow rate along with an increase followed by a reduction in the gas turbine overall efficiency with the increase in the pressure ratio. Gas turbine overall efficiency and the coolant mass flow increase with the increase in (TIT). Therefore, the amount of coolant mass flow rate bled from the compressor for turbine blade cooling

will decrease by cooling down the coolant line. This helps in reducing the penalty on the overall efficiency and improving the gas turbine performance.

The cooling systems integration with the gas turbine cycle showed a great potential specially the TS-EMD configuration, with an increase in the overall efficiency from 42.57 % without cooling to 43.27%, 43.54% and 43.83% for TS-MD, TS-PMD and TS-EMD, respectively. Additionally, a reduction in the amount of coolant mass flow rate was observed from 4.584 kg/s without cooling to 3.708 kg/s, 3.66 kg/s and 3.607 kg/s for TS-MD, TS-PMD and TS-EMD, respectively. Moreover, the cooling fraction decreased from 4.72% without cooling to 3.93%, 3.917% and 3.902% for TS-MD, TS-PMD and TS-EMD, respectively. Furthermore, a reduction in the fuel mass flow rate was noticed from 2.713 kg/s to 2.653 kg/s leading to a reduction in the carbon foot print which is vital in many fields, specially the industry sector. Hence, the TS-EMD can be considered the best configuration to be implemented with the gas turbine in order to improve its performance according to the obtained results.

Thermodynamic and exergoeconomic analyses were conducted to investigate the performance of the gas turbine power plant with and without integrating the cooling systems for the third configuration of intercooled, recuperated and reheated gas turbine. The effect of different variables on the gas turbine thermal and exergetic efficiency, net specific work and the total cost rate was investigated as well. Moreover, the exergoeconomic factor and relative cost difference variables were determined to assess the performance of each component and the manner of improving it.

The total coolant mass flow rate required to cool down the turbine blades has decreased from 3.349 kg/s in the base case to 2.977 kg/s when the TS-EMD cooling system was integrated. Thus, the thermodynamic penalty that occurs due to the coolant mass flow rate drained from the compressor decreased. This has led to an increase in the thermal efficiency from 52.16% in the base case to 53.12% for TS-EMD integration. This increase in the efficiency can be translated to millions of dollars saved, which is of a crucial important specially in the industrial sector.

Furthermore, utilizing the TS-EMD has led to a reduction in the amount of fuel mass flow rate, reducing the carbon foot print which is of a major importance nowadays according to the recent United Nations reports and guidelines as they are trying to work towards a more sustainable and greener environment.

From the exergoeconomic point of view, the integration of the TS-EMD cooling system has led to a reduction in the exergy destruction rate, followed by an augmentation in the exergetic efficiency, along a reduction in the investment cost flow rate and the cost rate of exergy. Thus, out of the three cooling systems investigated, the TS-EMD had the best effect when integrated with the gas turbine cycle.

The exergoeconomic factor and the relative cost difference were also determined to help assess each component in the system and the manner of improving its performance. The obtained results showed a promising potential as it will help improve the overall performance of the power plant and allow it to be more sustainable, environment friendly and cost effective by saving millions of dollars.

6.2. Recommendation

According to the obtained results, integration of Maisotsenko-Desiccant cooling systems with gas turbine power plants as an effective cooling technique has shown a great potential. Along the reduction in the carbon footprint, the augmentation in the thermodynamic and exergetic efficiency shall improve the performance of the power plant, saving huge amounts of money. As a recommendation, the usage of two stage and triple stage Maisotsenko-Desiccant cooling systems is highly advised as they provide better performance. Moreover, the incorporation of a recuperator with a reheated and intercooled gas turbine is a must since the reheater increases the temperature at which heat is rejected, and the intercooler decreases the temperature at which head is added. Thus, intercooling and reheating will always reduce the thermal efficiency unless they are integrated with a recuperator.

As for future research work, the ratio of the two divided processed air streams entering the working dry channel and the product channel is worth looking into. Investigating diverse ratios and percentages may yield different results. Furthermore, the integration of Maisotsenko-Desiccant cooling systems with combined or even steam power plants should be investigated from thermodynamic and exergoeconomic points of view.

References

[1] P. Tebbe, "Engaged In Thermodynamics," Minnesota State University, 2014. [Online]. [Accessed 2015].

[2] M. Farzaneh-Gord and . M. Deymi-Dashtebayaz, "Effect of various inlet air cooling methods on gas turbine performance," *Energy,* vol. 36, no. 2, pp. 1196-1205, 2011.

[3] Y. S. Najjar, "Gas turbine cogeneration systems: a review of some novel cycles," *Applied Thermal Engineering,* vol. 20, no. 2, pp. 179–197, 2000.

[4] A. Poullikkas, "An overview of current and future sustainable gas turbine technologies," *Renewable and Sustainable Energy Reviews,* vol. 9, no. 5, pp. 409–443, 2005.

[5] M. Jonsson and . J. Yan, "Humidified gas turbines—a review of proposed and implemented cycles," *Energy,* vol. 30, no. 7, pp. 1013–1078, 2005.

[6] E. Kakaras, . A. Doukelis and S. Karellas, "Compressor intake-air cooling in gas turbine plants," *Energy,* vol. 29, no. 12-15, pp. 2347–2358, 2004.

[7] A. M. Bassily, "Effects of evaporative inlet and aftercooling on the recuperated gas turbine cycle,*" Applied Thermal Engineering,* vol. 21, no. 18, pp. 1875–1890, 2001.

[8] A. A. Zadpoor and A. H. Golshan, "Performance improvement of a gas turbine cycle by using a desiccant-based evaporative cooling system," *Energy,* vol. 31, no. 14, pp. 2652–2664, 2006.

[9] S. o. oyedepo and O. Kilanko, "Thermodynamic analysis of a gas turbine power plant modelled with an evaporative cooler," *International Journal of Thermodynamics,* vol. 17, pp. 14-20, 2014.

[10] M. F. Gord and M. J. Maghrebi, "Exergy of natural gas flow in Iran's natural gas fields," *International Journal of Exergy,* vol. 6, no. 1, 2009.

[11] M. F. Gord and M. D. Dashtebayaz, "A new approach for enhancing performance of a gas turbine (case study: Khangiran refinery)," *Applied Energy,* vol. 86, no. 12, pp. 2750–2759, 2009.

[12] S. Boonnasaa, . P. Namprakaia and T. Muangnapohb, "Performance improvement of the combined cycle power plant by intake air cooling using an absorption chiller," *Energy,* vol. 31, no. 12, pp. 2036–2046, 2006.

[13] R. Gareta, L. M. Romeo and A. Gil, "Methodology for the economic evaluation of gas turbine air cooling systems in combined cycle applications," *Energy,* vol. 29, no. 11, pp. 1805–1818, 2004.

[14] M. Ameri, and S. H. Hejazi, "The study of capacity enhancement of the Chabahar gas turbine installation using an absorption chiller," *Applied Thermal Engineering,* vol. 24, no. 1, pp. 59–68, 2004.

[15] S. O. Singh and B. N. Prasad, "Influence of different means of turbine blade cooling on the thermodynamic performance of combined cycle," *Applied Thermal Engineering,* vol. 28, pp. 2315–2326, 2008.

[16] R. S. Amano, "Advances in gas turbine blade cooling," *WIT Transactions on Engineering Sciences,* vol. 61, pp. 149-157, 2008.

[17] R. C. Wilcock, . J. B. Young and . J. H. Horlock, "The Effect of turbine blade cooling on the cycle efficiency of gas turbine power cycles," *Journal of Engineering for Gas Turbines and Power,* vol. 127, no. 1, pp. 109-120, 2005.

[18] J. F. Louis, K. Hiraoka and M. A. El Masri, "A Comparitive Study of the Influence of Different Means of Turbine Blade Cooling on Gas Turbine Performance," *ASME,* 1983.

[19] E. Sciubba, "Air-cooled gas turbine cycles – part 1: An analytical method for the preliminary assessment of blade cooling flow rates," *Energy,* vol. 83, no. 1, pp. 104–114, 2015.

[20] A. R. Al Ali and I. Janajreh, "Numerical Simulation of Turbine Blade Cooling via Jet Impingemen," *Energy Procedia,* vol. 75, pp. 3220-3229, 2015.

[21] A. K. Mohapatra and S. , "Thermodynamic assessment of impact of inlet air cooling techniques on gas turbine and combined cycle performance," *Energy,* vol. 68, no. 15, pp. 191-203, 2014.

[22] S. O. Singh and B. N. Prasad, "Comparative performance analysis of cogeneration gas turbine cycle for different blade cooling means," *International Journal of Thermal Sciences,* vol. 48, pp. 1432–1440, 2009.

[23] M. K. Sahu and S. Sanjay , "Investigation of the effect of air film blade cooling on thermoeconomics of gas turbine based power plant cycle," *Energy,* vol. 115, pp. 1320-1330, 2016.

[24] M. Jonsson and O. Bolland, "Gas Turbine Cooling Model for Evaluation of Novel Cycles," in *ECOS,* Trondheim, Norway, 2005.

[25] J. D. Spelling, "Hybrid Solar Gas-Turbine Power Plants A Thermo-Economic Analysis (Doctoral Thesis)," KTH Royal Institute of Technology, Stockholm, Sweden, 2013.

[26] M. El-Masri, "On thermodynamics of gas-turbine cycles: part 2—a model for expansion in cooled turbines," *Journal of Engineering for Gas Turbines and Power,* vol. 108, no. 1, pp. 151, 1986.

[27] J. Horlock, D. Watson and T. Jones, "Limitations on gas turbine performance imposed by large turbine cooling flows," *Journal of Engineering for Gas Turbines and Power*, vol. 123, no. 3, pp. 487, 2001.

[28] A. Shukla and O. Singh, "Thermodynamic investigation of parameters affecting the execution of steam injected cooled gas turbine based combined cycle power plant with vapor absorption inlet air cooling," *Applied Thermal Engineering*, vol. 122, pp. 380-388, 2017.

[29] Apostolidis, "Turbine Cooling and Heat Transfer Modelling for Gas Turbine Performance Simulation," Ph.D, Cranfield University, 2015.

[30] Sanjay and B. Prasad, "Energy and exergy analysis of intercooled combustion-turbine based combined cycle power plant," *Energy*, vol. 59, pp. 277-284, 2013.

[31] R. Fernandes, "Investigation of Pin Fin Cooling Channels for Applications in Gas Turbines," Ph.D, Embry-Riddle Aeronautical University, 2016.

[32] B. Sunden and G. Xie, "Gas Turbine Blade Tip Heat Transfer and Cooling: A Literature Survey," *Heat Transfer Engineering*, vol. 31, no. 7, pp. 527-554, 2010.

[33] C. Du, L. Li, X. Fan and Z. Feng, "Rotational influences on aerodynamic and heat transfer behavior of gas turbine blade vortex cooling with bleed holes," *Applied Thermal Engineering*, vol. 121, no.5, pp. 302-313, 2017

[34] N. Nagaiah, "Multi-Objective Design Optimization of Gas Turbine Blade with Emphasis on Internal Cooling," Ph.D, University of Central Florida, 2012.

[35] W. Zhou, "Novel Cooling Strategies for Improved Protection of Gas Turbine Blades," Ph.D, Iowa State University, 2016.

[36] W. Siddique, "Design of Internal Cooling Passages: Investigation of Thermal Performance of Serpentine Passages," Ph.D, Royal Institute of Technology, 2011.

[37] V. Maisotsenko and L. Gillan, "Maisotsenko open cycle used for gas turbine power generation," in *Proceedings of ASME Turbo Expo 2003*, Georgia, 2003.

[38] H. Caliskan, A. Hepbasli, I. Dincer and V. Maisotsenko, "Thermodynamic performance assessment of a novel air cooling cycle: Maisotsenko cycle," *International Journal of Refrigeration*, vol. 34, no.4, pp. 980-990, 2011.

[39] M. Saghafifar and . M. Gadalla, "Innovative inlet air cooling technology for gas turbine power plants using integrated solid desiccant and Maisotsenko cooler," *Energy*, vol. 87, no.1, pp. 663-677, 2015.

[40] M. Saghafifar and M. Gadalla, "Performance assessment of integrated PV/T and solid desiccant air-conditioning systems for cooling buildings using Maisotsenko cooling cycle," *Solar Energy*, vol. 127, pp. 79-95, 2016.

[41] M. Gadalla and M. Saghafifar, "Performance assessment and transient optimization of air precooling in multi-stage solid desiccant air conditioning systems," *Energy Conversion and Management*, vol. 119, no.1, pp. 187-202, 2016.

[42] R. Bhargava and A. Peretto, "A Unique Approach for Thermoeconomic Optimization of an Intercooled, Reheat, and Recuperated Gas Turbine for Cogeneration Applications," *Journal of Engineering for Gas Turbines and Power*, vol. 124, no. 4, pp. 881, 2002.

[43] Y. Sanjay, O. Singh and B. Prasad, "Energy and exergy analysis of steam cooled reheat gas–steam combined cycle," *Applied Thermal Engineering*, vol. 27, no. 17-18, pp. 2779-2790, 2007.

[44] S. Göktun and H. Yavuz, "Thermal efficiency of a regenerative Brayton cycle with isothermal heat addition," *Energy Conversion and Management*, vol. 40, no. 12, pp. 1259-1266, 1999.

[45] C. McDonald and D. Wilson, "The utilization of recuperated and regenerated engine cycles for high-efficiency gas turbines in the 21st century," *Applied Thermal Engineering*, vol. 16, no. 8-9, pp. 635-653, 1996.

[46] R. Bhargava, M. Bianchi, S. Campanari, A. De Pascale, G. Negri di Montenegro and A. Peretto, "A Parametric Thermodynamic Evaluation of High Performance Gas Turbine Based Power Cycles," *Journal of Engineering for Gas Turbines and Power*, vol. 132, no. 2, pp. 022001, 2010.

[47] Sanjay, "Investigation of effect of variation of cycle parameters on thermodynamic performance of gas-steam combined cycle," *Energy*, vol. 36, no. 1, pp. 157-167, 2011.

[48] J. Horlock, D. Watson and T. Jones, "Limitations on Gas Turbine Performance Imposed by Large Turbine Cooling Flows," *Journal of Engineering for Gas Turbines and Powe*r, vol. 123, no. 3, pp. 487, 2001.

[49] J. Young and R. Wilcock, "Modeling the Air-Cooled Gas Turbine: Part 1—General Thermodynamics," *Journal of Turbomachinery*, vol. 124, no. 2, pp. 207, 2002.

[50] Sanjay, O. Singh and B. Prasad, "Influence of different means of turbine blade cooling on the thermodynamic performance of combined cycle," *Applied Thermal Engineering*, vol. 28, no. 17-18, pp. 2315-2326, 2008.

[51] I. Kwon, D. Kang and T. Kim, "Using coolant modulation and pre-cooling to avoid turbine blade overheating in a gas turbine combined cycle power plant fired with low calorific value gas," *Applied Thermal Engineering*, vol. 60, no. 1-2, pp. 285-294, 2013.

[52] Sanjay, O. Singh and B. Prasad, "Comparative Evaluation of Gas Turbine Power Pant Performance for Different Blade Cooling Means," Proceedings of the Institution of Mechanical Engineers, Part A: *Journal of Power and Energy*, vol. 223, no. 1, pp. 71-82, 2008.

[53] J. Young and J. Horlock, "Defining the efficiency of a cooled turbine," *Journal of Turbomachinery*, vol. 128, no. 4, pp. 658, 2006.

[54] A. Valero, M. A. Lozano, L. Serra, G. Tsatsaronis, J. Pisa, C. Frangopoulos and M. R. Von Spakovsky, "CGAM problem: Definition and conventional solution" *Energy*, vol. 19, no. 3, pp. 279-286, 1994.

[55] C. Frangopoulos, "Application of the thermoeconomic functional approach to the CGAM problem," *Energy*, vol. 19, no. 3, pp. 323-342., 1994.

[56] G. Tsatsaronis and J. Pisa, "Exergoeconomic evaluation and optimization of energy systems — application to the CGAM problem," *Energy*, vol. 19, no. 3, pp. 287-321, 1994.

[57] A. Valero, M. Lozano, L. Serra and C. Torres, "Application of the exergetic cost theory to the CGAM problem," *Energy*, vol. 19, no. 3, pp. 365-381, 1994.

[58] M. Von Spakovsky, "Application of engineering functional analysis to the analysis and optimization of the CGAM problem," *Energy*, vol. 19, no. 3, pp. 343-364, 1994.

[59] P. Sahoo, "Exergoeconomic analysis and optimization of a cogeneration system using evolutionary programming," *Applied Thermal Engineering*, vol. 28, no. 13, pp. 1580-1588, 2008.

[60] D. Kim, "A new thermoeconomic methodology for energy systems", *Energy*, vol. 35, no. 1, pp. 410-422, 2010.

[61] A. Mohammadi Khoshkar Vandani, F. Joda and R. Bozorgmehry Boozarjomehry, "Exergic, economic and environmental impacts of natural gas and diesel in operation of combined cycle power plants," *Energy Conversion and Management*, vol. 109, no.1, pp. 103-112, 2016.

[62] S. Bakhshmand, R. Saray, K. Bahlouli, H. Eftekhari and A. Ebrahimi, "Exergoeconomic analysis and optimization of a triple-pressure combined cycle plant using evolutionary algorithm," *Energy*, vol. 93, no.1, pp. 555-567, 2015.

[63] A. Marzouk and A. Hanafi, "Thermo-Economic Analysis of Inlet Air Cooling in Gas Turbine Plants," *Journal of Power Technologies*, vol. 93, no. 2, pp. 90-99, 2013.

[64] J. Xiong, H. Zhao, C. Zhang, C. Zheng and P. Luh, "Thermoeconomic operation optimization of a coal-fired power plant," *Energy*, vol. 42, no. 1, pp. 486-496, 2012.

[65] S. Seyyedi, H. Ajam and S. Farahat, "A new approach for optimization of thermal power plant based on the exergoeconomic analysis and structural optimization method: Application to the CGAM problem," *Energy Conversion and Management*, vol. 51, no. 11, pp. 2202-2211, 2010.

[66] R. Karaali and İ. Öztürk, "Thermoeconomic optimization of gas turbine cogeneration plants," *Energy*, vol. 80, no.1, pp. 474-485, 2015.

[67] P. Ahmadi, I. Dincer and M. Rosen, "Exergy, exergoeconomic and environmental analyses and evolutionary algorithm based multi-objective optimization of combined cycle power plants," *Energy*, vol. 36, no. 10, pp. 5886-5898, 2011.

[68] M. Sahu and S. , "Comparative exergoeconomic analysis of basic and reheat gas turbine with air film blade cooling," *Energy*, vol. 132, no.1, pp. 160-170, 2017.

[69] M. Sahu and Sanjay, "Comparative exergoeconomics of power utilities: Air-cooled gas turbine cycle and combined cycle configurations," *Energy*, vol. 139, no.5, pp. 42-51, 2017.

[70] M. Sahu and Sanjay, "Thermoeconomic investigation of basic and intercooled gas turbine based power utilities incorporating air-film blade cooling," *Journal of Cleaner Production*, vol. 170, no.1, pp. 842-856, 2018.

[71] M. Sahu and Sanjay, "Thermoeconomic investigation of power utilities: Intercooled recuperated gas turbine cycle featuring cooled turbine blades," *Energy*, vol. 138, no.1, pp. 490-499, 2017.

[72] M. Sahu and Sanjay, "Exergoeconomic investigation of power utility based on air film blade cooled gas turbine cycle," *Applied Thermal Engineering*, vol. 122, no.5, pp. 738-746, 2017.

[73] A. M. Al-Ibrahim and A. Varnham, "A review of inlet air-cooling technologies for enhancing the performance of combustion turbines in Saudi Arabia," *Applied Thermal Engineering*, vol. 30, no.14-15, pp. 1879-1888, 2010.

[74] C. B. Meher-Homji and T. . R. Mee, "Inlet Fogging of Gas Turbine Engines: Part A — Theory, Psychrometrics and Fog Generation," in *ASME Turbo Expo 2000: Power for Land, Sea, and Air*, *Munich*, 2000.

[75] H. P. Blanco, . K. H. Kim and S. Ream, "Evaporatively-cooled compression using a high-pressure refrigerant," *Applied Energy*, vol. 84, no. 10, pp. 1028-1043, 2007.

[76] B. Mohanty and G. Paloso Jr, "Enhancing gas turbine performance by intake air cooling using an absorption chiller," *Heat Recovery Systems and CHP*, vol. 15, no. 1, pp. 41-50, 1995.

[77] M. Gadalla and . M. Saghafifar, "Performance assessment and transient optimization of air precooling in multi-stage solid desiccant air conditioning systems," *Energy Conversion and Management*, vol. 119, no. 1, pp. 182-202, 2016.

[78] Y. S. Touloukian and M. Tadash, "Thermo-physical Properties of Matter vol. 6" in *Thermo-physical Properties of Matter, vol. 6, The TPRC Data Series, IFI/Plenum*, New York, Washington, 1970.

[79] J. H. Horlock, Advanced Gas Turbine Cycles, Cambridge, UK: Elsevier Science, 2003.

[80] G. Panaras, E. Mathioulakis and V. Belessiotis, "Solid desiccant air-conditioning systems – Design parameters" *Energy*, vol. 36, no. 5, p. 2399–2406, 2011.

[81] C. Nóbrega and . N. Brum, "An analysis of the heat and mass transfer roles in air dehumidification by solid desiccants," *Energy and Buildings,* vol. 50, pp. 251-258, 2012.

[82] G. Panaras, E. Mathioulakis, V. Belessiotis and N. Kyriakis, "Experimental validation of a simplified approach for a desiccant wheel model," *Energy and Buildings*, vol. 42, no. 10, p. 1719–1725, 2010.

[83] K. Wicker, "Life below the wet bulb: The Maisotsenko cycle," *Power*, Arvada, Colo, 2003.

[84] S. Seyyedi, H. Ajam and S. Farahat, "A new approach for optimization of thermal power plant based on the exergoeconomic analysis and structural optimization method: Application to the CGAM problem," *Energy Conversion and Management*, vol. 51, no. 11, pp. 2202-2211, 2010.

[85] A. Bejan, G. Tsatsaronis and M. Moran, Thermal design and optimization. *New York*: Wiley, 1996.

[86] T. George and C. Frank, "Thermoeconomics", *Encyclopedia of Science and Technology*. pp. 659-680, 2002.

[87] W. El-Damaty and M. Gadalla, "Analysis of Integrated Cooling Systems for Gas Turbine Power Plants," in *International Mechanical Engineering Congress and Exposition, IMECE*, 2017.

[88] W. El-Damaty and M. Gadalla, "Assesments of Gas Turbine's Cooling Systems Integrated with Bottoming Cycle," in *Congress and Exhibition, Power & Energy, 2018.*

[89] J. Chattopadhyay, Rahul Singh and O. Prakash, *Renewable energy and its innovative technologies*, 1st ed. 2017, pp. 69-88.

[90] M. Sahu, " Exergoeconomic Analysis of Air Film Cooled Complex Gas Turbine Based Power Plant Cycles," Ph.D., National Institute of Jamshedpur, 2018.

[91] "UN Environment Annual Report 2017", Unenvironment.org, 2018. [Online]. Available: https://www.unenvironment.org/annualreport/2017/index.php?page=0&lang=en [Accessed: 27- Oct- 2018].

Vita

Waleed Moustafa El-Damaty was born in 1993, in Alexandria, Egypt. He received his primary and secondary education in Cairo, Egypt. He received his B.Sc. degree in Energy Engineering from Helwan University in 2014.

In September 2016, he joined the Mechanical Engineering master's program in the American University of Sharjah as a graduate teaching assistant. During his master's study, he authored 2 papers which was presented in international conferences with a third paper accepted for publication. His research interests are in power plants, gas turbines and sustainability.